



## AD-A159 646

LIQUID-VAPOR FLOW REGIME TRANSITIONS FOR USE IN  
DESIGN OF HEAT TRANSFER LOOPS IN SPACECRAFT -  
AN INVESTIGATION OF TWO-PHASE FLOW IN ZERO  
GRAVITY CONDITIONS

Thomas W. Lovell

AETA Corporation  
117 Silver Street  
Dover, New Hampshire 03820

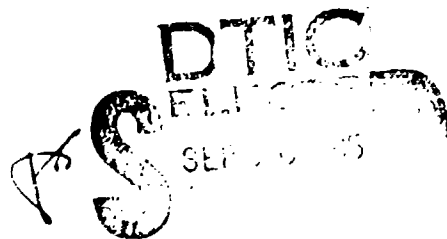
May 1985

Final Report for Period 21 September 1984 - 21 March 1985

Approved for public release; distribution unlimited.

DTIC FILE COPY

FLIGHT DYNAMICS LABORATORY  
AIR FORCE WRIGHT AERONAUTICAL LABORATORIES  
AIR FORCE SYSTEMS COMMAND  
WRIGHT-PATTERSON AIR FORCE BASE, OHIO 45433-6553




85 09 30 015

# NOTICE

When Government drawings, specifications, or other data are used for any purpose other than in connection with a definitely related Government procurement operation, the United States Government thereby incurs no responsibility nor any obligation whatsoever; and the fact that the government may have formulated, furnished, or in any way supplied the said drawings, specifications, or other data, is not to be regarded by implication or otherwise as in any manner licensing the holder or any other person or corporation, or conveying any rights or permission to manufacture use, or sell any patented invention that may in any way be related thereto.

This report has been reviewed by the Office of Public Affairs (ASD/PA) and is releasable to the National Technical Information Service (NTIS). At NTIS, it will be available to the general public, including foreign nations.

This technical report has been reviewed and is approved for publication.



KENT L. WEAVER  
Project Engineer



PAUL D. LINDQUIST  
Technical Manager

FOR THE COMMANDER



SOLOMON R. METRES  
Chief  
Vehicle Equipment Division  
Flight Dynamics Laboratory

"If your address has changed, if you wish to be removed from our mailing list, or if the addressee is no longer employed by your organization please notify AFWAL/FIEE, W-PAFB, OH 45433 to help us maintain a current mailing list".

Copies of this report should not be returned unless return is required by security considerations, contractual obligations, or notice on a specific document.

UNCLASSIFIED

SECURITY CLASSIFICATION OF THIS PAGE

AD-A159 646

## REPORT DOCUMENTATION PAGE

1a. REPORT SECURITY CLASSIFICATION <b>UNCLASSIFIED</b>			1b. RESTRICTIVE MARKINGS N/A										
2a. SECURITY CLASSIFICATION AUTHORITY			3. DISTRIBUTION/AVAILABILITY OF REPORT  Approved for public release, distribution in unlimited.										
2b. DECLASSIFICATION/DOWNGRADING SCHEDULE													
4. PERFORMING ORGANIZATION REPORT NUMBER(S)			5. MONITORING ORGANIZATION REPORT NUMBER(S)  AFWAL-TR-85 -3021										
6a. NAME OF PERFORMING ORGANIZATION  Aeta Corporation		6b. OFFICE SYMBOL (If applicable)	7a. NAME OF MONITORING ORGANIZATION  AFWAL/FIEED										
6c. ADDRESS (City, State and ZIP Code)  117 Silver Street Dover, New Hampshire 03820			7b. ADDRESS (City, State and ZIP Code)  AFWAL/FIEED W-PAFB, OH 45433-6553										
8a. NAME OF FUNDING/SPONSORING ORGANIZATION  FLIGHT DYNAMICS LABORATORY		8b. OFFICE SYMBOL (If applicable)	9. PROCUREMENT INSTRUMENT IDENTIFICATION NUMBER  F33615-84-C-3413										
8c. ADDRESS (City, State and ZIP Code)  Wright-Patterson AFB, OH 45433-6553			10. SOURCE OF FUNDING NOS. <table border="1"><thead><tr><th>PROGRAM ELEMENT NO.</th><th>PROJECT NO.</th><th>TASK NO.</th><th>WORK UNIT NO.</th></tr></thead><tbody><tr><td>65502F</td><td>3005</td><td>30</td><td>14</td></tr></tbody></table>		PROGRAM ELEMENT NO.	PROJECT NO.	TASK NO.	WORK UNIT NO.	65502F	3005	30	14	
PROGRAM ELEMENT NO.	PROJECT NO.	TASK NO.	WORK UNIT NO.										
65502F	3005	30	14										
11. TITLE (Include Security Classification) LIQ-VAP FLOW REGIME TRANSITIONS-Two Phase Invest in Zero-G Condition													
12. PERSONAL AUTHOR(S) THOMAS W. LOVELL													
13a. TYPE OF REPORT FINAL	13b. TIME COVERED FROM 21Sep84 to 21Mar85		14. DATE OF REPORT (Yr., Mo., Day) May 1985	15. PAGE COUNT 122									
16. SUPPLEMENTARY NOTATION													
17. COSATI CODES <table border="1"><thead><tr><th>FIELD</th><th>GROUP</th><th>SUB. GR.</th></tr></thead><tbody><tr><td>22</td><td>02</td><td></td></tr><tr><td>20</td><td>13</td><td></td></tr></tbody></table>			FIELD	GROUP	SUB. GR.	22	02		20	13		18. SUBJECT TERMS (Continue on reverse if necessary and identify by block number)	
FIELD	GROUP	SUB. GR.											
22	02												
20	13												
19. ABSTRACT (Continue on reverse if necessary and identify by block number)  This program was funded through the Small Business Innovation Research (SBIR) Program. The behavior of viscous (or low velocity) two-phase vapor-liquid flow under zero gravity was simulated in the laboratory by using two immiscible fluids of equal density flowing together in a one inch diameter glass tube. The fluids used were Polypropylene Glycol (PPG) which simulated the liquid phase and water which simulated the vapor phase. Various tests were conducted varying flow rates and entrance conditions. Four existing flow regime models were analyzed, modeled on a computer, and extrapolated to predict zero-gravity conditions. The flow regimes were the Horizontal Dukler-Taitel, Vertical Dukler-Taitel, Vertical Weisman and Horizontal Weisman. None of these models when extrapolated to zero-g conditions agreed well with the lab data, and some of the observed flow regimes were not predicted at all.													
20. DISTRIBUTION/AVAILABILITY OF ABSTRACT  UNCLASSIFIED/UNLIMITED <input type="checkbox"/> SAME AS RPT. <input checked="" type="checkbox"/> DTIC USERS <input type="checkbox"/>			21. ABSTRACT SECURITY CLASSIFICATION  UNCLASSIFIED										
22. NAME OF RESPONSIBLE INDIVIDUAL  KENT L. WEAVER		22b. TELEPHONE NUMBER (Include Area Code) (513) 255-4853	22c. OFFICE SYMBOL  AFWAL/FIEE										

## PREFACE

The work outlined in this report was supported by the Air Force under Contract No. F33615-84-C-3413, and was a Phase I SBIR award from WPAFB.

The contract's Program Manager, Mr. Kent Weaver of the Air Force Wright Aeronautical Laboratories, Wright Patterson Air Force Base, was most encouraging and helpful to us in focusing our activities. We are especially grateful for his assistance in providing relevant background reference materials and for his critical review of our early results when he visited our facilities during the course of the contract.

We are also appreciative of the efforts of the Director of the Consulting Center, Dr. J. Morrison and the Chairman of the Chemical Engineering Department, Dr. S. Fan of the University of New Hampshire for their cooperation in making their experimental and videotaping facilities available to us at reduced cost. This was definitely a major contributing factor in permitting us to provide such comprehensive results in such a short time and with the limited budget provided by this Phase I contract.

Dr. V.K. Mathur, a member of the faculty at the University of New Hampshire and a Senior Consulting Associate of the AETA Corporation, along with Dr. Horst Richter of Dartmouth College, were instrumental in assuring that the contract was expeditiously carried out and in reviewing the final results. We are grateful for their assistance.

Accession For	
NRIS GRA&I	X
ERIC TAB	
Unannounced	
Dr. Richter	
By	
Dr. Richter	
Approved	
Dr. Richter	
Dist	
A-1	



# TABLE OF CONTENTS

	PAGE
Preface	iii
Table of Figures	vi
<b>INVESTIGATION OF TWO PHASE FLOW IN ZERO GRAVITY CONDITIONS</b>	<b>1</b>
Executive Summary	1
Overview of Findings	3
<b>I. BACKGROUND AND OUTLINE OF PHASE I WORK ORIGINALLY PROPOSED</b>	<b>5</b>
<b>II. EXPERIMENTAL WORK</b>	<b>6</b>
Fluids Used	6
Experimental Apparatus and Procedure	6
Experimental Results	10
<b>III. SIGNIFICANCE AND ASSESSMENT OF EXPERIMENTAL RESULTS</b>	<b>13</b>
Significance of What Has Been Experimentally Observed	13
Assessment of Experimental Limitations	19
<b>IV. COMPUTER MODELING: COMPARISON OF FOUR FLOW REGIME MODES</b>	<b>20</b>
Summary of Computer Modeling of Existing Flow Regime Maps	37
<b>V. COMPARISON OF LAB RESULTS WITH THE FOUR FLOW REGIME MAPS</b>	<b>37</b>
Dukler-Taitel Horizontal Flow Regime Map	37
Weisman Horizontal Flow Regime Map	50
Dukler-Taitel Vertical Flow Regime Map	50
Weisman Vertical Flow Regime Map	64
<b>VI. COMMENTARY ON FLOW REGIME MAPS</b>	<b>64</b>
The Weisman Map (Vertical and Horizontal)	64
The Dukler-Taitel Horizontal Flow Regime Map	72
The Dukler-Taitel Vertical Flow Regime Map	72
<b>VII. ANALYTICAL WORK</b>	<b>73</b>
<b>VIII. CONCLUSIONS</b>	<b>76</b>
References	77
Appendix A - Entrainment Analysis	78
Appendix B - Laboratory Data	82

# TABLE OF FIGURES

	PAGE
FIGURE 1 Laboratory Apparatus	8
FIGURE 2 Entrance Geometries	9
FIGURE 3 Flow Regime Definitions	11
FIGURE 4 Observed Flow Regimes: Labdata 1	12
FIGURE 5 Observed Flow Regimes: Labdata 2	14
FIGURE 6 Observed Flow Regimes: Labdata 3	15
FIGURE 7 Observed Flow Regimes: Labdata 4	16
FIGURE 8 Observed Flow Regimes: Labdata 5	17
FIGURE 9 Observed Flow Regimes: Labdata 6	18
FIGURE 10 Dukler-Taitel Horizontal Flow Regimes (Freon 11)	22
FIGURE 11 Weisman Horizontal Flow Regimes (Freon 11)	23
FIGURE 12 Weisman Horizontal Map (log G vs. log X)	24
FIGURE 13 Dukler-Taitel Vertical Map (Freon 11)	25
FIGURE 14 Weisman Vertical Map (Freon 11)	26
FIGURE 15 Weisman Vertical Map (log G vs log X)	27
FIGURE 16 Dukler Taitel Horizontal (with iso-G and iso-X lines)	29
FIGURE 17 Weisman Horizontal (with iso- $J_f$ and iso $J_g$ lines)	30
FIGURE 18 Dukler-Taitel Horizontal (0.1-G)	31
FIGURE 19 Dukler-Taitel Horizontal (0.01-G)	32
FIGURE 20 Dukler-Taitel Horizontal (0.001-G)	33
FIGURE 21 Weisman Horizontal (0.1-G)	34
FIGURE 22 Weisman Horizontal (0.01-G)	35
FIGURE 23 Weisman Horizontal (0.001-G)	36
FIGURE 24 Dukler-Taitel Vertical (0.1-G)	38
FIGURE 25 Dukler-Taitel Vertical (0.01-G)	39
FIGURE 26 Dukler-Taitel Vertical (0.001-G)	40
FIGURE 27 Weisman Vertical (0.1-G)	41
FIGURE 28 Weisman Vertical (0.01-G)	42
FIGURE 29 Weisman Vertical (0.001-G)	43
FIGURE 30 Labdata 1 Compared to Dukler-Taitel Horizontal Predictions	44
FIGURE 31 Labdata 2 Compared to Dukler-Taitel Horizontal Predictions	45
FIGURE 32 Labdata 3 Compared to Dukler-Taitel Horizontal Predictions	46
FIGURE 33 Labdata 4 Compared to Dukler-Taitel Horizontal Predictions	47
FIGURE 34 Labdata 5 Compared to Dukler-Taitel Horizontal Predictions	48
FIGURE 35 Labdata 6 Compared to Dukler-Taitel Horizontal Predictions	49
FIGURE 36 Weisman Horizontal Labdata 1 Compressed on G vs X plot	51
FIGURE 37 Labdata 1 Compared to Weisman Horizontal Predictions	52
FIGURE 38 Labdata 2 Compared to Weisman Horizontal Predictions	53

# TABLE OF FIGURES (CONTINUED)

	PAGE
FIGURE 39 Labdata 3 Compared to Weisman Horizontal Predictions	54
FIGURE 40 Labdata 4 Compared to Weisman Horizontal Predictions	55
FIGURE 41 Labdata 5 Compared to Weisman Horizontal Predictions	56
FIGURE 42 Labdata 6 Compared to Weisman Horizontal Predictions	57
FIGURE 43 Labdata 1 Compared to Dukler-Taitel Vertical Predictions	58
FIGURE 44 Labdata 2 Compared to Dukler-Taitel Vertical Predictions	59
FIGURE 45 Labdata 3 Compared to Dukler-Taitel Vertical Predictions	60
FIGURE 46 Labdata 4 Compared to Dukler-Taitel Vertical Predictions	61
FIGURE 47 Labdata 5 Compared to Dukler-Taitel Vertical Predictions	62
FIGURE 48 Labdata 6 Compared to Dukler-Taitel Vertical Predictions	63
FIGURE 49 Weisman Vertical Flow Regime Map Predictions (G vs X)	65
FIGURE 50 Labdata 1 Compared to Weisman Vertical Predictions	66
FIGURE 51 Labdata 2 Compared to Weisman Vertical Predictions	67
FIGURE 52 Labdata 3 Compared to Weisman Vertical Predictions	68
FIGURE 53 Labdata 4 Compared to Weisman Vertical Predictions	69
FIGURE 54 Labdata 5 Compared to Weisman Vertical Predictions	70
FIGURE 55 Labdata 6 Compared to Weisman Vertical Predictions	71

# **LIQUID-VAPOR FLOW REGIME TRANSITIONS FOR USE IN DESIGN OF HEAT TRANSFER LOOPS IN SPACECRAFT**

**AN**

## **INVESTIGATION OF TWO PHASE FLOW IN ZERO GRAVITY CONDITIONS**

### **EXECUTIVE SUMMARY**

There is presently a fair understanding of flow regime behavior on earth (i.e., in a one-G gravity field). However, the Phase I work at low flow velocities just completed has shown:

a) The various existing models do not predict the same flow regime behavior at zero or minimal gravity for Freon-11, a common coolant.

b) The four models analyzed, Horizontal Dukler-Taitel, Vertical Dukler-Taitel, Vertical Weisman, and Horizontal Weisman, do not agree with the lab data collected. Regimes are predicted which do not appear to occur. Some of the observed regimes are not predicted at all.

c) Current flow regime models do not extrapolate well and are not valid in zero gravity conditions. Such flow regime maps apparently cannot be used for conditions far from their range of experimental verification. This was already concluded from our preliminary work.

The behavior of viscous (or low velocity) two-phase vapor-liquid flow under zero gravity was simulated in the laboratory with two immiscible fluids of equal density flowing together in a 0.025m (1") diameter pipe. Computer modeling was performed by extrapolating four current flow regime prediction schemes to almost zero gravity. The different model predictions were compared with each other by using the properties of Freon-11. These same four flow regime models were also tested against our own lab data. Based on the data, an analytical basis for the prediction of vapor-liquid flow regimes in zero gravity was initiated.

The chosen experimental fluids were water and polypropylene glycol (PPG) which has a molecular weight of about 2000. The results of the experiments showed that flow regimes such as inverse annular flow (i.e., the high viscosity fluid - the "liquid" - flowed in the core of the pipe, while the low viscosity fluid - the "vapor" - flowed at the pipe perimeter) was observed under a number of conditions. Furthermore, it was found that flow regime behavior in zero gravity is very sensitive to entrance conditions. This result was expected, since for horizontal flow, the gravity force is perpendicular to the flow direction and tends to stratify the flow. Thus, gravity minimizes the observed differences between varying entrance effects.

However, when gravity is eliminated, entrance geometries and effects become much more pronounced.

Additional findings of significance requiring verification for usefulness in spacecraft heat exchanger designs include:

(1) Flow regimes only occasionally observed on earth (i.e., inverse annular, inverse slug, and inverse churn) are likely to occur frequently in zero gravity. These regimes have not been previously studied very well. However, they have occurred in our zero gravity simulations of two-phase flow and need further study.

(2) Analytical work for zero gravity vapor-liquid flow regime prediction can be of use. Preliminary work has been conducted and reported herein. We suggest the use of three dimensionless groups, which include all the relevant parameters in zero gravity vapor-liquid flow, would be adequate.

In order to improve our understanding of zero-gravity two-phase flow the following work will be necessary in Phase 2 activity:

- a) varying entrance geometries and/or conditions (to more closely simulate real equipment).
- b) varying the viscosities of the fluids used.
- c) varying the surface tensions of the fluids used.
- d) study of entrainment and de-entrainment phenomena, in combination with zero gravity simulation, to accurately predict the point at which inverse annular flow occurs in a zero gravity vapor-liquid flow.

## OVERVIEW OF FINDINGS

### **SIGNIFICANCE OF PHASE I WORK FOR IMPROVING HEAT TRANSFER IN SPACECRAFT**

It is important to reduce both the weight and pumping power requirements of spacecraft heat transfer systems. A major advantage in weight and power reduction would be accomplished by the design of heat transfer equipment utilizing phase change (liquid to vapor and back to liquid) of such fluids as freon or ammonia. However, before such equipment can be designed reliably or optimally, a knowledge of pressure drop and heat transfer of such vapor-liquid systems is necessary. **Before pressure drop or heat transfer can be predicted confidently, a knowledge of flow regime behavior in zero gravity is mandatory.**

The present results give insights into the prediction of flow regime behavior in zero gravity. **First, the experiments performed suggest that certain flow regimes will readily occur in zero gravity which have not been often observed on earth.** One such flow regime is "Inverse Annular Flow" - liquid flows in the core of the pipe and vapor flows around the perimeter. When this behavior occurs in a heat transfer loop, boiling heat transfer is hindered. However, this flow regime would probably enhance condensation. The experiments also suggest that with proper choice of entrance conditions a designer can probably eliminate undesirable flow regimes and create desirable flow regimes to enhance heat transfer. **These results are significant because they offer the beginnings of guidance in designing effective heat transfer systems for spacecraft.**

**Second, both the experiments and computer modeling work show that four present widely accepted flow regime models cannot be extrapolated to zero or even minimal gravity.** None of the four models came even close to matching lab results. Regimes were predicted which did not occur or which occurred at significantly different flow rates. Other flow regimes occurred which were not predicted. All four flow regime models contradicted each other at minimal gravity and were only in fair agreement at normal gravity. None tolerated an input condition of zero gravity. Some seemed to contradict even themselves at minimal gravity. That is, their own flow regime boundaries over-lapped in ways that make it hard to know which flow regime was being predicted. **These results are all significant because they show that present models are inapplicable at zero gravity and cannot give any useful detail to designers of spacecraft heat transfer systems.**

By exploring these flow regime models we found that two of the existing semi-analytical models are based on physical behavior which does not occur in zero gravity (e.g., stratified flow, bubble rise velocity). Two other flow regime models appear to be simply curve fits with exponents and coefficients adjusted to correlate to some set of data. Thus, the apparent

inadequacies of these models is not surprising. The significance of this result is that simple modification of the existing models is not sufficient to predict flow regime behavior (and therefore heat transfer coefficients and pressure drops) in zero gravity conditions.

Analytical work started during the Phase I effort has also shown that three dimensionless quantities should be sufficient to describe flow regimes in zero gravity. Furthermore, the analysis and experiments point to de-entrainment mechanisms as a key to predicting inverse annular flow. Beyond this, some preliminary analysis based on physical behavior in zero gravity and upon simple, generally valid correlations shows some promise of predicting flow regime behavior at zero gravity. These results will help to create effective engineering tools for reliable and optimized vapor-liquid, zero gravity heat transfer designs.

## I. BACKGROUND AND OUTLINE OF PHASE I WORK ORIGINALLY PROPOSED WORK

There have been previous studies aimed at zero gravity flow regime behavior [1,2,4,5,6,7]. Some have been performed in drop towers. These experiments give a few seconds of zero gravity experimental run time. They are usually limited to studies of bubble growth during boiling. Other studies have been performed in parabolic looping aircraft. These studies yield 20-40 seconds of zero gravity per experimental run. They are valuable but very costly studies of condensation and boiling at zero gravity. Analytical studies of zero gravity behavior have also been performed. These studies may give useful insights to flow regime behavior in zero gravity. However, without a close tie-in to experimental work, two phase flow analysis can become speculative on the one hand or may totally miss important physical phenomena on the other hand.

To overcome the limitations of each of the above types of studies, the overall objectives of this project, as originally proposed, consisted of three parts:

- 1) Perform flow visualization experiments with water and an immiscible fluid of equal density. The purpose of these experiments was to explore what flow regimes exist under zero gravity conditions, especially at low flow velocities. The hypothesis is that at high speed flows, the flow regimes already observed on earth are very close to what will be observed in the absence of gravity, because for high speed flows, gravity is only a secondary effect (momentum, drag, etc. being primary effects). In fact, there is some support for this hypothesis in the literature of Sky Lab experiments [1]. However at low velocities, vapor-liquid flow regime behavior in zero gravity does not match behavior observed on earth. This was also found in the Sky Lab work. Therefore, liquid-liquid experiments with low speed flows, where inertial effects are less important, were proposed as a good simulation of zero gravity flow regime behavior.

- 2) Computerize several flow regime maps from the literature (original proposal was for a minimum of two flow regime maps) and compare their predictions at zero gravity. Also, to check how well these same flow regime models predicted the experimental results from above. If the mathematics of the maps did not permit gravity to be equated to zero, then a parametric study of predicted flow regimes was to be performed as the gravity term approached zero.

- 3) Begin new analysis for the prediction of zero gravity flow regime behavior. This analysis was to be based on the lab results and the evaluation of the numerical modeling done with the flow regime maps mentioned above.

As a result of our Phase I effort we were able to accomplish all three of the above goals. In fact, we have evaluated four flow regime models. In addition, we have demonstrated successfully that video taping of some of the flow visualization experiments is useful for the data analysis. Through video tape review, experiments can be observed repetitively, analyzed more affectively and shared usefully with other researchers.

## II. EXPERIMENTAL WORK

### Fluids Used

Experiments were done with polypropylene glycol (PPG) which has a molecular weight of 2000 and water to simulate liquid-vapor flow in zero gravity. The PPG has a specific gravity of 1.005. Therefore, buoyancy effects were virtually eliminated. Because of its high viscosity, (280 times that of water at room temperature), the PPG had been designated as the "liquid". Water had been designated as the "vapor" in these simulation experiments. The surface tension between these two liquids was approximately 62 dyne/cm according to the formula in Appendix A for calculating surface tension between any two liquids. The viscosity ratio and the surface tension between the two liquids were reasonably close to those of a liquid and vapor.

### Experimental Apparatus And Procedure

The experiments were performed in a 20 ft. long horizontal section of 1" ID glass tubing. Figure 1 shows the overall experimental arrangement. The entrance mixing section was varied during the course of the experiments in an attempt to eliminate or better understand the effect of entrance conditions. Figure 2 shows the four entrance geometries actually used. The flows of water and PPG were controlled by hand valves. The flow rates of each liquid were measured by rotameters. Both the water and the PPG were stored in holding tanks and pumped separately to the entrance section. Before running any experiment, the temperatures of both liquids were equalized. This procedure ensured that fluid properties would remain constant as they flowed through the visualization section. After flowing together through the 20 ft. flow visualization section, the two fluids were discharged into a separation tank.

The small density difference (1/2%) was usually enough to separate the two fluids if left overnight. However, at some of the higher flow rates, the PPG emulsified in the water, and overnight separation would not occur. In these cases, it was necessary to break the emulsion by essentially boiling off the water. Any recovery method (either settling or boiling of water) always resulted in the loss of some PPG (usually 10-20%).

The available stored quantity of PPG was the limiting factor in determining how many and with what frequency experiments could

be run. Observation time was limited according to how much PPG had been recovered and was stored. In the beginning, observation times were 5-10 minutes for each PPG/water flow setting. As experience was gained, many data points could be taken after 3-5 minutes of observation.

However, all of the phenomena could not be examined in sufficient detail due to the limited PPG supply. Therefore, at the suggestion of the University of New Hampshire (UNH), and with their help, we video-taped a few of the flow visualization runs and found the quality of filming to be well suited for review purposes. We also found that video-taping added to our ability to correctly, and in detail, observe explicit phenomena, analyze results, and share the experiments with other researchers. All data were taken with the Principal Investigator present, so as to assure consistent operation of the tests and accurate definition of flow regimes.

The involvement of Dr. Horst Richter, Professor of Engineering at Dartmouth College, a nationally recognized expert in two phase flow, as a senior consultant to the project, greatly enhanced our ability to evaluate the experimental results. The availability of the laboratory, computer and videotaping facilities of the nearby University of New Hampshire, a subcontractor added to the project as it evolved, made an important contribution to the success of our project. This was made possible by Dr. V.K. Mathur, Professor of Chemical Engineering at UNH, who also serves AETA as a Senior Consulting Associate.

FIGURE 1 LABORATORY APPARATUS

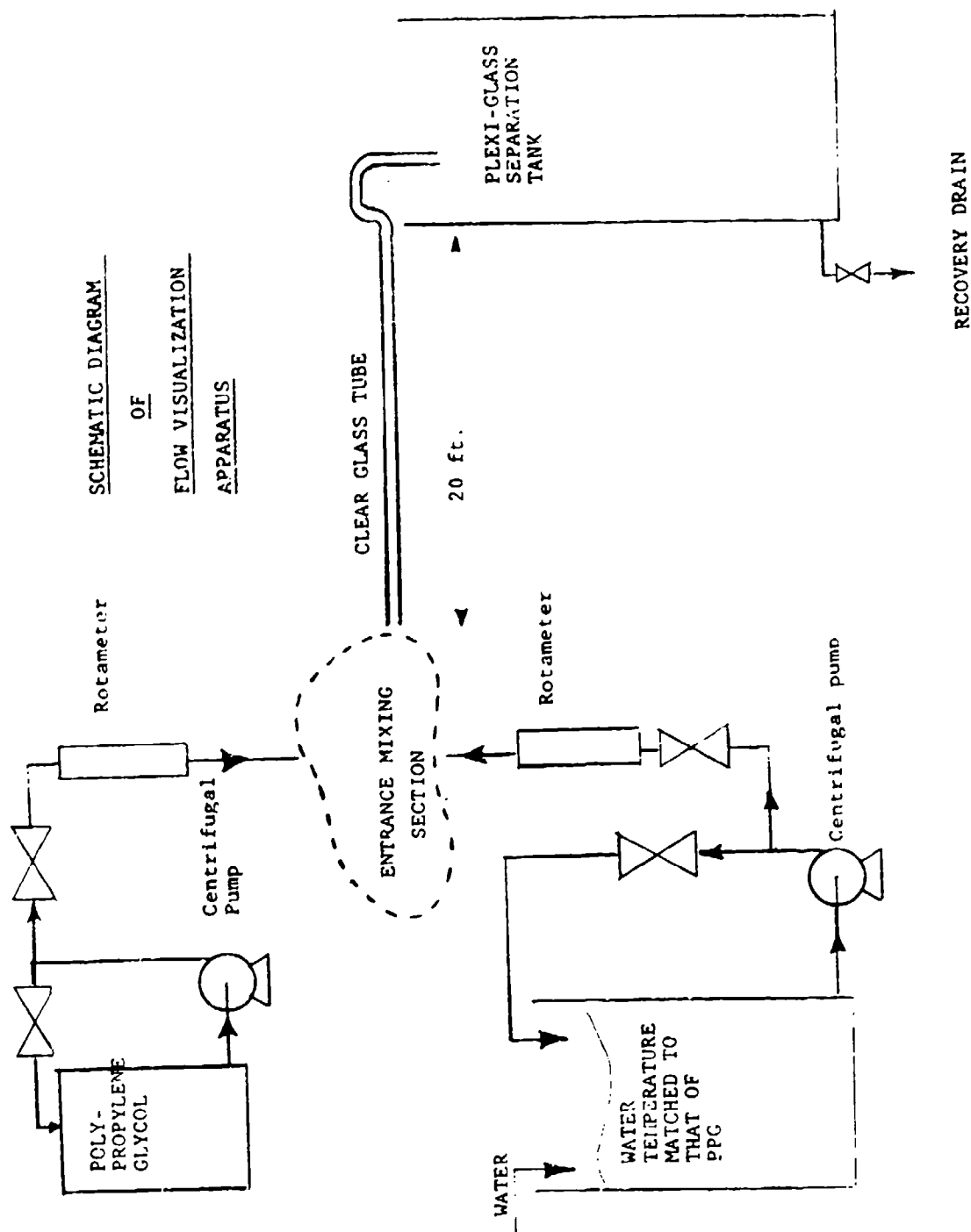
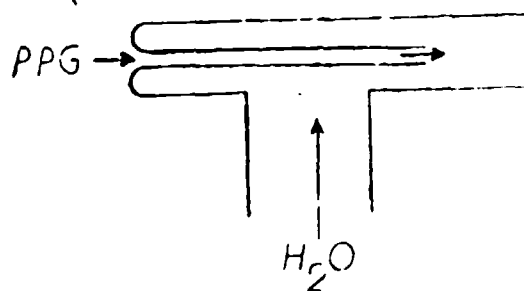
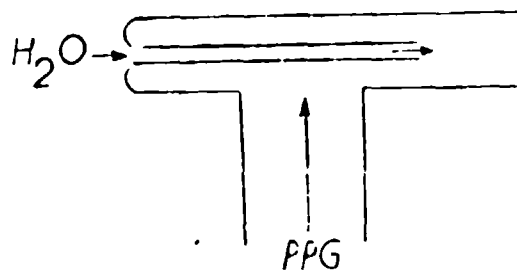


FIGURE 2 ENTRANCE GEOMETRIES

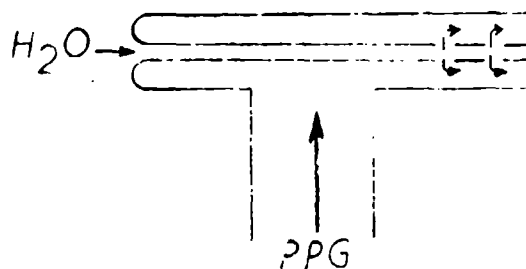
ENTRANCE CONDITIONS USED IN PHASE I EXPERIMENTS



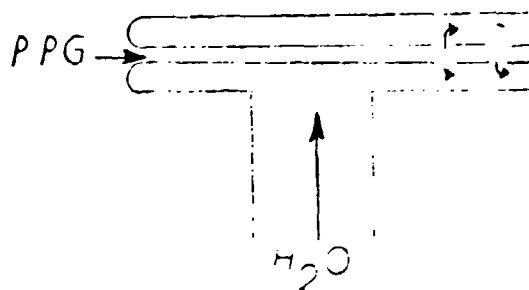
Used for LABDATA 1



Used for LABDATA 2



Used for LABDATA 3



Used for LABDATA 4,5,6

## Experimental Results

The observed flow regimes were classified according to the definitions presented in Figure 3. The flow regimes observed for each entrance condition are presented separately. That is, for each entrance condition studied, a low speed area of the flow regime map is presented. Since entrance effects were difficult to eliminate the data are presented on separate plots. However, as will be seen, entrance effects are not so dominant so as to totally change the observed flow regimes. Rather, entrance effects serve to shift the boundaries of the flow regimes.

Data are presented on log-log plots of superficial gas velocity ( $J_g$ ) versus superficial liquid velocity ( $J_f$ ). This is a way flow regime maps have been presented in the past, and it is an easy and straightforward way of presenting lab data. However, this plotting scheme is by no means general. There are too many factors (eg, viscosity, surface tension, density) left out of such plots to consider that  $J_g$  vs  $J_f$  could represent the observed flow regimes for any wide group of fluids or flow conditions.

Rather, the influencing factors are accounted for in a computer code and then output the predicted flow regimes on a  $J_g$  vs  $J_f$  map that is relevant only for the specific fluids and flow conditions under consideration. This is the same approach adopted by Dukler-Taitel [3,8] and Weisman [13]. Actually, Weisman chose to plot mass velocity ( $G$ ) versus quality ( $X$ ). However, this form is easily transposed to or from a  $J_g$  vs  $J_f$  plot. Some of the results were plotted on a  $G$  versus  $X$  plot. However, because the modeled vapor-liquid flows with liquid-liquid flows, the data points were somewhat compressed on a  $G$  vs.  $X$  plot. The  $J_f$  vs.  $J_g$  plot is more useful for the data presented here, as will be seen below. By choosing this simple form to present data, or computer predictions, results are easy to visualize. In the case of mathematical models for the flow regimes the computer handles the complexity of varying flow regime boundaries according to fluid properties, pipe diameter, pipe inclination, etc.

The following plots (Figs. 4-9) should be self-explanatory. They show observed flow regimes plotted against  $J_g$  and  $J_f$ . On each plot is a schematic diagram showing the entrance geometry. A key shows the flow regime indicated by the chosen symbols. The data from which these plots were generated is listed in Appendix B. Flow rates, Reynolds' Numbers, and some other calculated quantities of interest are also listed in Appendix B. A written description of the flow regimes observed is included for each data point.

**NOTE:** In all flow regime definitions, water is designated the "vapor" because its viscosity is much less than that of PPG.

**BUBBLE FLOW** - Water "bubbles" (i.e., drops) flow in a continuous flow of PPG.

**SLUG FLOW** - Bullet shaped bubbles of water of diameter almost equal to pipe, flow in a "train", separated by PPG.

**CHURN FLOW** - Water slugs become long (12 - 24"), chaotic, and very rough at PPG interface. Almost annular flow but PPG has small "bridges" across pipe diameter which interrupts the continuity of the water core.

**ANNULAR FLOW** - Continuous water core, PPG film (sometimes thick; sometimes thin) on perimeter. Almost always had some PPG drops in water core.

**DROP FLOW** - PPG flows in drops, within a continuous water flow which fills the pipe. The PPG drops were usually 1-10mm in diameter and spherical. Above this diameter (occasionally up to 2.5 cm), the PPG drops were usually quite irregular and began to coalesce to form PPG (i.e., "inverse") slugs. Some flow regimes classed as drop flow had a very thin PPG film on the pipe perimeter. But the film was so thin as to be negligible, not moving, or washed off in places.

**INVERSE SLUG FLOW** - Bullet shaped bubbles of PPG, diameter almost equal to pipe diameter, flow in a "train", separated by water flow. Sometimes water bubbles were entrained inside PPG slugs.

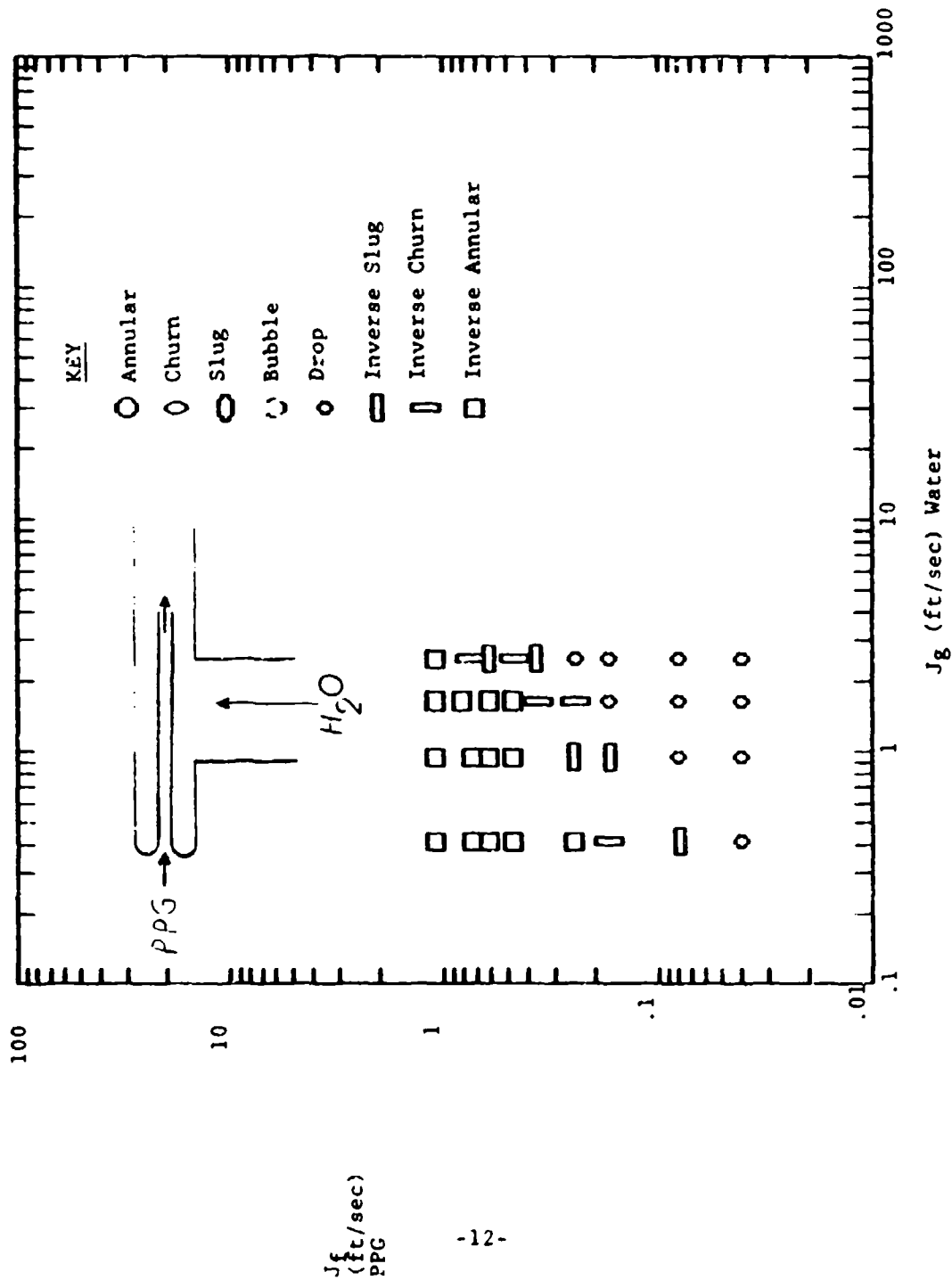
**INVERSE CHURN FLOW** - PPG slugs touched and because long (12-24") chaotic, and rough surfaced. Occasional water bridges across pipe diameter interrupted continuity of the core PPG flow.

**INVERSE ANNULAR FLOW** - Continuous PPG core, water flowed along pipe wall. Sometimes, but not always, some PPG drops also flowed in perimeter water.

FIGURE 3 FLOW REGIME DEFINITIONS

FIGURE 4

LABDATA 1  
Observed Flow Regimes: PPG-2000 and Water at 77°F



At first glance, Figs. 4-9 appear quite different. However, despite the changes caused by entrance conditions, a pattern of flow regimes emerges. In the lower right (high  $J_g$ , low  $J_f$ ), the **DROP** flow regime is evident. Moving diagonally upward to the left (decreasing  $J_g$  and increasing  $J_f$ ) the plots show a general move toward **INVERSE SLUG** flow, then **INVERSE CHURN** flow, then **INVERSE ANNULAR** flow.

The exact boundaries between flow regimes change with entrance conditions as described earlier. Normally, in one-G flow regime experiments the data would be presented with minimal or no entrance effects. However, entrance conditions that are often considered "standard" and "neutral", affected the flow regime boundaries. In fact, as Figures 8 and 9 show, at low flow rates, entrance geometry and the order in which the fluids are introduced both play an important role in determining the location of the flow regime boundaries. This fact alone suggests that in the absence of a "restoring" gravity force, the flow regime is very sensitive to entrance conditions. The gravity force tends to make observed flow regimes more uniform despite varying entrance conditions. Since we effectively eliminated the gravity (ie, buoyancy) force, any entrance condition will tend to have a significant effect on flow regime, even many pipe diameters downstream.

This result is not new. A number of studies have been performed which examine the effect of entrance conditions on two phase flow rates and flow regimes [Eqn. 10, p.338,340]. One conclusion of such studies has been that there is no such thing as "fully developed two phase flow". For example, with any significant pressure drop, the vapor phase is continuously expanding and, therefore, the flow is continually "developing".

### **III. SIGNIFICANCE AND ASSESSMENT OF EXPERIMENTAL RESULTS**

#### **Significance Of What Has Been Experimentally Observed**

The PPG/water experiments present a possible model of two phase (liquid-vapor) behavior in zero gravity. These experiments suggest that a number of significant phenomena may occur in zero gravity liquid-vapor flow. These observations and their significance for good design of heat transfer loops are listed below:

**Inverse Annular Flow** - This flow regime is defined as vapor flowing along the pipe wall and liquid flowing as a cylindrical core in the center of the pipe. It occurs for a variety of low - to - moderate vapor flow rates. In a boiling situation, this flow regime would hinder boiling and increase the risk of dry - out. It has already been observed in vertical boiling on earth [9]. The absence of gravity seemed to increase the likelihood of Inverse Annular Flow.

FIGURE 5 LABDATA 2  
Observed Flow Regimes: PPG - 2000 and WATER at 77°F

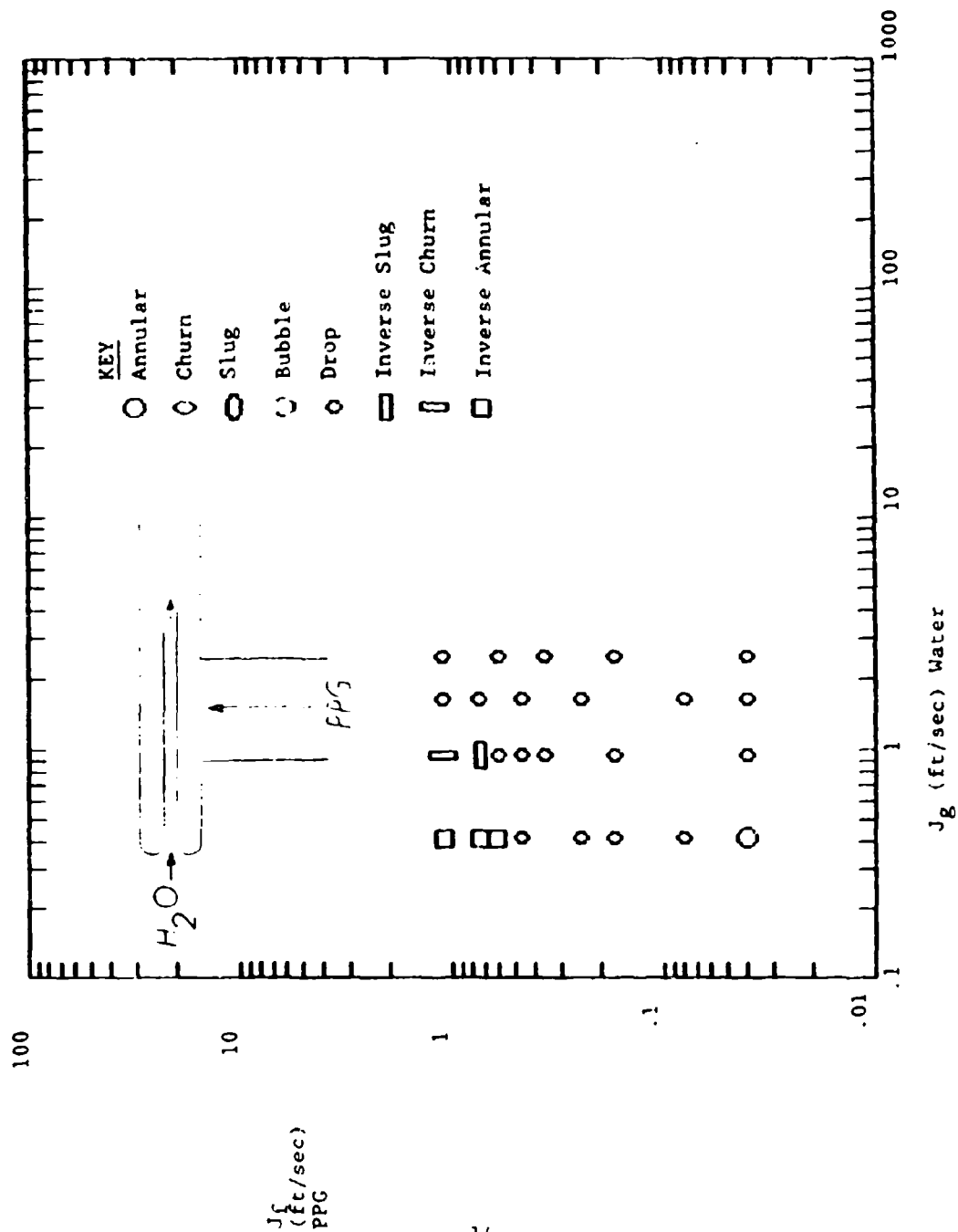


FIGURE 6 LABDATA 3  
Observed Flow Regimes: PPG - 2000 and WATER at 77°F

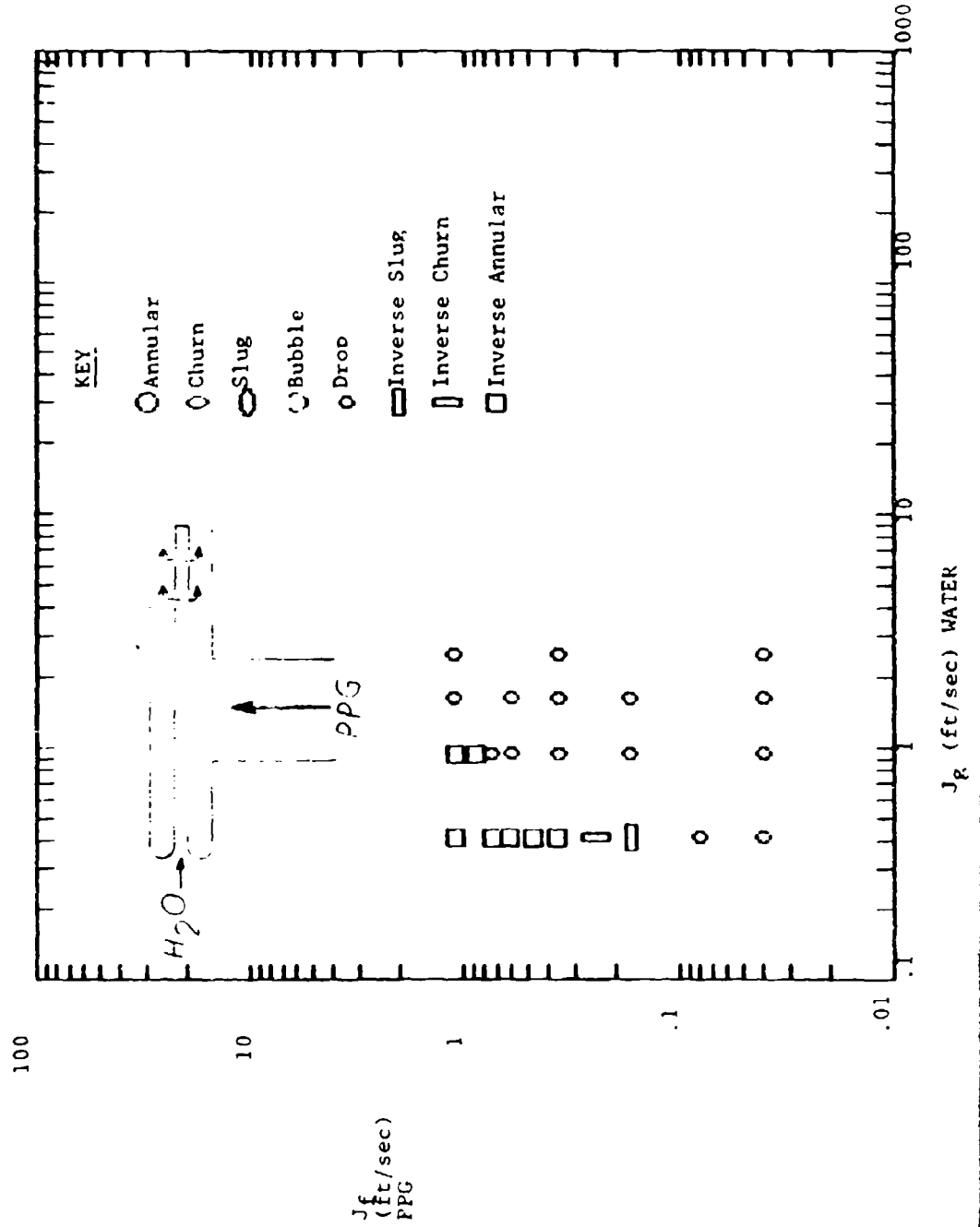


FIGURE 7 LABDATA 4  
Observed Flow Regimes: PPG-2000 and WATER at 77°F

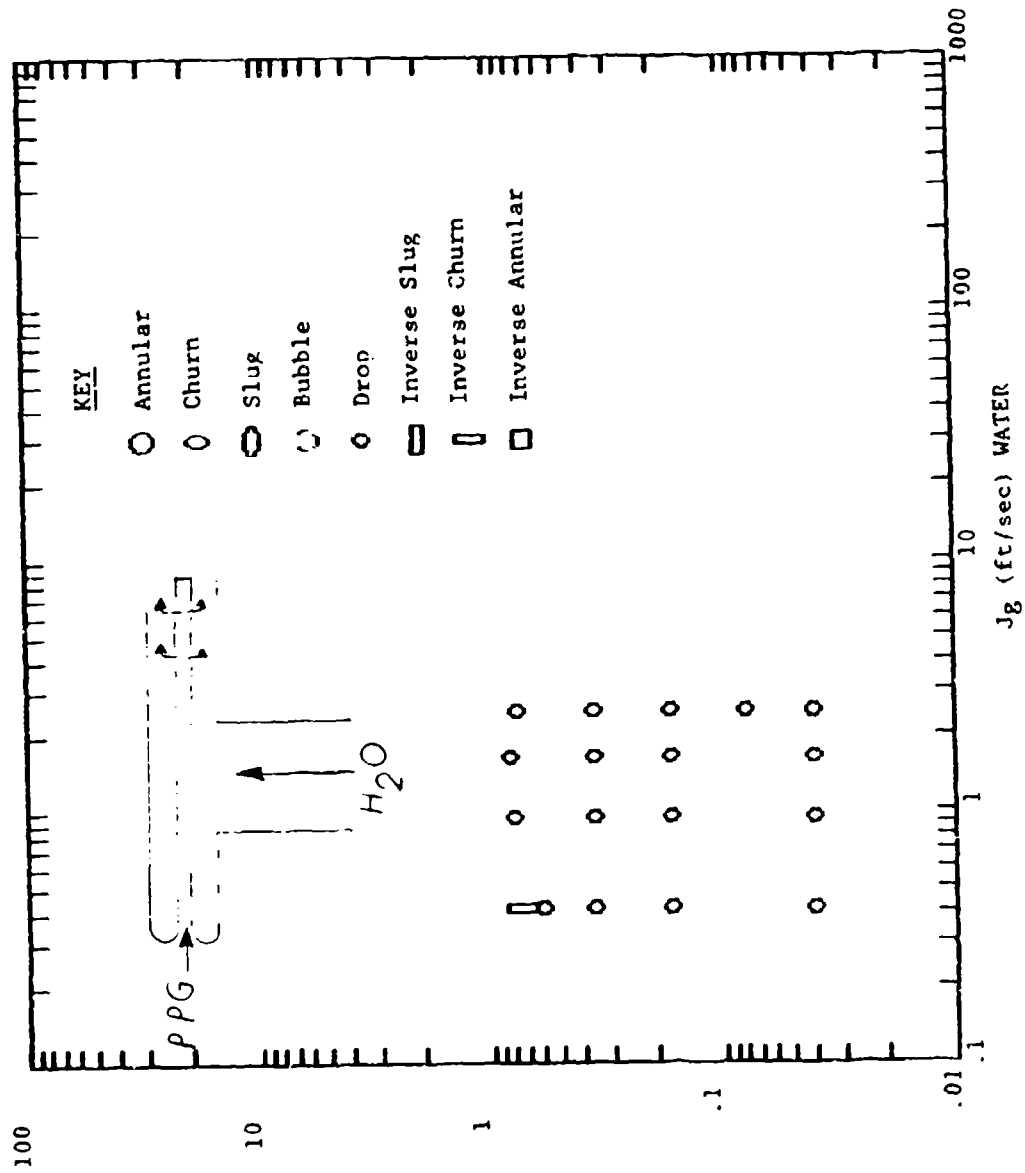


FIGURE 8 LABDATA 5  
Observed Flow Regimes: PPG-2000 and WATER at 77°F

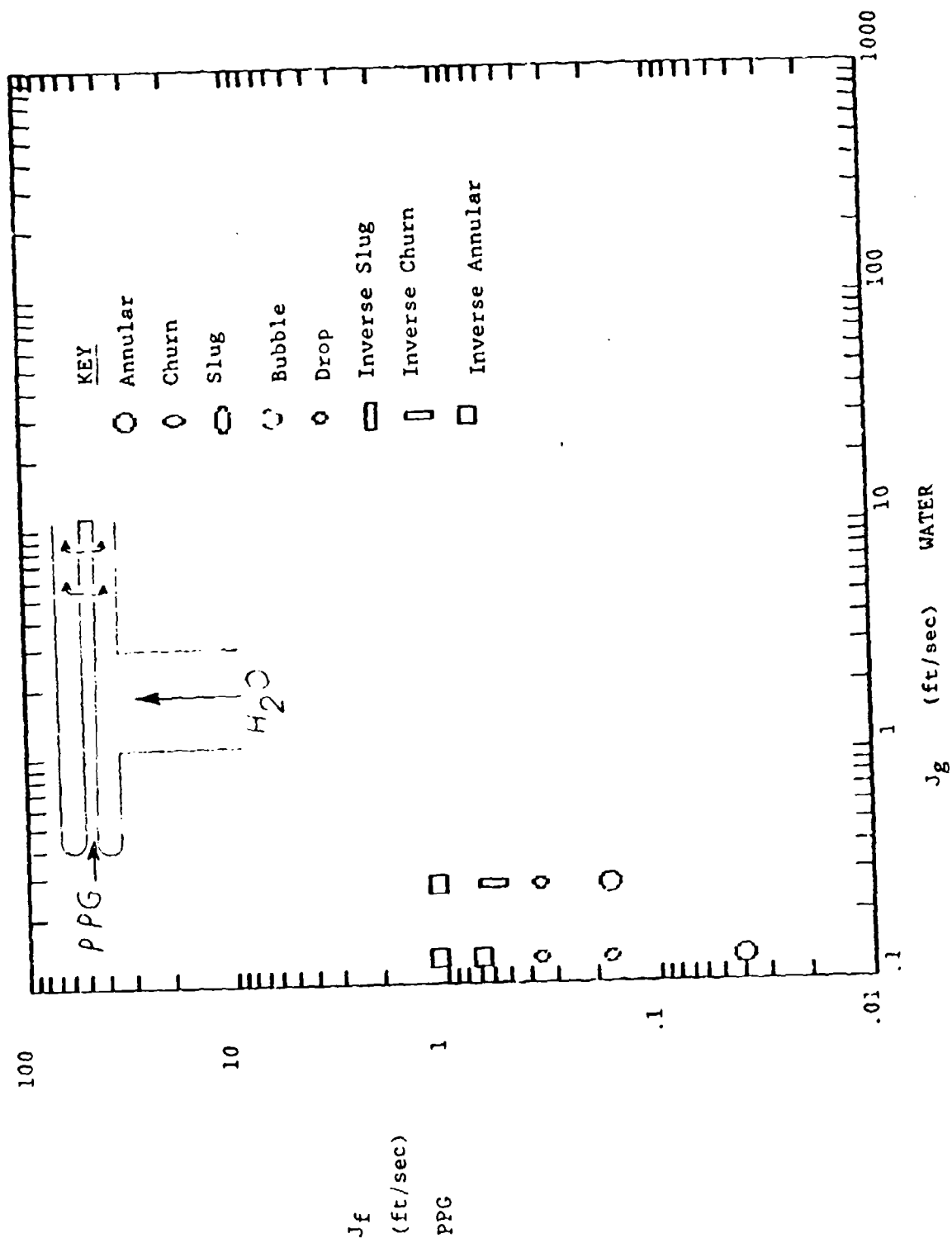
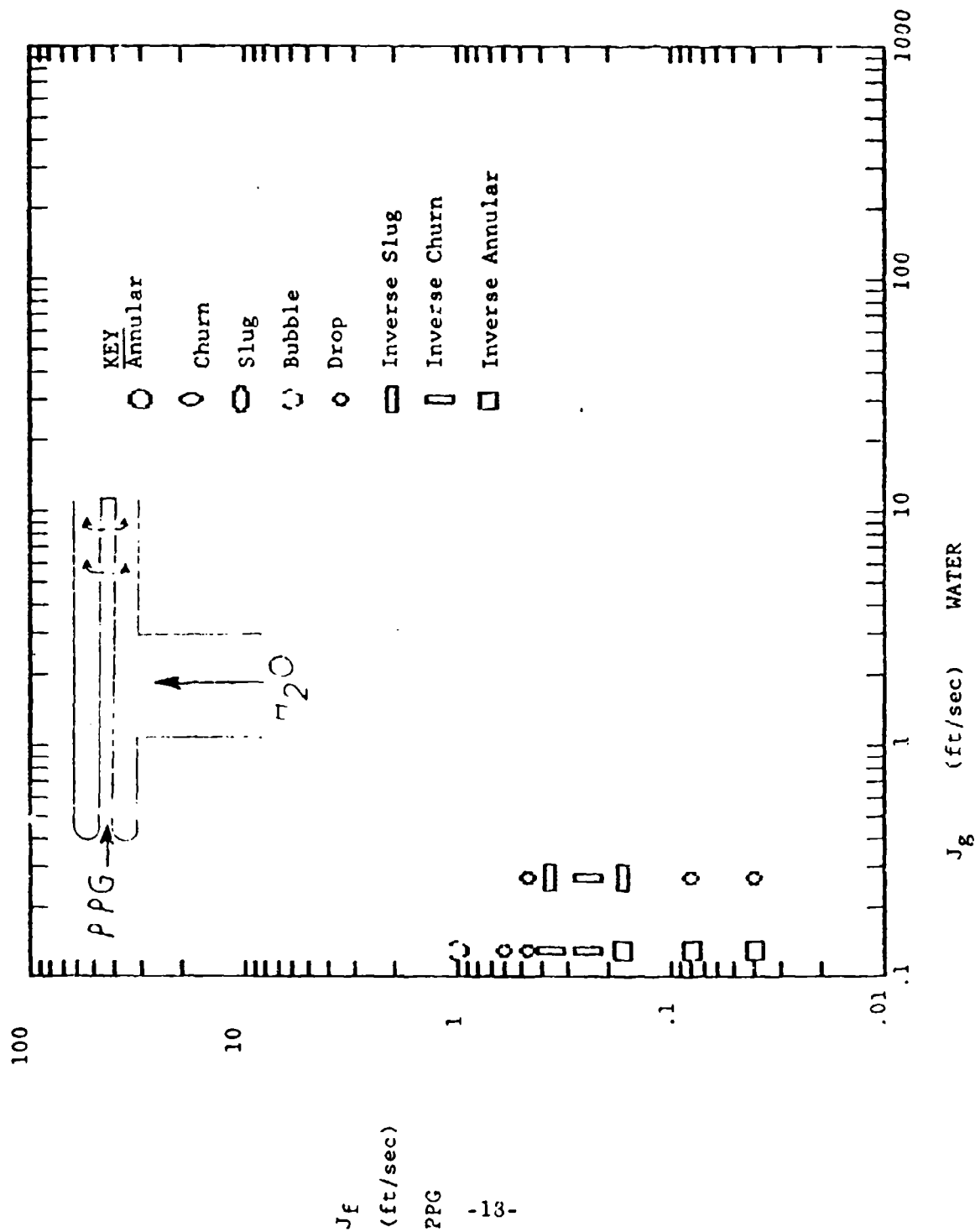


FIGURE 9 LABDATA 6  
Observed Flow Regimes: PPG - 2000 and WATER at 77°F



## **Entrance Effects -**

a) Entrance geometries have been found to be much more important than when gravity is present. Even at a distance of 240 pipe diameters, entrance conditions sometimes influence the flow regime. This observation implies that proper design of entrance geometry in heat exchangers and heat transfer loops would be a major control factor for producing desirable flow regimes.

b) The order of introducing fluids into the apparatus at low flow rates often causes a substantial difference in observed flow regimes. Again, without gravity flow regimes are quite sensitive to initial conditions. This point and the previous one are obviously closely related. Both suggest that an understanding of entrance conditions is an important factor leading to an ability to control flow regimes by proper equipment design. Both observations also suggest that, as is often the case with two phase flow, "transient" effects can be dominant over the full length of pipes.

**Slug and Churn Flows** - As expected, these intermittent flow regimes were observed. Some ideas were gained as to when they occur and under what conditions they can be avoided. Entrance conditions play an important role here as well. Proper choice of entrance geometry may be a powerful and inexpensive way of controlling these flow regimes.

**Liquid Film on Pipe Perimeter** - This thin film, technically annular flow, sometimes occurs and is sometimes washed away. The experiments have tentatively suggested that under high enough vapor flow rates, the liquid film may be washed from the wall. Such a result would hinder boiling, but probably enhance condensation.

## **Assessment of Experimental Limitations**

The validity of the present results can be divided into three categories:

1) Entrance effects are very significant and perhaps critically important. To categorize them, further work is needed and may well necessitate simulating the expected entrance conditions found in typical spacecraft heat transfer loops.

2) The very basis for "eliminating" gravity (by choosing two liquids of equal density) creates a problem in that the two fluids, if not in annular or inverse annular flow, have very similar inertia. For example, with drop flow, the de-entrainment mechanism is minimal. With de-entrainment eliminated, inverse annular flow probably appears earlier than it would otherwise. That is, a core of water flow is overloaded with PPG drops, which do not de-entrain. The PPG drops, being of equal

inertia with the water, follow every twist and turn of the water flow - centrifugal force is virtually eliminated - and are never re-deposited on the wavy annular film from which they were stripped. The water core becomes more and more overloaded until the PPG drops coalesce, first as "Inverse Slug" flow; then as "Inverse Churn" flow; then as a continuous core of PPG, in "inverse annular" flow. Inverse annular flow will generally occur in zero gravity, but not so readily as in the experiments we have performed.

3) The high viscosity of the PPG, although chosen in an attempt to match liquid-to-vapor viscosity ratio, keeps the liquid dominated by laminar effects. This is a problem in attempting to simulate actual fluid flows. It is virtually impossible to simulate all flow conditions and properties of any flow without actually running an experiment "in situ" with the exact fluids and conditions in question.

Experiments with other fluids of equal density are necessary. One such combination is water and PPG-400 which has a viscosity only 40 times that of water. Another possibility is water and a solution of two fluids, both immiscible in water, but whose solution has a density equal to that of water. The advantage of working with such a solution of fluids would be that surface tension and viscosity could be varied. This ability would help to gain a much better idea of how fluid properties affect flow regimes, while still under "zero gravity" conditions.

We do not expect there is a "perfect simulation". However, by studying the effect of property variation on flow regime, we would expect an analysis to predict (i.e., by more confident extrapolation) flow regimes under zero gravity. Additionally, with a wider data base there would be more confidence that the analysis had included all relevant physical phenomena.

#### IV. COMPUTER MODELING: COMPARISON OF FOUR FLOW REGIME MODELS

Four flow regime models were computerized and compared:

- 1) Dukler-Taitel Horizontal Flow Regime Map
- 2) Dukler-Taitel Vertical Flow Regime Map
- 3) Weisman Horizontal Flow Regime Map
- 4) Weisman Vertical Flow Regime Map

The two Dukler-Taitel maps are semi-empirical attempts to predict flow regime. The flow regime boundaries are derived by various physical arguments which are based on many other experimental observations and results. Many of the results taken from other investigators are empirical correlations. However, with various physical arguments, Dukler-Taitel have attempted to synthesize valid, somewhat analytical co-current flow regime maps, one for vertical flows and one for horizontal flows. Both

maps were derived for non-zero gravity. The horizontal map allows for laminar flow, but it does not include any effect due to surface tension anywhere in the analysis. The vertical map does include the effect of surface tension, but does not allow for laminar flow. Both of these omissions suggest that the maps will be inappropriate for low speed zero gravity flows.

The Weisman maps appear to consist of pure correlations which do allow for surface tension, and appear to handle laminar flows. We have seen no physical arguments associated with any of the Weisman correlations. This fact makes further modification difficult. It also means that when the correlations give overlapping flow regimes, interpretation of results remains ambiguous.

The four flow regime maps are presented in Figures 10-15, for Freon - 11 at 25°C, saturation pressure, 1" ID horizontal tubes, and gravity = 32.17 ft/sec<sup>2</sup>. The Dukler-Taitel Maps are presented in the form of  $\log J_f$  vs.  $\log J_g$ , as is common. The Weisman Maps are presented first in their  $J_f$  vs.  $J_g$  form and then in their usual  $G$  vs  $X$  format. As stated earlier, for the set of experiments performed, the  $J_f$  vs  $J_g$  form is the better one to use.

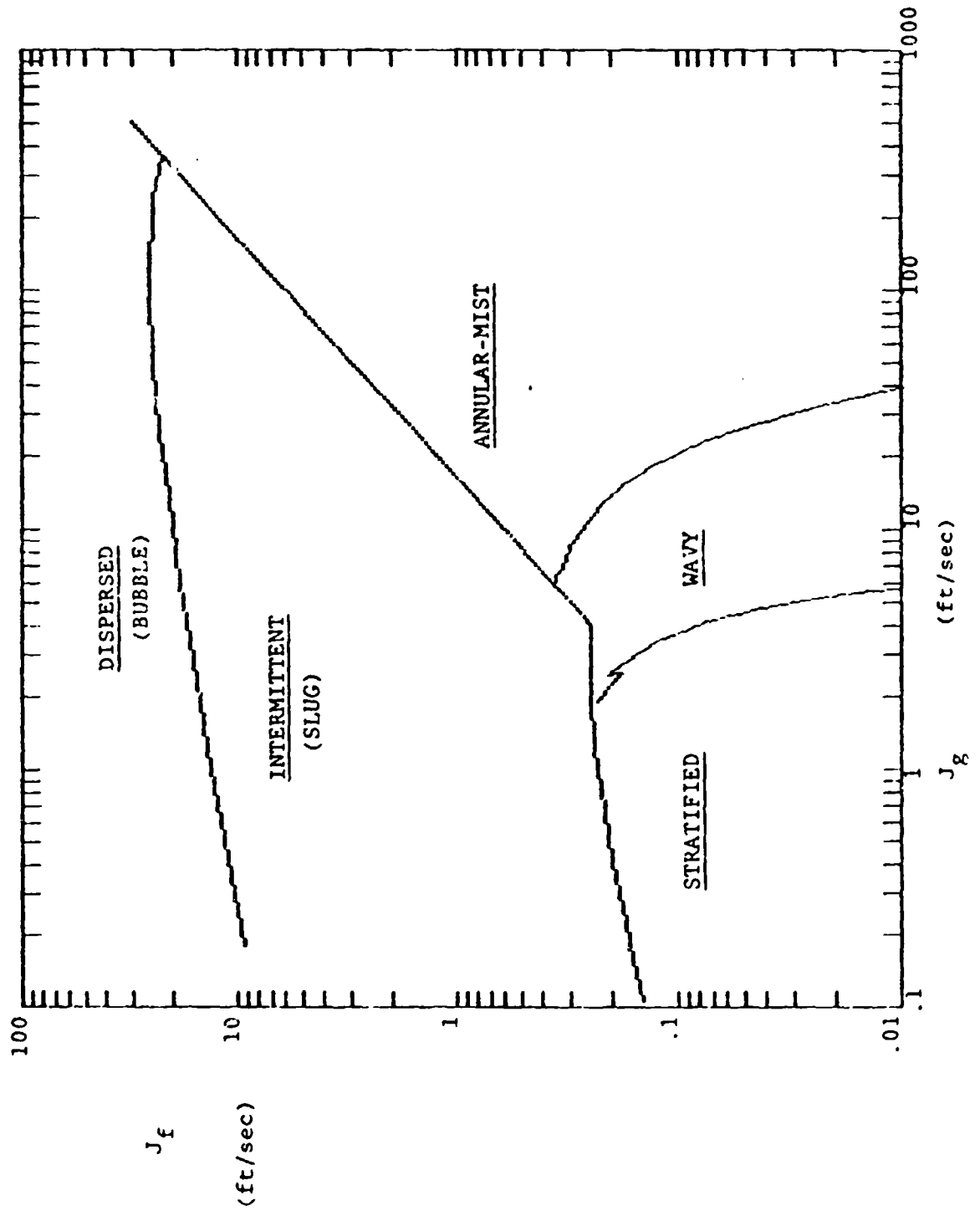
To help the reader to transpose more intuitively between these two co-ordinate systems, Figure 16 shows lines of constant mass flow and quality plotted on a  $\log J_f$  -  $\log J_g$  grid. Likewise Figure 17 shows lines of constant  $J_f$  and  $J_g$  plotted on a  $\log G$  -  $\log X$  grid.

A quick glance shows that the two horizontal maps and the two vertical maps roughly agree with each other. The same flow regimes are identified in roughly the same regions of the plots.

However closer inspection reveals little agreement between the maps. Note that the Weisman horizontal map has a negative slope on the boundary of the annular mist and slug flow regimes. The Dukler horizontal map has a positive slope. Note also the small size of Weisman's dispersed flow regime, and Dukler's larger size. Considering that these results show up easily on log-log plots, one must realize how significantly different these predictions really are. Similar observations can be made regarding the vertical flow regime maps. Dukler's annular boundary line is vertical, Weisman's is exactly the same line as on his horizontal map. The size, and extent of the dispersed region is different for each map. A significant disagreement is found where Dukler's vertical map predicts no bubbly flow at all (except finely dispersed bubbles), while the Weisman vertical map predicts both bubble flow and finely dispersed bubble flow. Again, on log-log plots, absolute differences are usually minimized. Here, however, a quick inspection reveals major differences in the absolute flow values for which various regimes will occur.

DUKLER-TAITEL Horizontal Flow Regime Map Predictions  
 for FREON-11, 25 C, Saturation Pressure  
 Vapor-Liquid Flow in 1" i.d. horizontal pipe  
 GRAVITY = 32.17 ft/sec/sec (1-G)

FIGURE 10



WEISMAN Horizontal Flow Regime Map Predictions  
for FREON-11, 25 C, Saturation Pressure  
Vapor-Liquid Flow in 1" i.d. horizontal pipe  
GRAVITY = 32.17 ft/sec/sec (1-G)

FIGURE 11

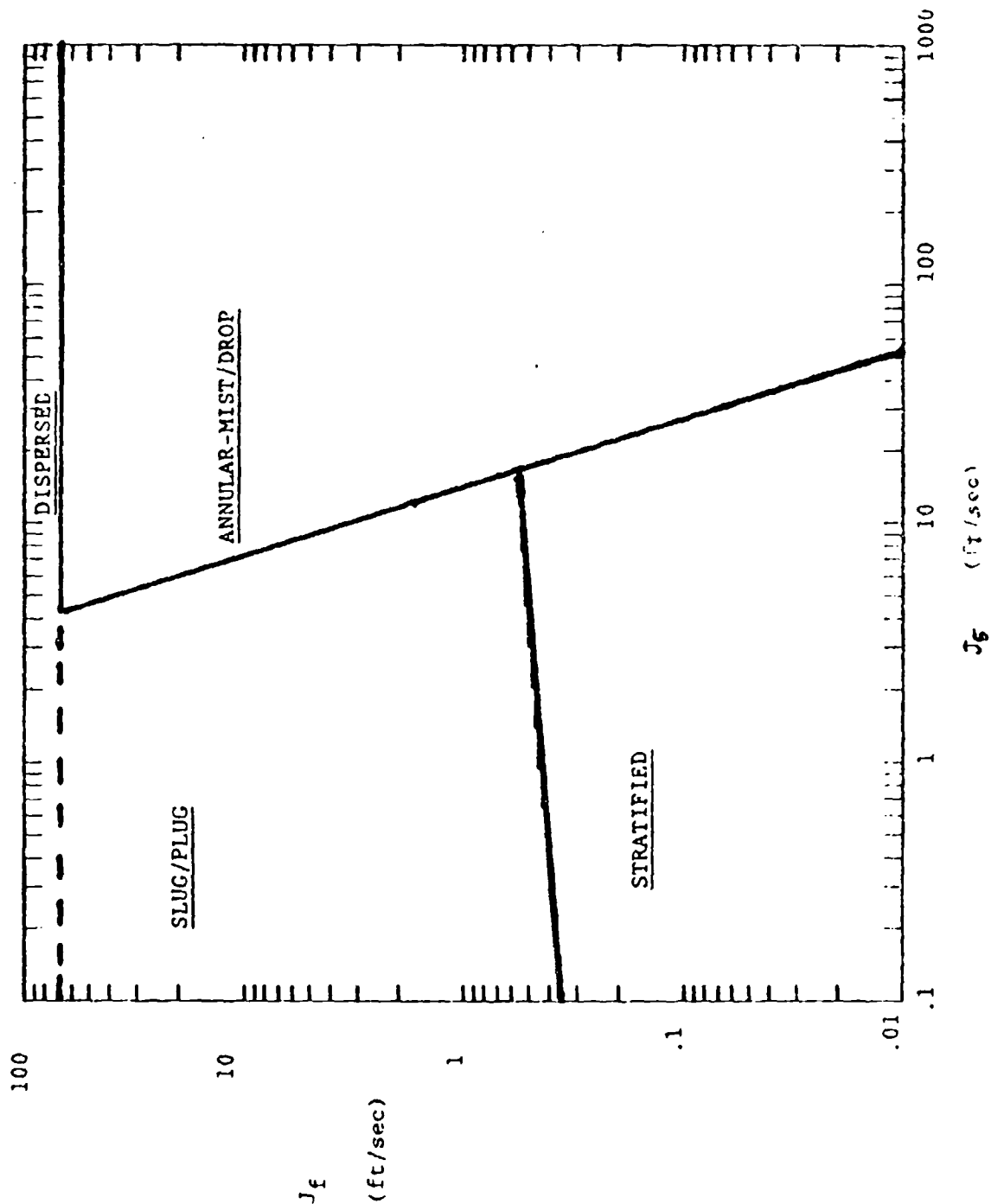
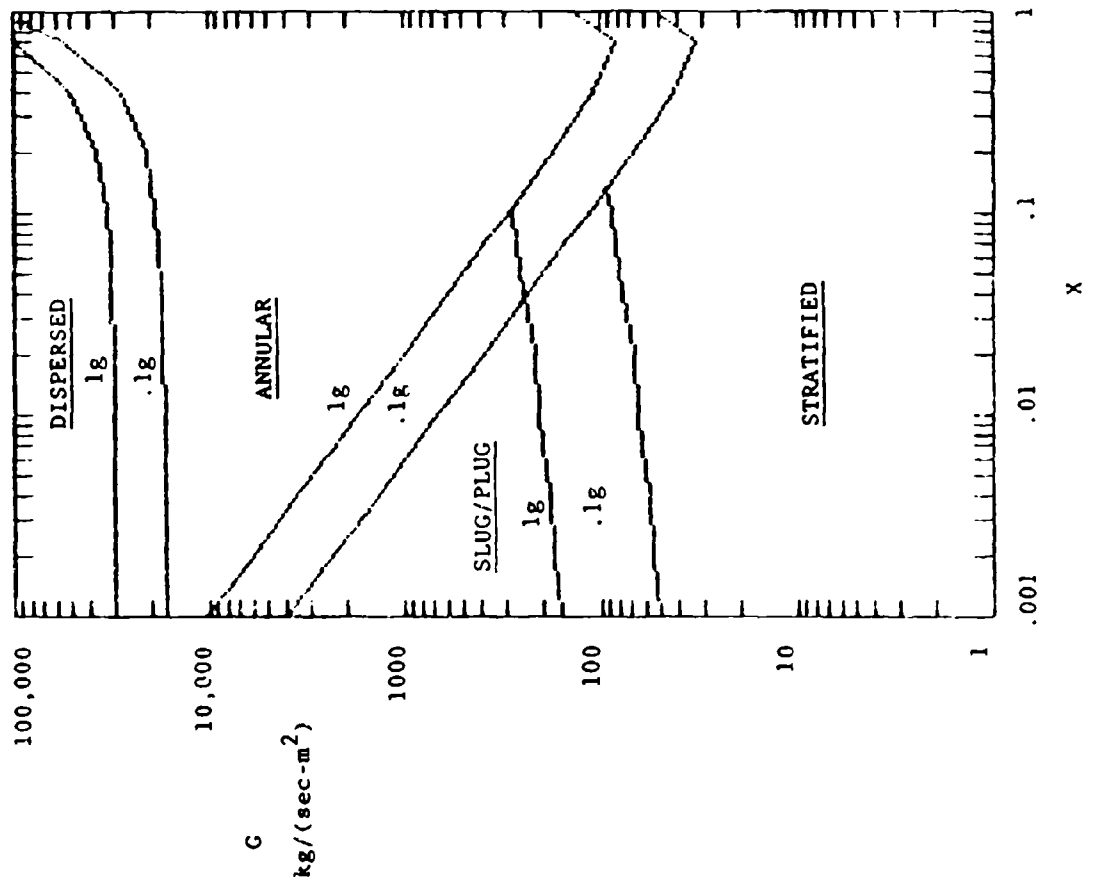


FIGURE 12

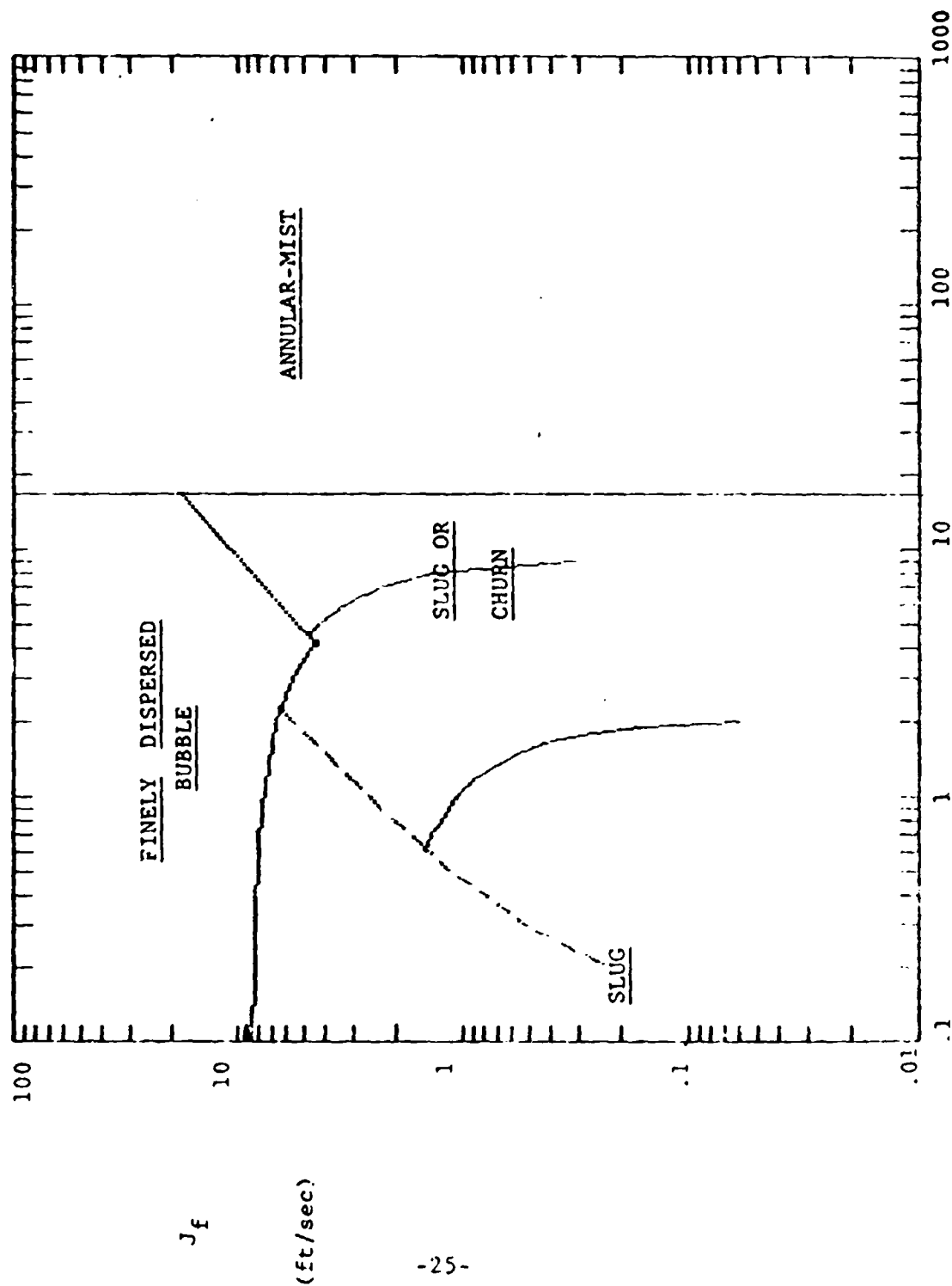


WEISMAN Horizontal  
Flow Regime Map Predictions  
for Freon 11 at 25°C, saturated  
pressure, 1" i.d. tube,  
horizontal orientation

Mass Velocity plotted against  
Quality (MKS units)

Change in predicted flow regime  
boundaries shown as gravity  $x$   
is reduced from  $1g$  ( $9.8 \text{ m/sec}^2$ )  
to  $.1g$  ( $.98 \text{ m/sec}^2$ )

DUKLER-TAITEL Vertical Flow Regime Map Predictions  
 for FREON-11, 25 C, Saturation Pressure  
 Vapor-Liquid Flow in 1" i.d. horizontal pipe  
 GRAVITY = 32.17 ft/sec/sec (1-G)



WEISMAN Vertical Flow Regime Map Predictions  
 for FREON-11, 25 C, Saturation Pressure  
 Vapor-Liquid Flow in 1" i.d. horizontal pipe  
 GRAVITY = 32.17 ft/sec/sec (1-G)

FIGURE 14

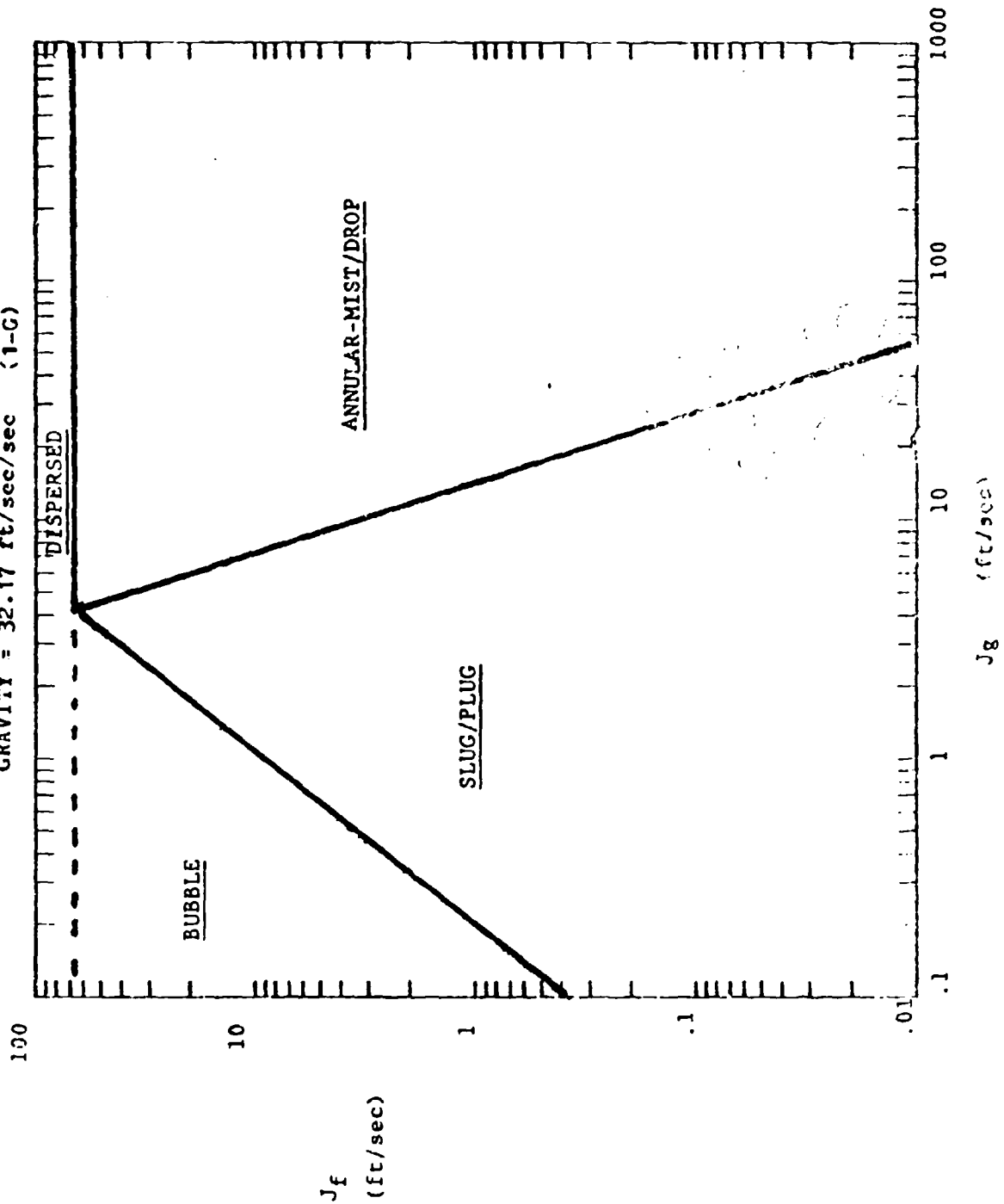
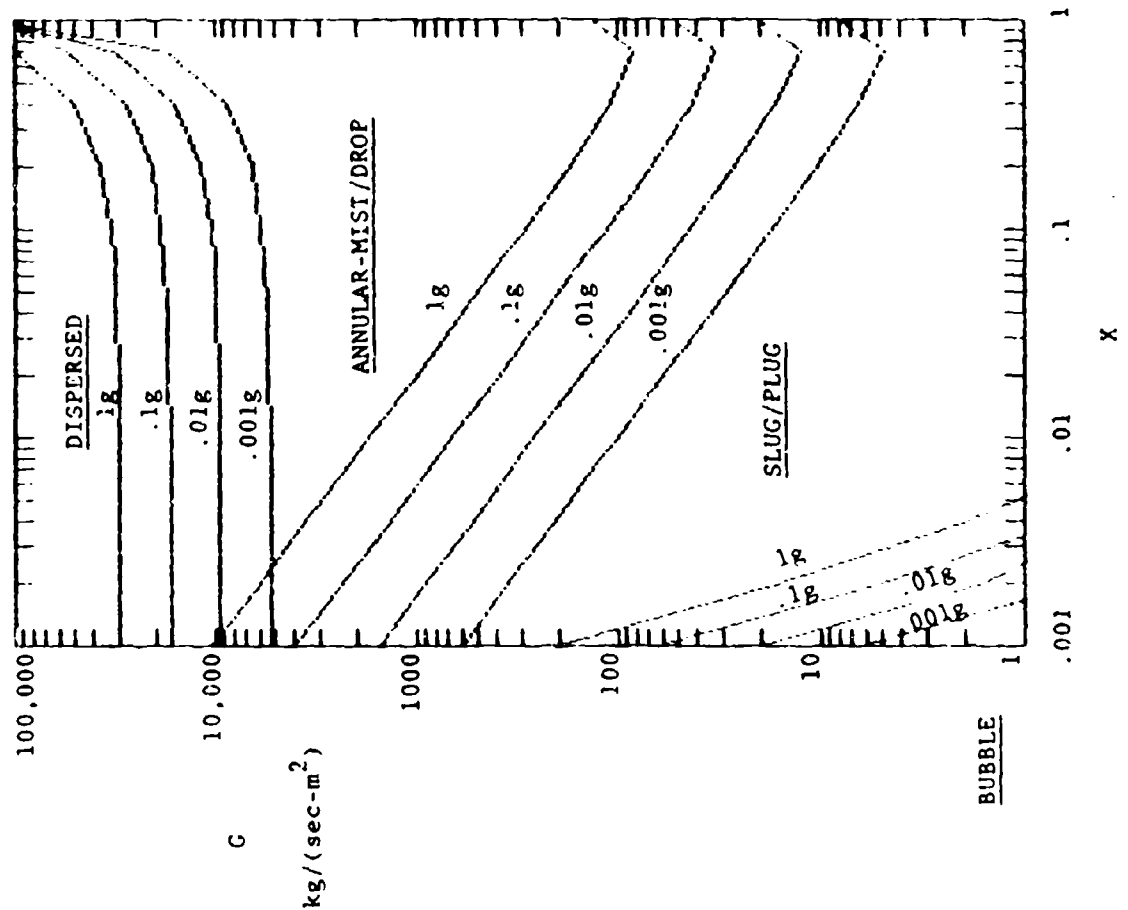


FIGURE 15



WEISMAN Vertical  
Flow Regime Map Predictions

Freon 11, 25° C., saturated  
pressure, 1" i.d. tubes,  
vertical orientation

Mass Velocity plotted against  
Quality (MKS units)

Change in predicted flow regime  
boundaries shown as gravity  
is reduced from:  
1g (9.8 m/sec<sup>2</sup>,  
to  
.1g (.98 m/sec<sup>2</sup>)  
to  
.01g (.098 m/sec<sup>2</sup>)  
to  
.001g (.0098 m/sec<sup>2</sup>)

Two conclusions can be drawn, since these conditions certainly seem similar to some of the most common data used. Investigators are either disagreeing on what flow regimes they observe or, these flow regime maps may not be generally valid, and have been chosen as approximations to a certain set of data.

The flow regime boundaries on the Weisman maps appear to be pure curve fits. Graphically, these curves plot to straight lines on  $\log J_f - \log J_g$  plots. Therefore, we conclude that the Weisman curves were created by drawing straight line boundaries through  $\log J_f - \log J_g$  data plots of flow regimes. This method is appropriate if the experimental data base is wide enough. Many functions plot to straight lines on log-log plots. However, if the data is limited, we have reservations about the generality of such a correlation scheme. This already raises some concern of the validity of extrapolation to what these maps predict for flow regimes in zero gravity. Unfortunately, none of these maps is based on a mathematics which can tolerate zero for a gravity term. The best that can be done is to reduce gravity to a small term and to compare the maps. We have chosen to reduce gravity successively in steps from 1-G to 0.1-G to 0.01-G to 0.001-G.

Figures 18-20 show the predictions of the Dukler-Taitel Horizontal map for Freon - 11 in a 1" i.d. horizontal tube as gravity is successively reduced from 1-G to 0.001-G. As might be expected, stratified and wavy flow move downward and "off" the log-log plot. The slug flow regime takes over where the stratified regime was predicted. The dispersed flow regime (i.e., finely dispersed bubbles) expands to include where slug flow regime existed. Other than that, the map maintains a logical (not necessarily accurate) picture of predicted flow regimes.

Figures 21-23 shows the Weisman horizontal map in  $\log J_f - \log J_g$  form as gravity is reduced from .1-G to .001-G. (The maps are still for Freon-11 under the same conditions as above - only the gravity term is changed). The basic trend occurs as in the Dukler map predictions. The stratified region disappears (taken over by the slug/plug regime) and the dispersed region gets larger on the map. However, when .001 - G is assumed there is no agreement between the Dukler and Weisman horizontal maps. Comparing Figure 23 (Weisman) to Figure 20 (Dukler) shows disagreement in the size, shape and extent of all three flow regimes regions predicted.

DUKLER-TAITEL Horizontal Flow Regime Map Predictions  
 for FREON-11, 25 C, Sat. Press., 1" i.d. horiz. tube  
 GRAVITY = 32.17 ft/sec/sec (1-G)  
 Lines of Constant MASS VELOCITY and QUALITY shown

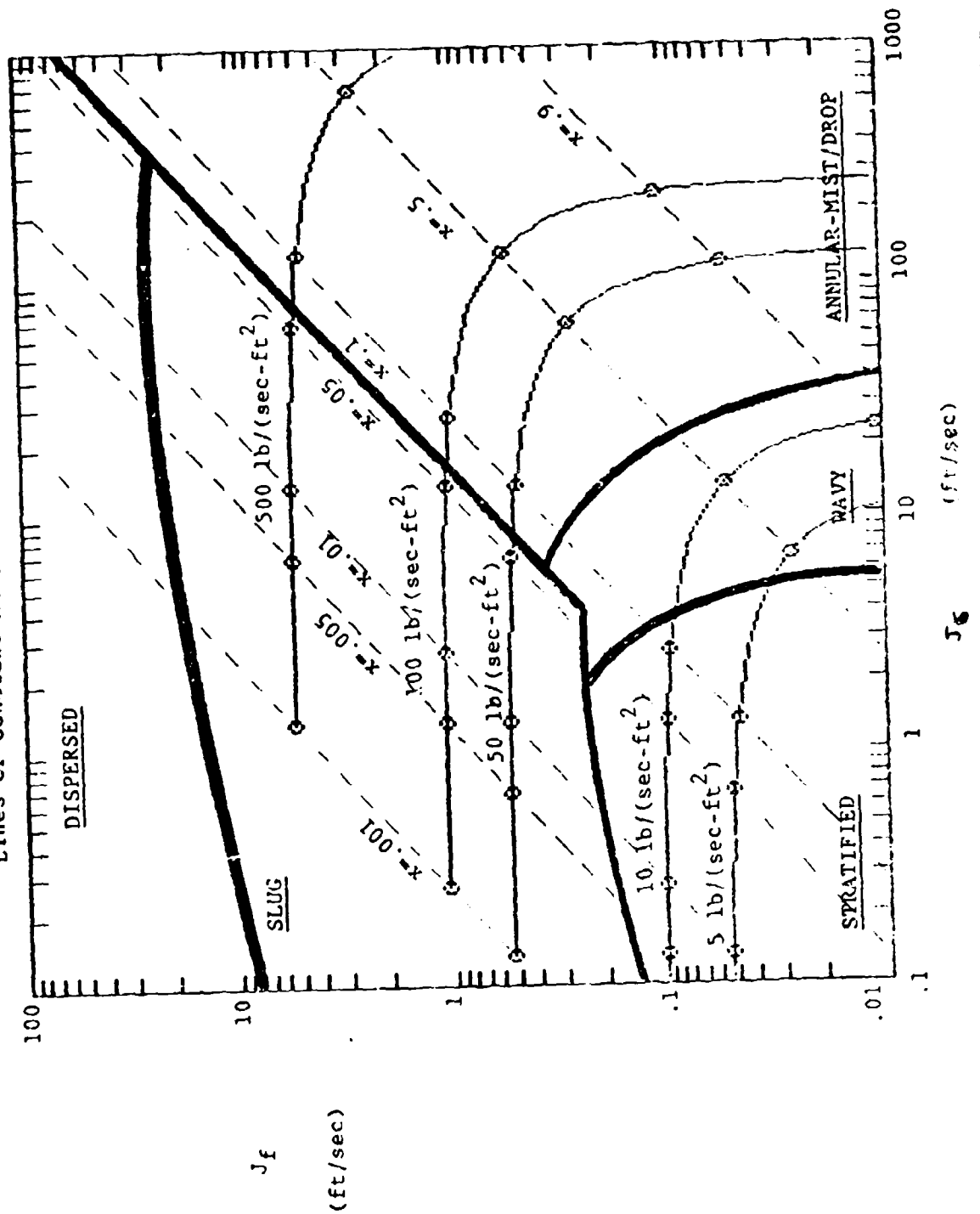
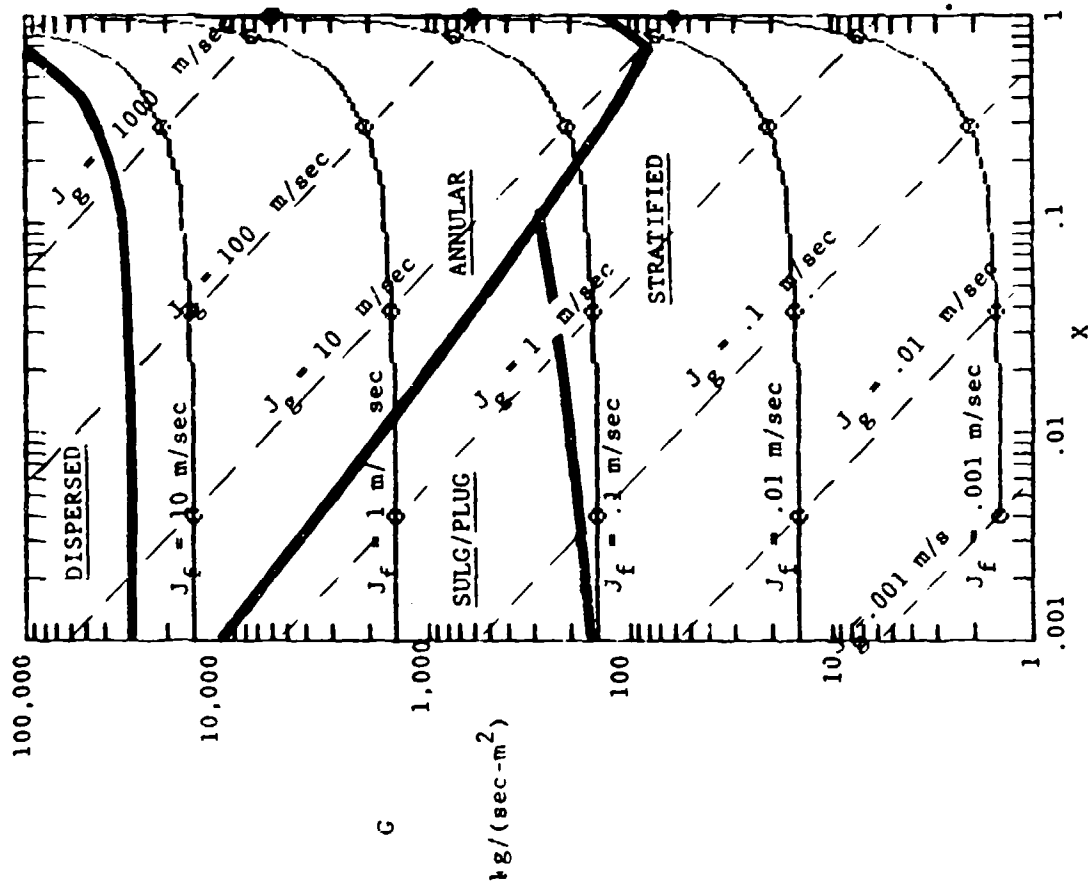


FIGURE 17



CHISMAN Horizontal  
Flow Regime Map Predictions  
for Freon 11 at 25°C, sat. pressure,  
1" i.d. horizontal tube

Mass Velocity vs Quality  
(MKS units)

Lines of constant  $J_f$  and  $J_g$  shown

DUKLER-TAITEL Horizontal Flow Regime Map Predictions  
 for FREON-11, 25 C, Saturation Pressure  
 Vapor-Liquid Flow in 1" i.d. horizontal pipe  
 GRAVITY = 3.217 ft/sec/sec (0.1-G)

FIGURE 1C

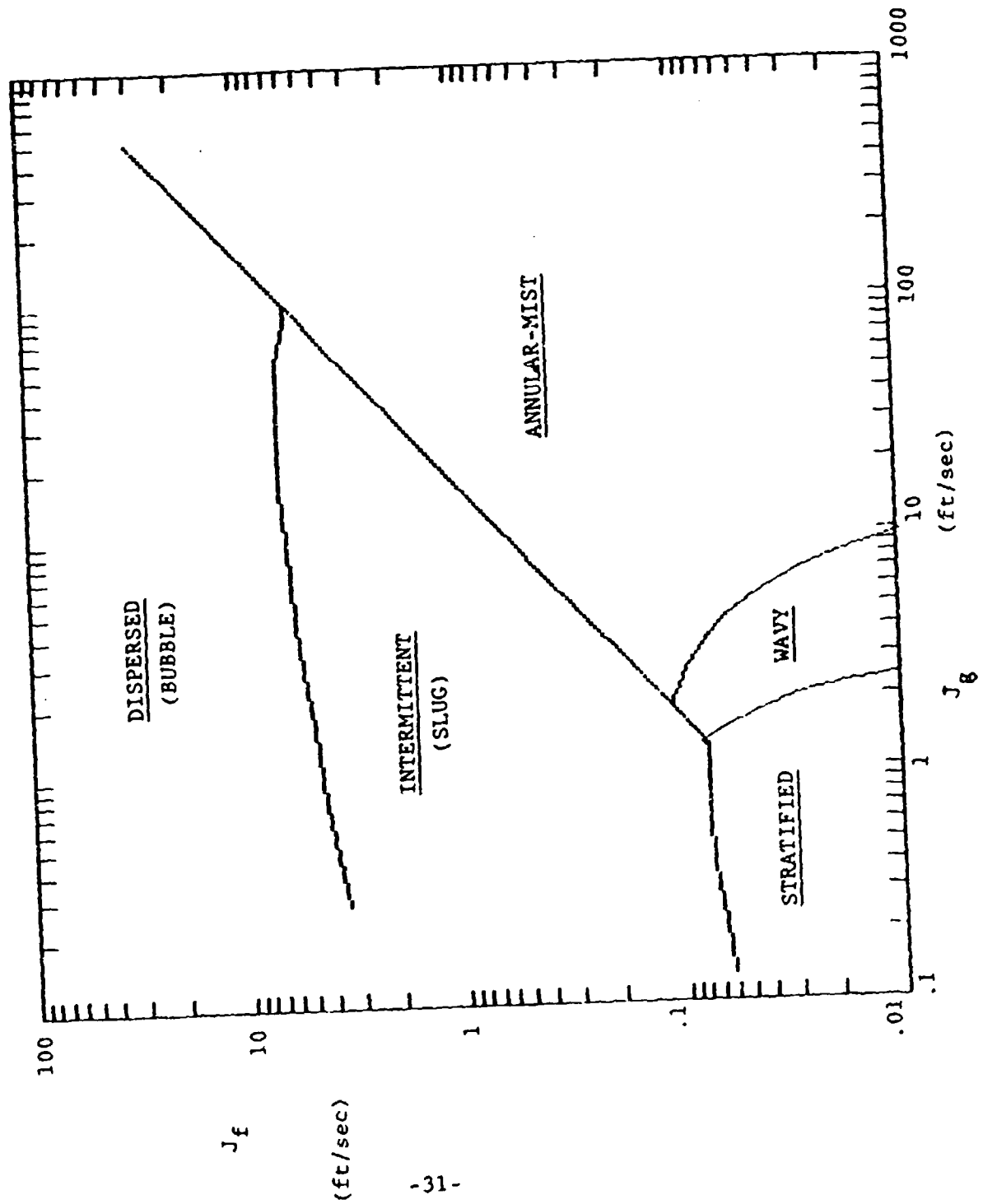
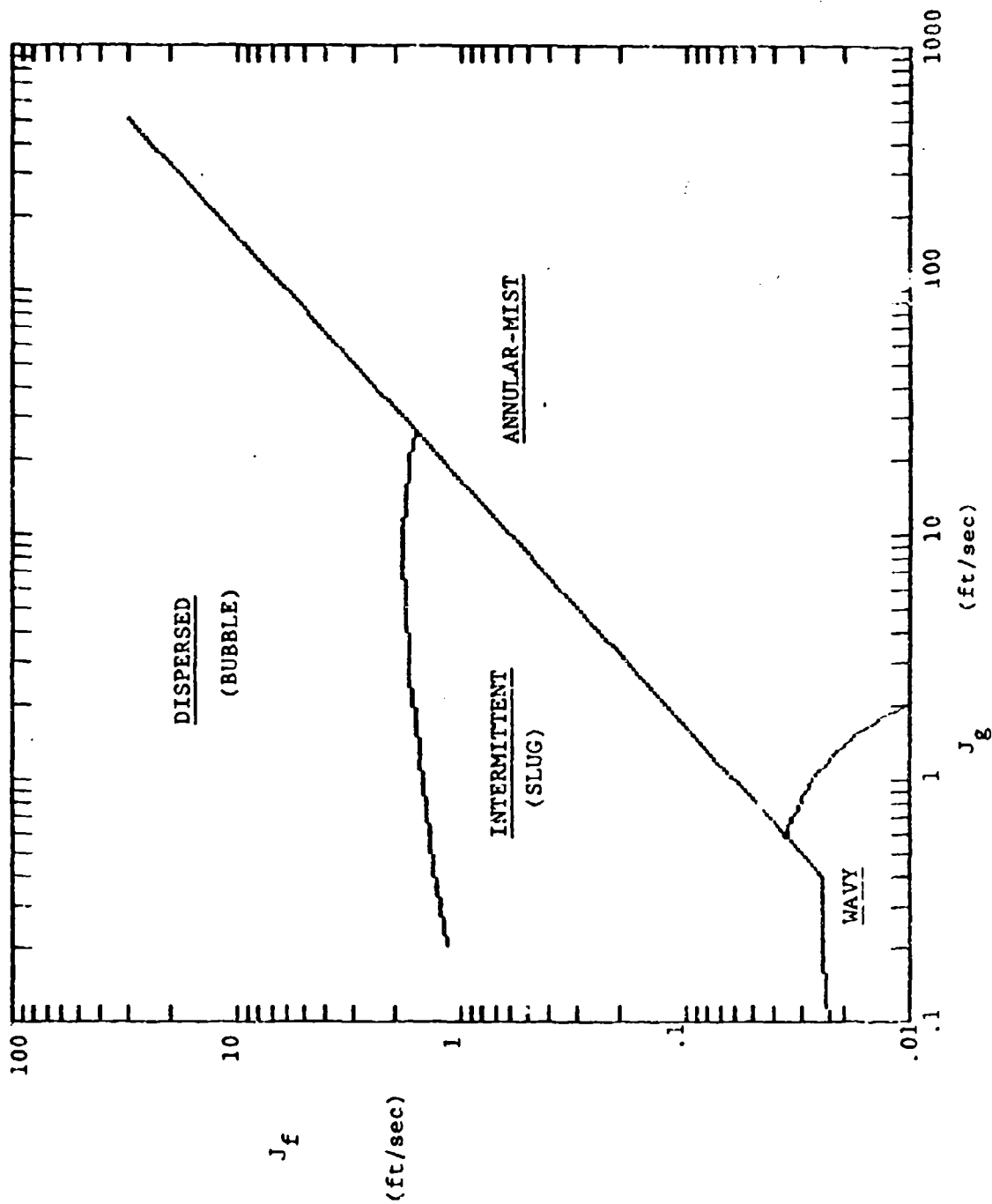


FIGURE 19

DUKLER-TAITEL Horizontal Flow Regime Map Predictions  
for FREON-11, 25 C, Saturation Pressure  
Vapor-Liquid Flow in 1" i.d. horizontal pipe  
GRAVITY = .3217 ft/sec/sec (0.01-G)



DUKLER-TAITEL Horizontal Flow Regime Map Predictions  
 for FREON-11, 25 C, Saturation Pressure  
 Vapor-Liquid Flow in 1" i.d. horizontal pipe  
 GRAVITY = .03217 ft/sec/sec (0.001-G)

FIGURE 20

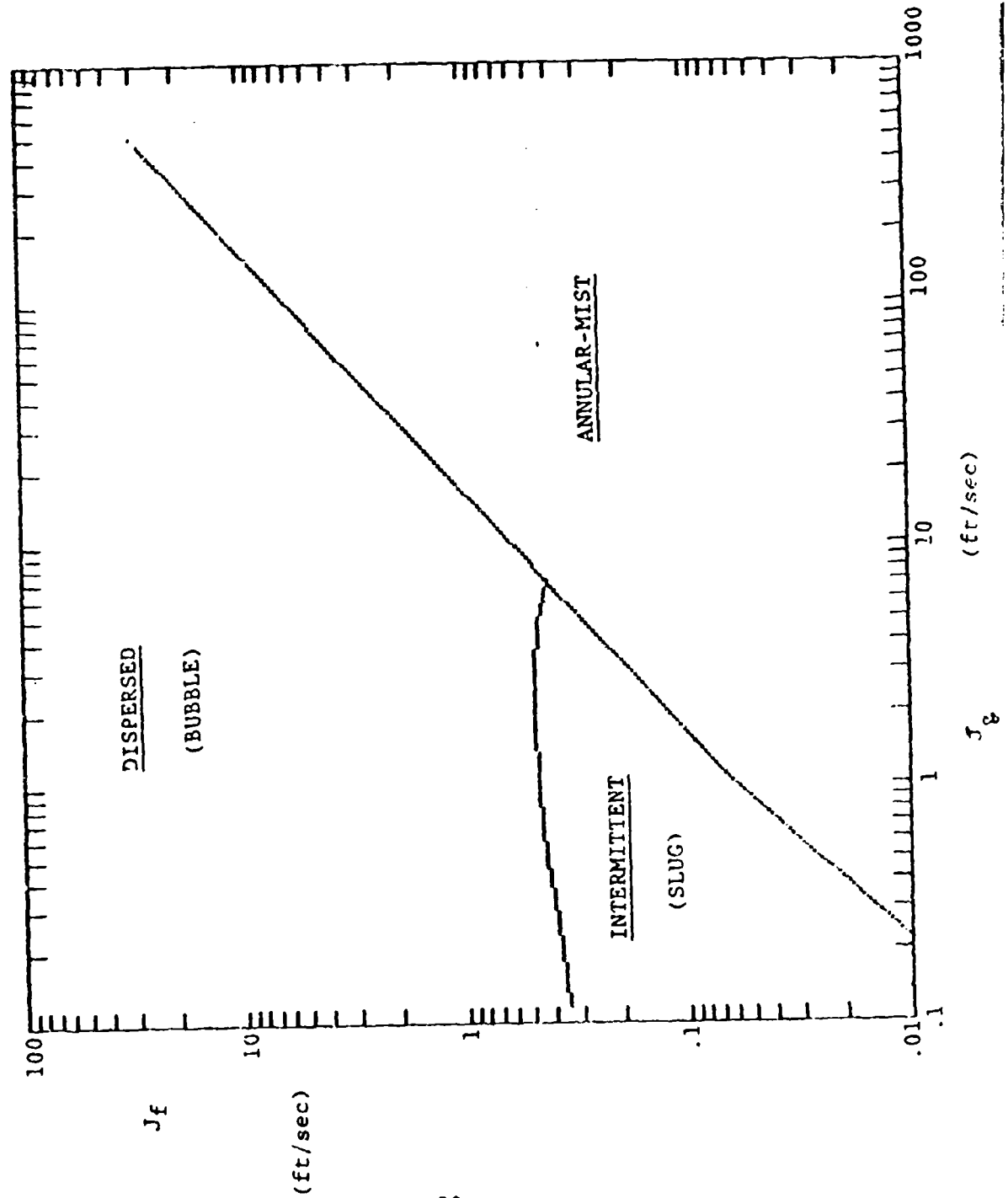


FIGURE 21

WEISMAN Horizontal Flow Regime Map Predictions  
for FREON-11, 25 C, Saturation Pressure  
Vapor-Liquid Flow in 1" i.d. horizontal pipe  
GRAVITY = 3.217 ft/sec/sec (.1-G)

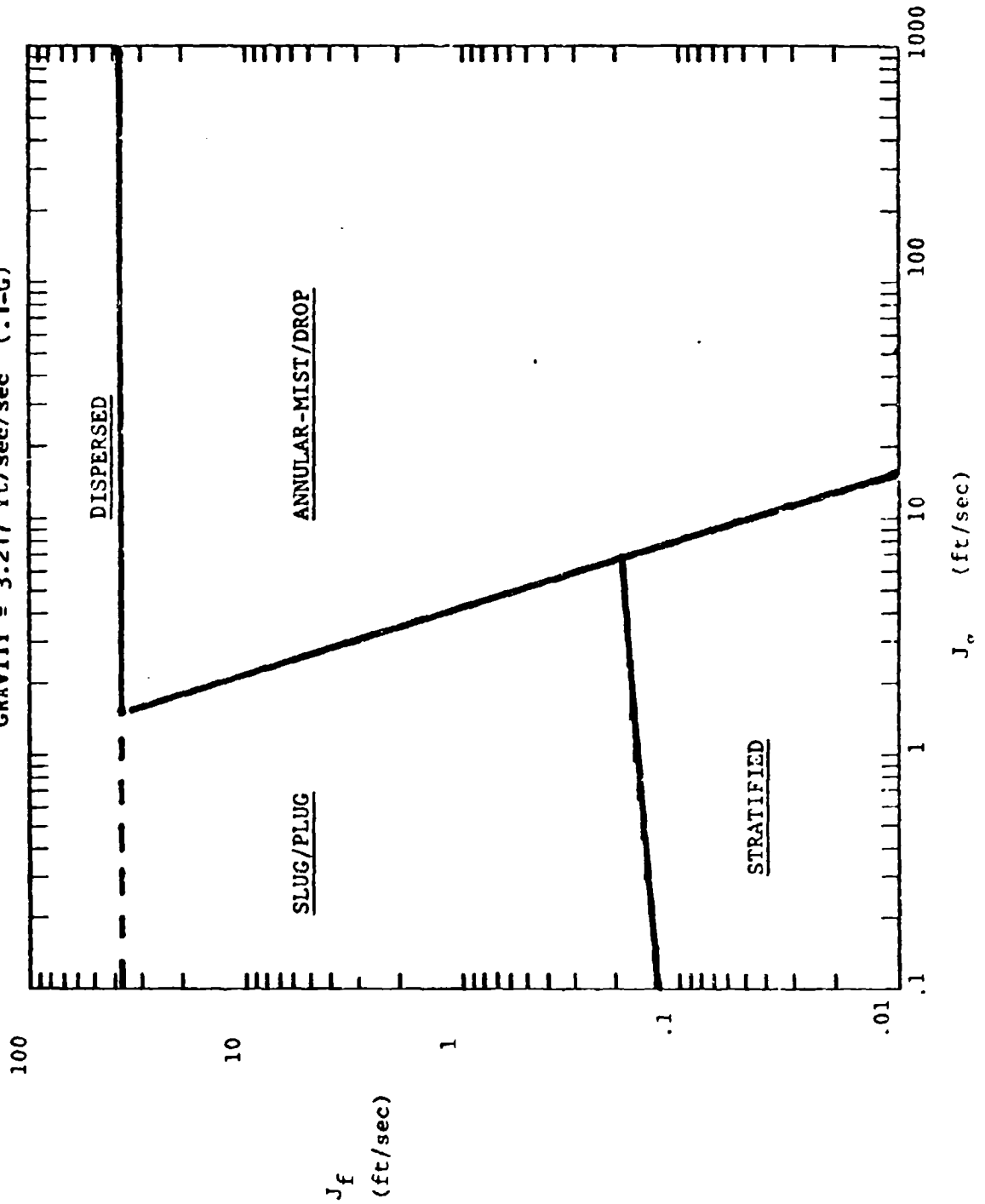


FIGURE 22

WEISMAN Horizontal Flow Regime Map Predictions  
for IREON-11, 25 C, Saturation Pressure  
Vapor-Liquid Flow in 1" i.d. horizontal pipe  
GRAVITY = .3217 ft/sec/sec (.01-G)

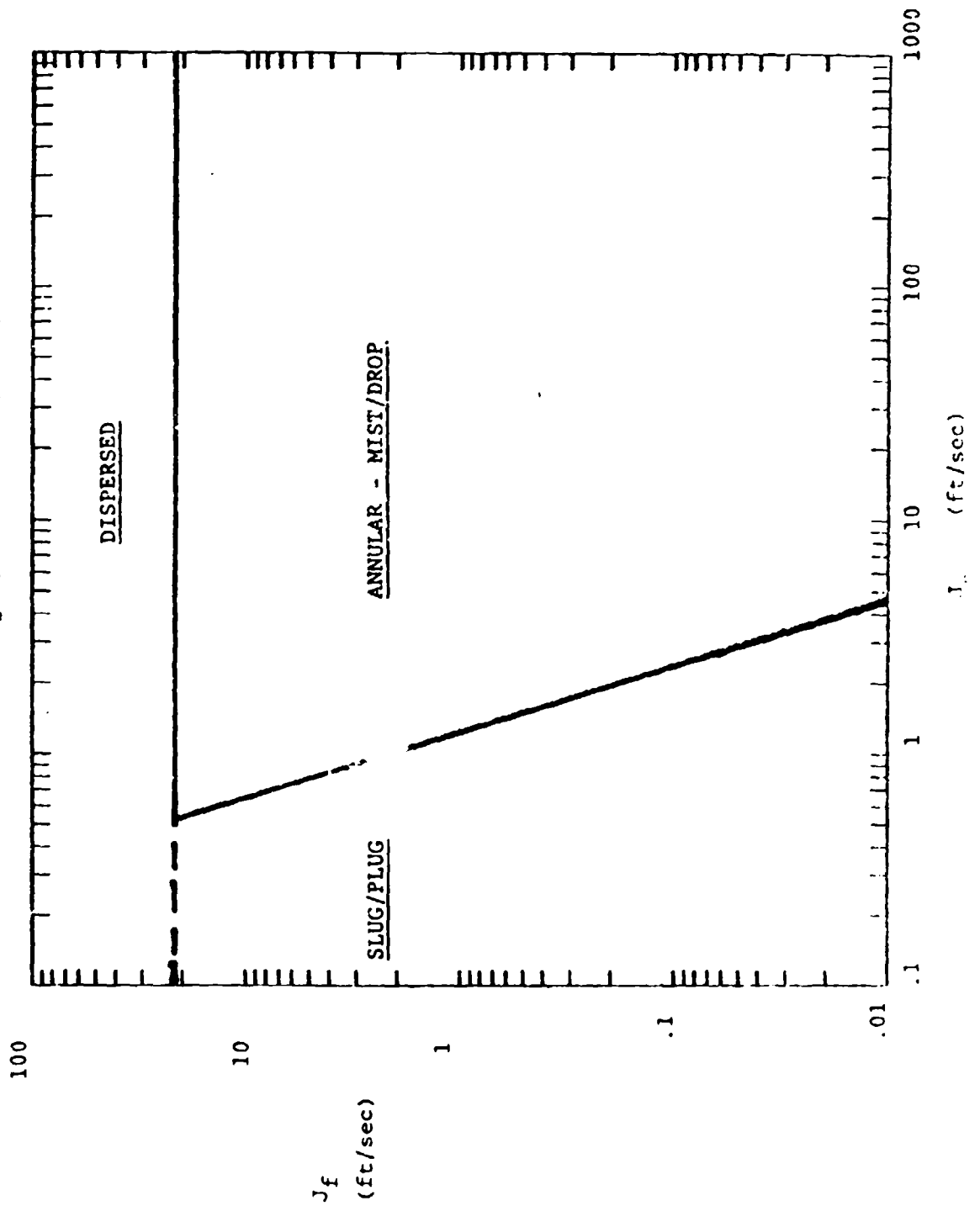
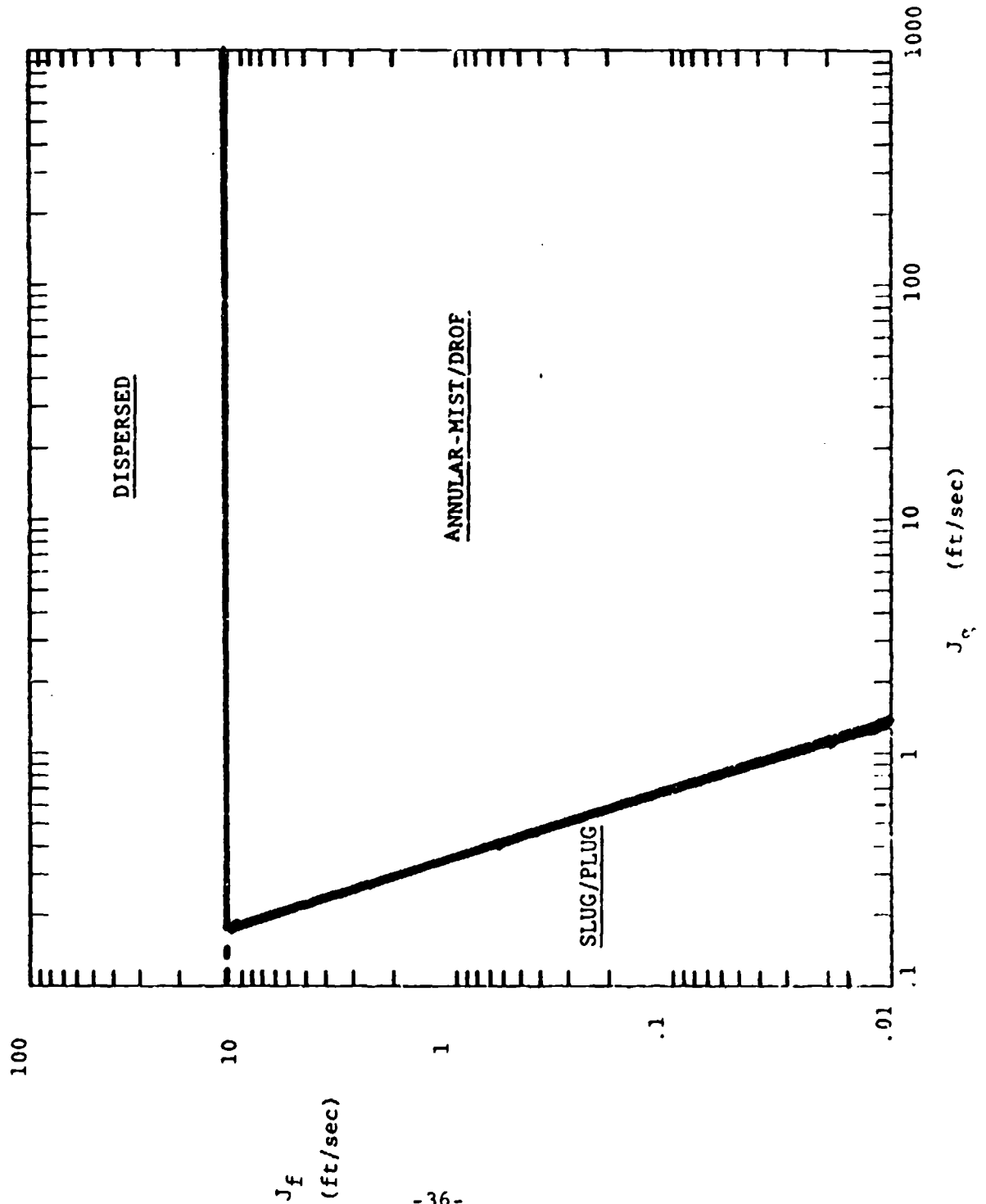


FIGURE 23

WEISMAN Horizontal Flow Regime Map Predictions  
for FREON-11, 25 C, Saturation Pressure  
Vapor-Liquid Flow in 1" i.d. horizontal pipe  
GRAVITY = .03217 ft/sec/sec (.001-G)



Figures 24-26 show predictions for the same Freon-11 conditions as in 1" I.D. vertical tube, as gravity is reduced from .1-G to .001-G on Dukler's Vertical flow regime map. The three flow regimes that are predicted for a low gravity force are annular, slug, and dispersed (bubble) flow regimes. In this case, annular flow predominates all values of large vapor flow. This result disagrees with both previous horizontal maps, which always showed a region of dispersed flow at sufficiently large liquid flow rates.

Figures 27-29 show the predictions for Freon-11 in a 1" I.D. vertical tube, as gravity is reduced from .1-G to .001-G on Weisman's vertical flow regime map. Because this map contains identical mathematics to the Weisman horizontal map, "agreement" between these two maps is perfect at low gravity values. The only difference between Weisman vertical and horizontal maps is replacement of a bubble flow regime boundary with a stratified flow regime boundary. Therefore, once the stratified and bubble flow regimes disappear, due to decrease in the gravity constant, the results should be identical.

#### **Summary of Computer Modeling of Existing Flow Regime Maps**

It is encouraging that all four maps predict the existence of the same three flow regimes at minimal (.001) gravity. However, the predictions for the sizes, ranges and shapes of these three flow regimes on the map are substantially different. The annular regime boundary for example, is variously predicted as being vertical, as having significant negative slope (i.e.,  $-60^\circ$ ) and as having significant positive slope (i.e.,  $+45^\circ$ ).

Possibly these differences in prediction can be reconciled analytically. However, before such a step is attempted, it is worthwhile to see how well each of these maps matches laboratory data of flow regimes when the buoyancy force is minimized by using liquids of nearly equal density. After such a comparison has been made, the value of the various flow regime modeling schemes may be uncovered.

#### **V. COMPARISON OF LAB RESULTS WITH THE FOUR FLOW REGIME MAPS**

##### **Dukler-Taitel Horizontal Flow Regime Map:**

Figures 30-35 show the previously presented lab data with the Dukler-Taitel Horizontal flow regime map predictions overlaid on the same scale. These Dukler-Taitel predictions are for the actual laboratory conditions used (ie, 1" I.D., density and viscosity of water and PPG-2000 respectively). It is of interest to note that the Dukler horizontal flow regime map predictions for our lab data are quite similar to predictions for Freon-11 at reduced gravity. This fact indicates that, so far as the

FIGURE 24

DUKLER-TAITEL Vertical Flow Regime Map Predictions  
for FREON-11, 25 C, Saturation Pressure  
Vapor-Liquid Flow in 1" i.d. horizontal pipe  
GRAVITY = 3.217 ft/sec/sec (0.1-G)

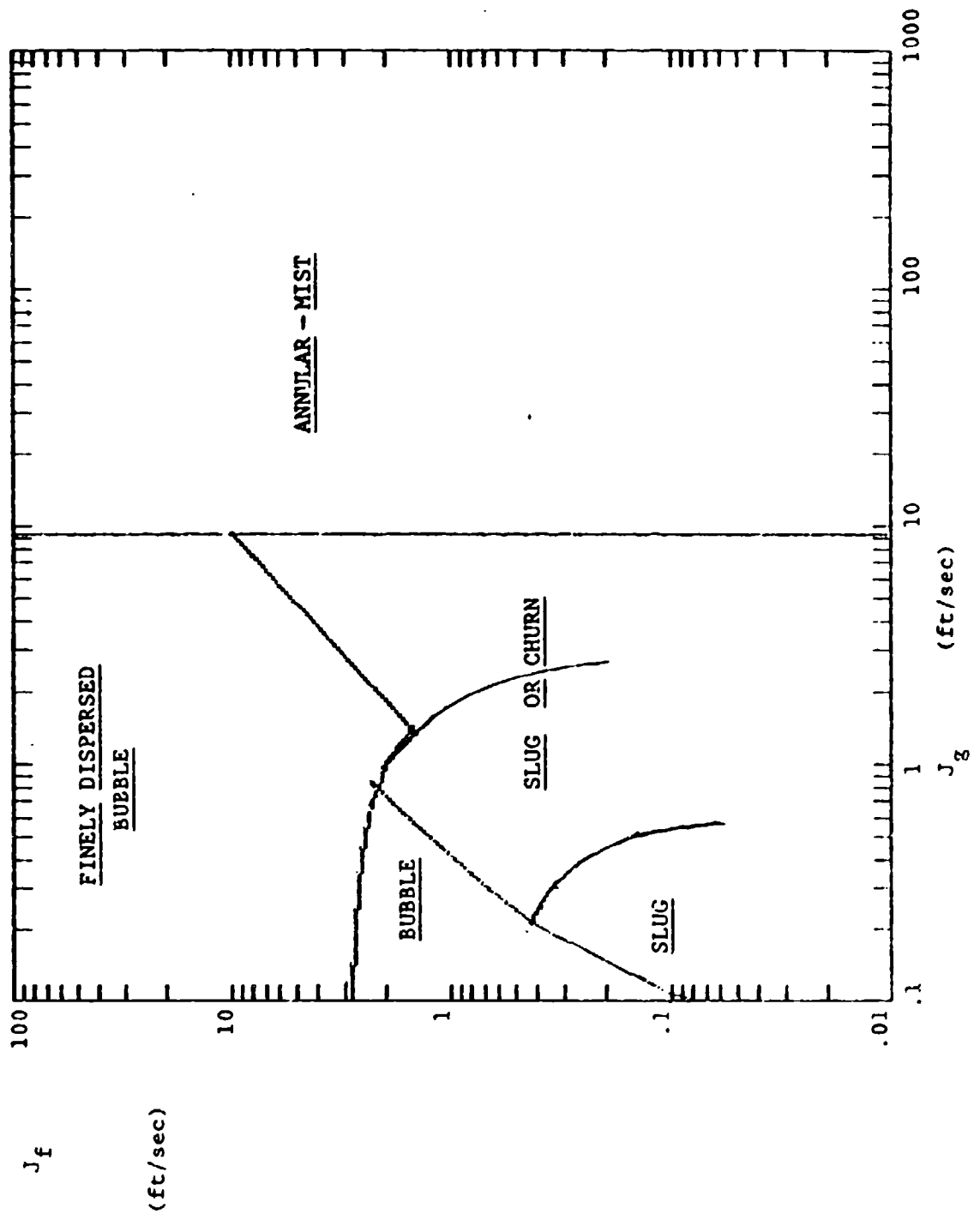


FIGURE 25

DUKLER-TAITEL Vertical Flow Regime Map Predictions  
for FREON-11, 25 C, Saturation Pressure  
Vapor-Liquid Flow in 1" i.d. horizontal pipe  
GRAVITY = .3217 ft/sec/sec (0.01-G)

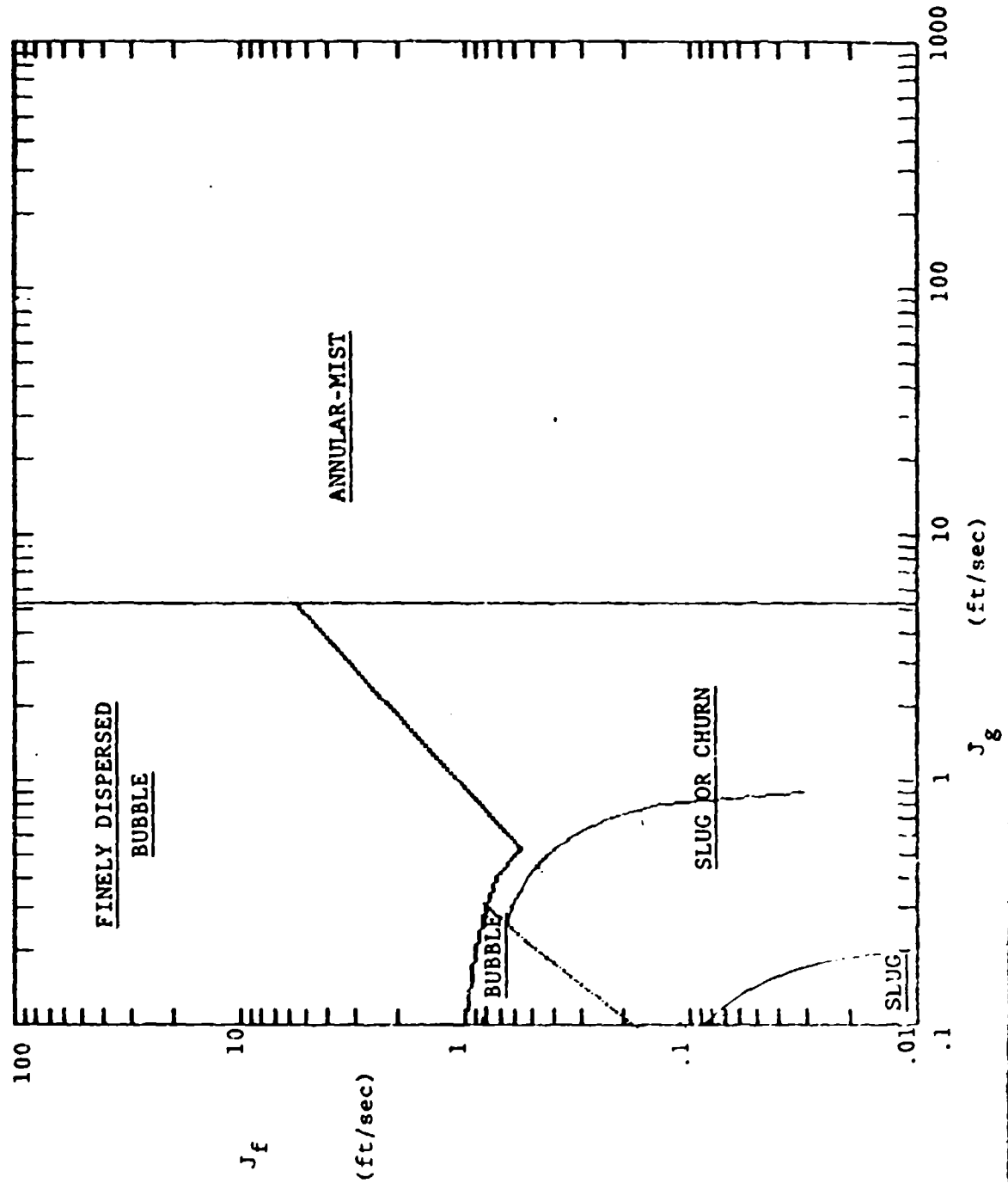


FIGURE 26

DUKLER-ITTEL Vertical Flow Regime Map Predictions  
for FREON-11, 25 C, Saturation Pressure  
Vapor-Liquid Flow in 1" i.d. horizontal pipe  
GRAVITY = .03217 ft/sec/sec (0.001-G)

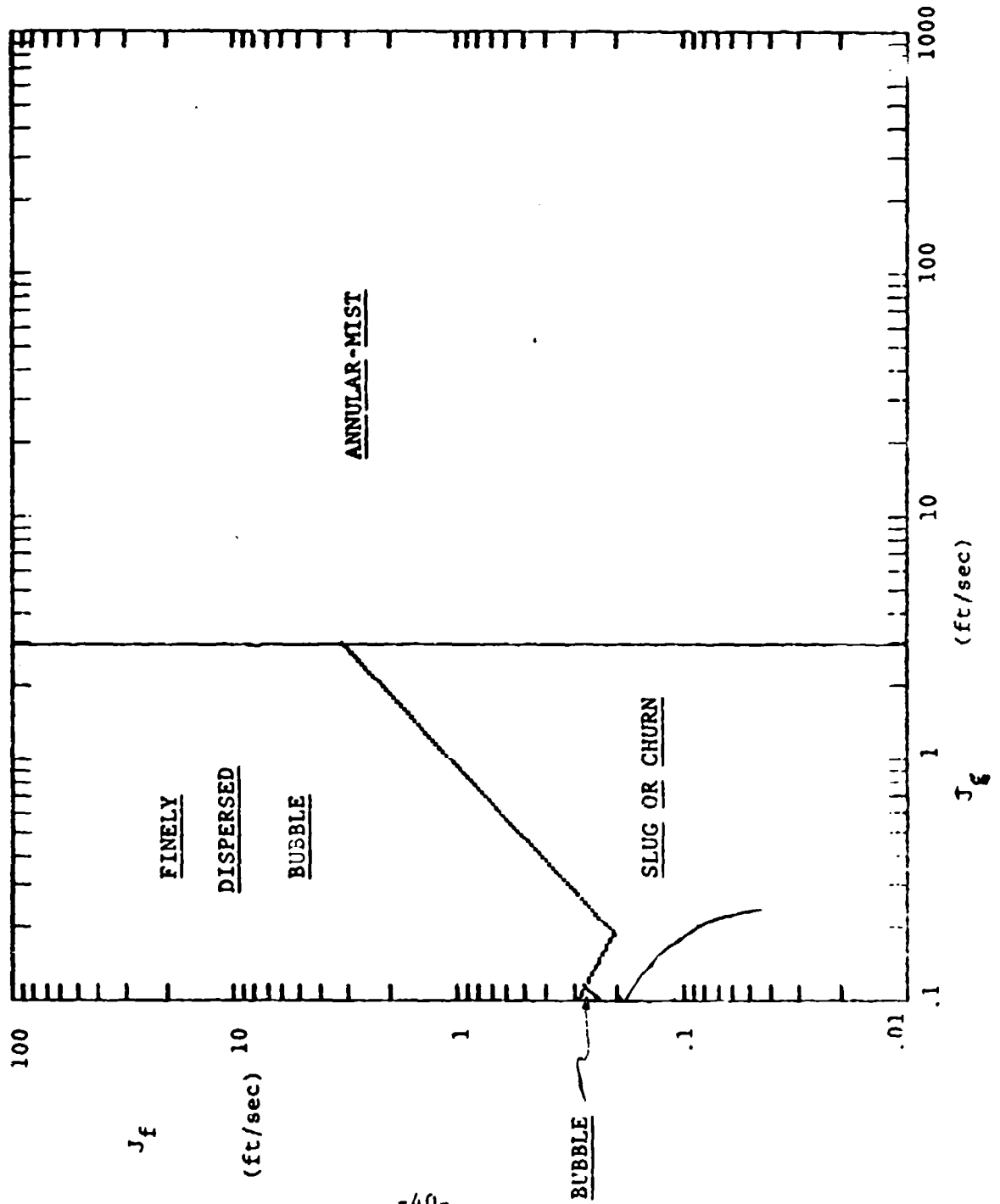


FIGURE 27

WEISMAN Vertical Flow Regime Map Predictions  
for FREON-11, 25 C, Saturation Pressure  
Vapor-Liquid Flow in 1" i.d. horizontal pipe  
GRAVITY = 3.217 ft/sec/sec (.1-G)

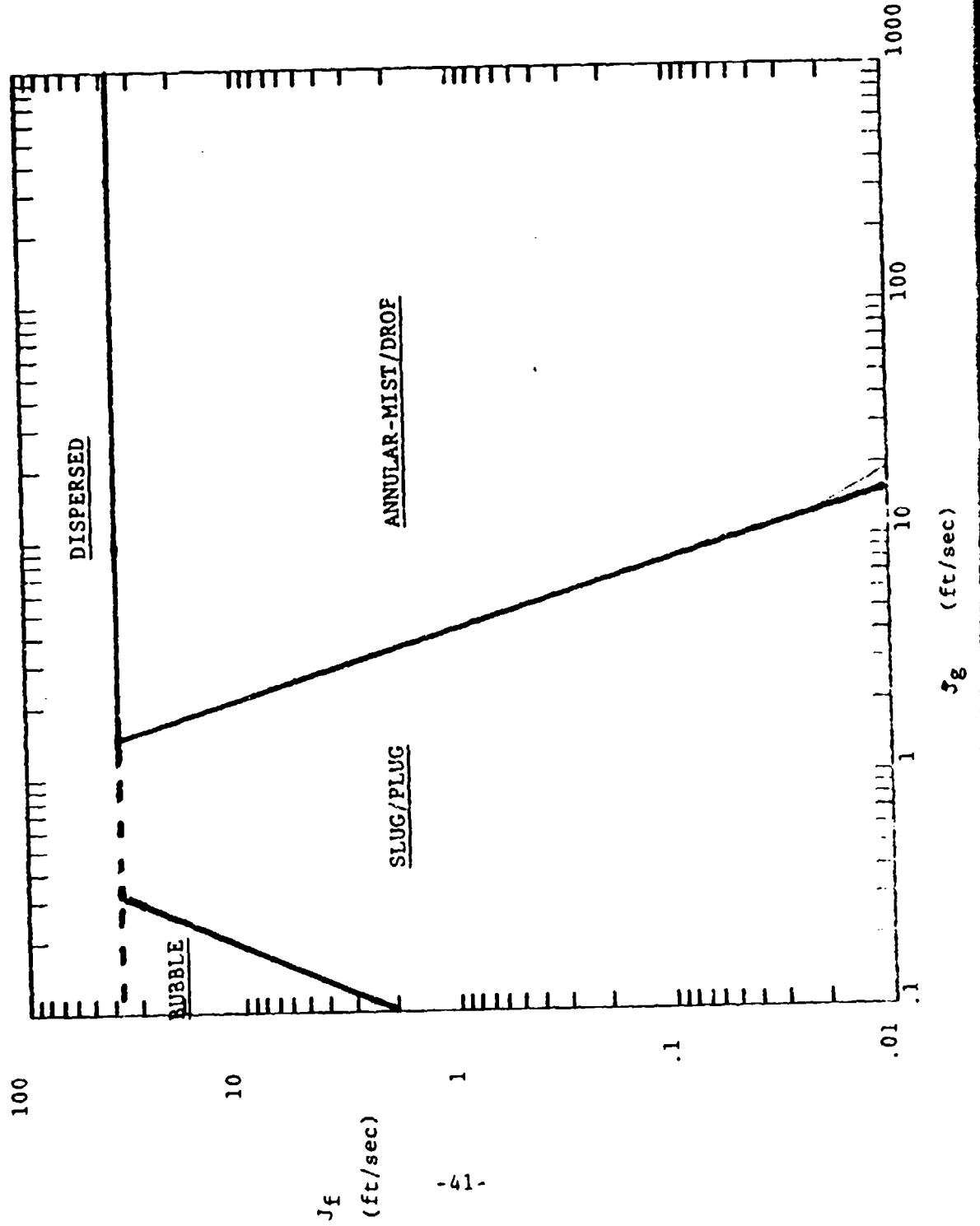


FIGURE 28

WEISMAN Vertical Flow Regime Map Predictions  
for FREON-11, 25 C, Saturation Pressure  
Vapor-Liquid Flow in 1" i.d. horizontal pipe  
GRAVITY = .3217 ft/sec/sec (.01-G)

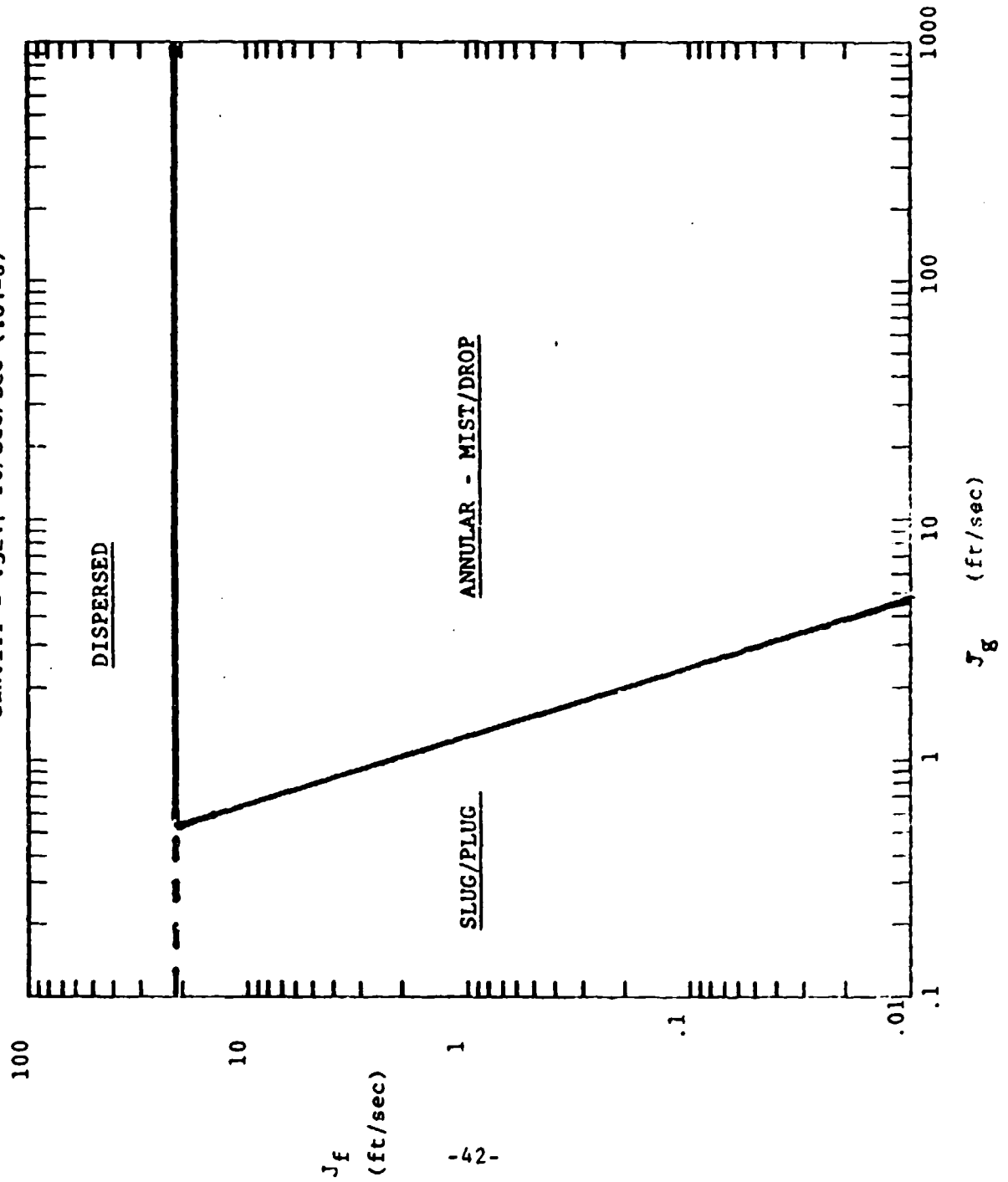


FIGURE 29

WEISMAN Vertical Flow Regime Map Predictions  
for FREON-11, 25 C, Saturation Pressure  
Vapor-Liquid Flow in 1" i.d. horizontal pipe  
GRAVITY = .03217 ft/sec/sec (.001-G)

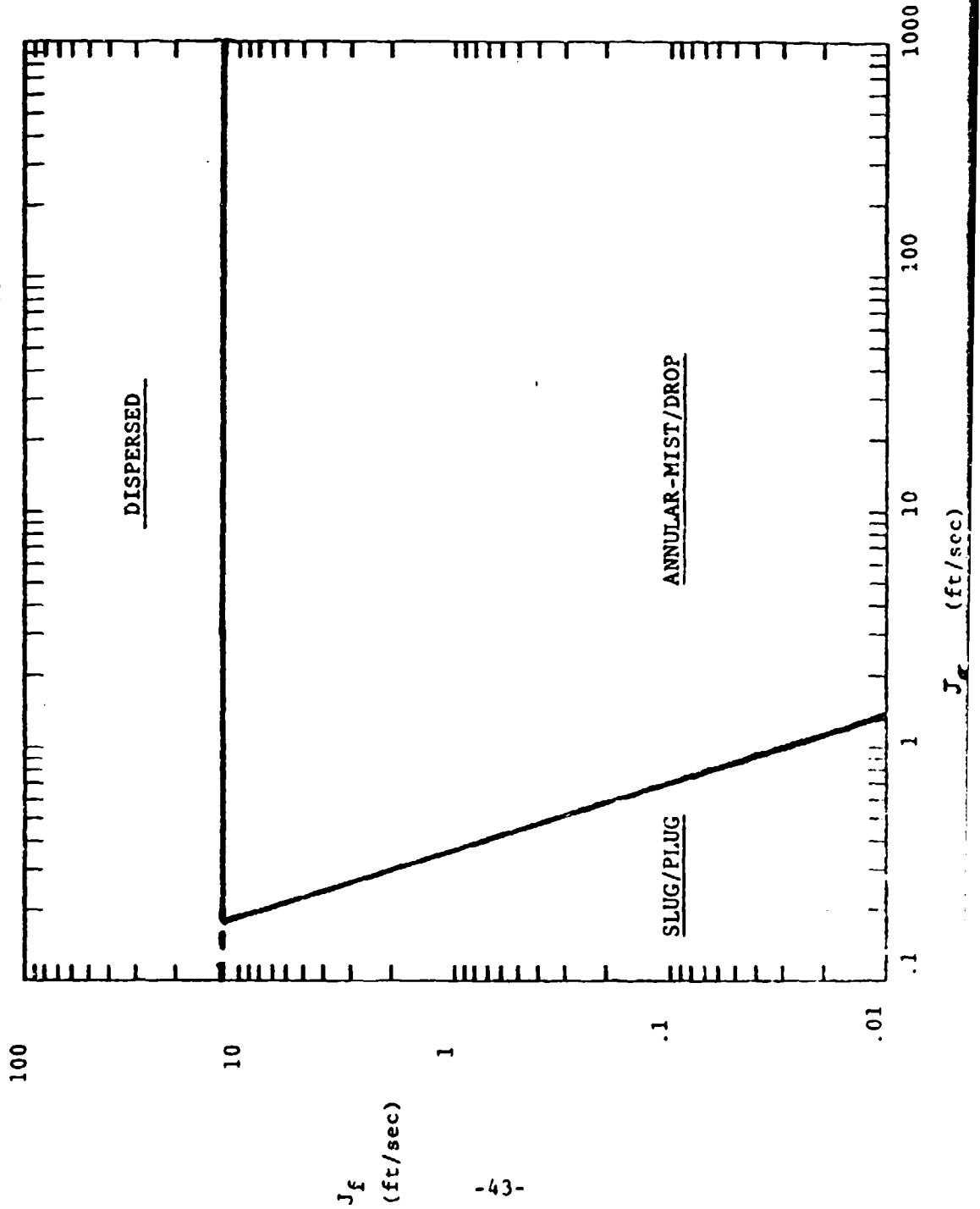


FIGURE 30

LABDATA 1  
PPG-2000 and WATER at 77° F  
Compared to Dukler-Taitel Horizontal Flow Regime Map Predictions  
(Predicted Flow Regimes are UNDERLINED)

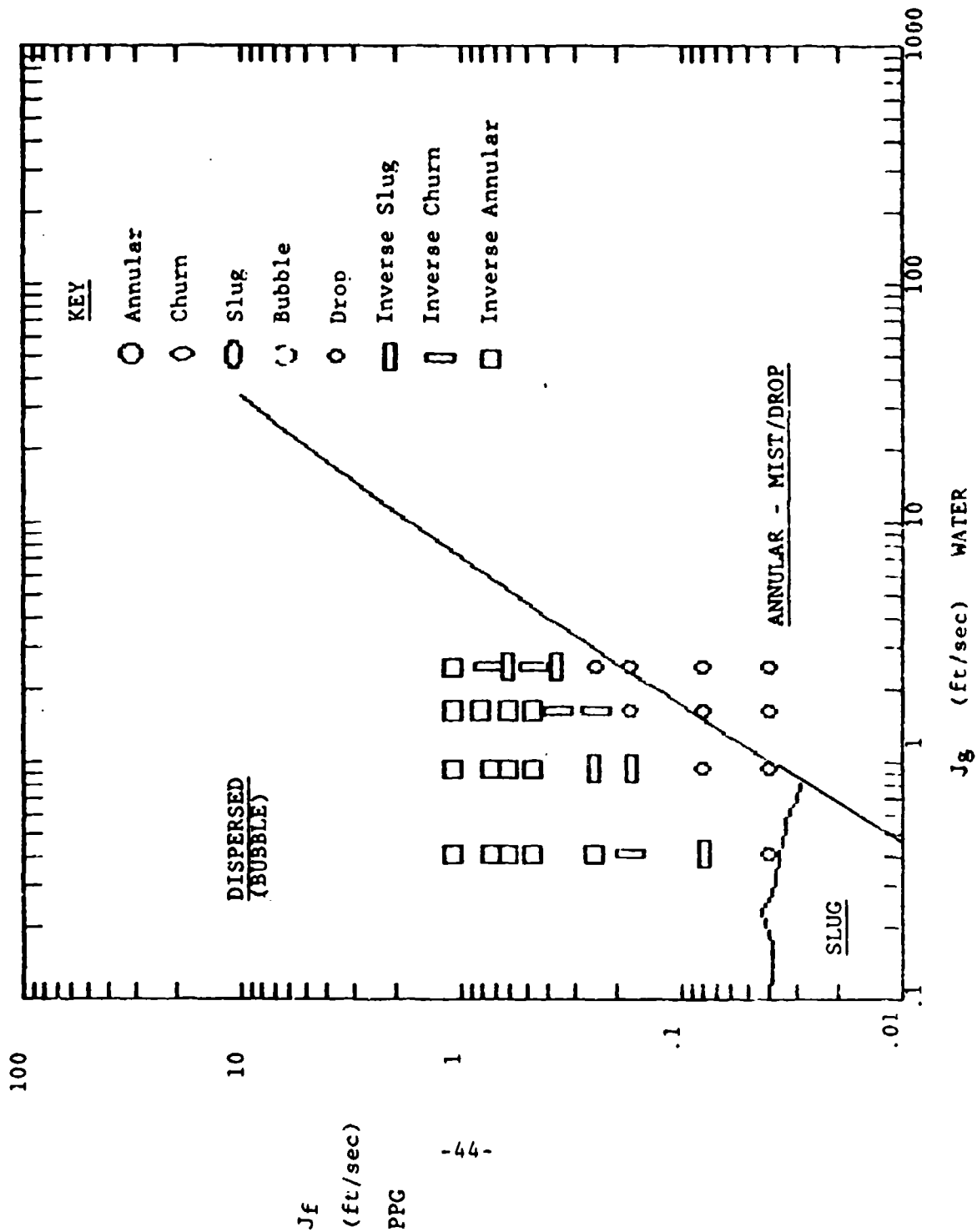


FIGURE 31

LABDATA 2  
 PPG-2000 and WATER at 77° F  
 Compared to Dukler-Taitel Horizontal Flow Regime Map Predictions  
 (Predicted Flow Regimes are UNDERLINED)

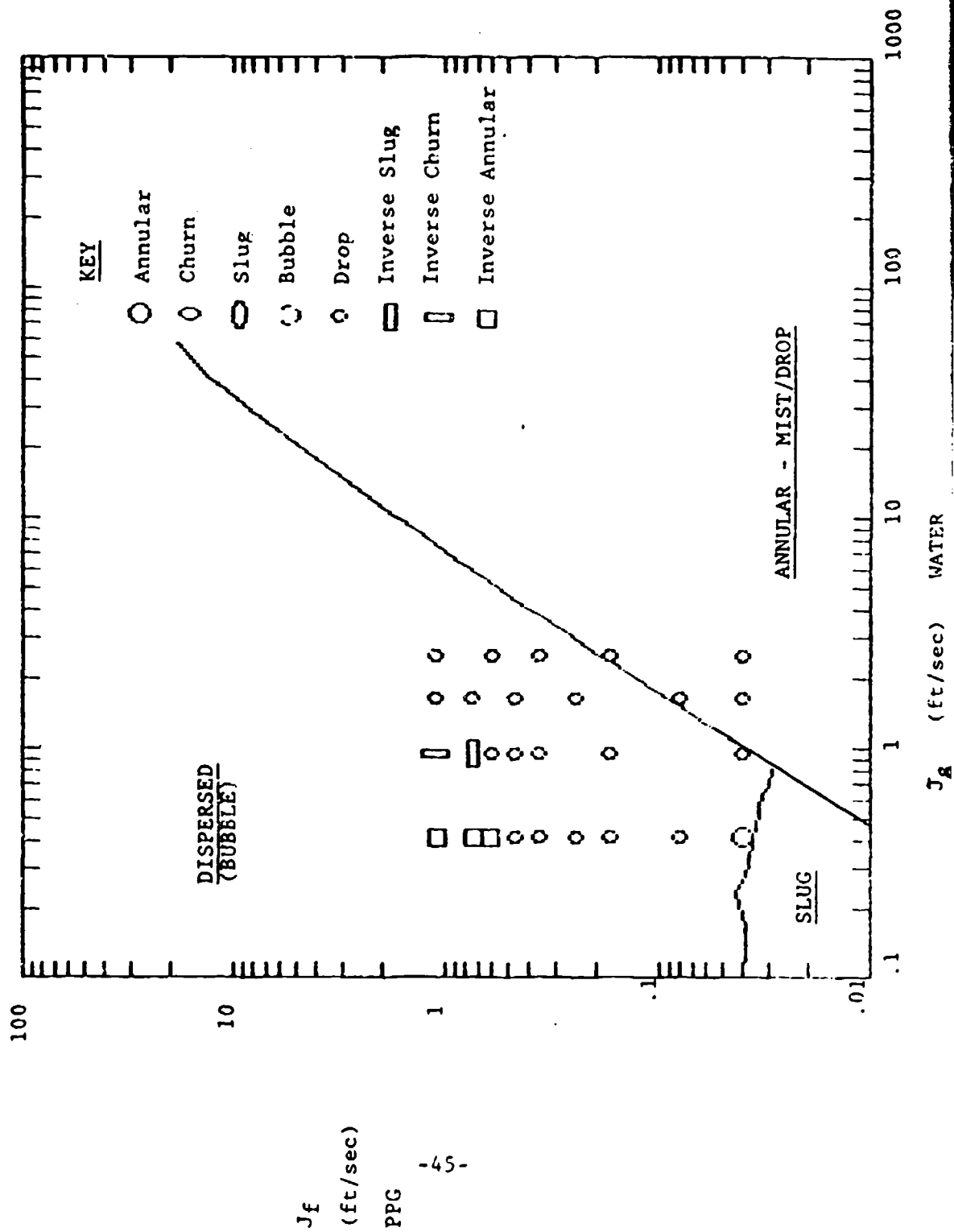


FIGURE 32

LABDATA 3  
PPG-2000 and WATER at 77°F  
Compared to Dukler-Taitel Horizontal Flow Regime Map Predictions  
(Predicted Flow Regimes are UNDERLINED)

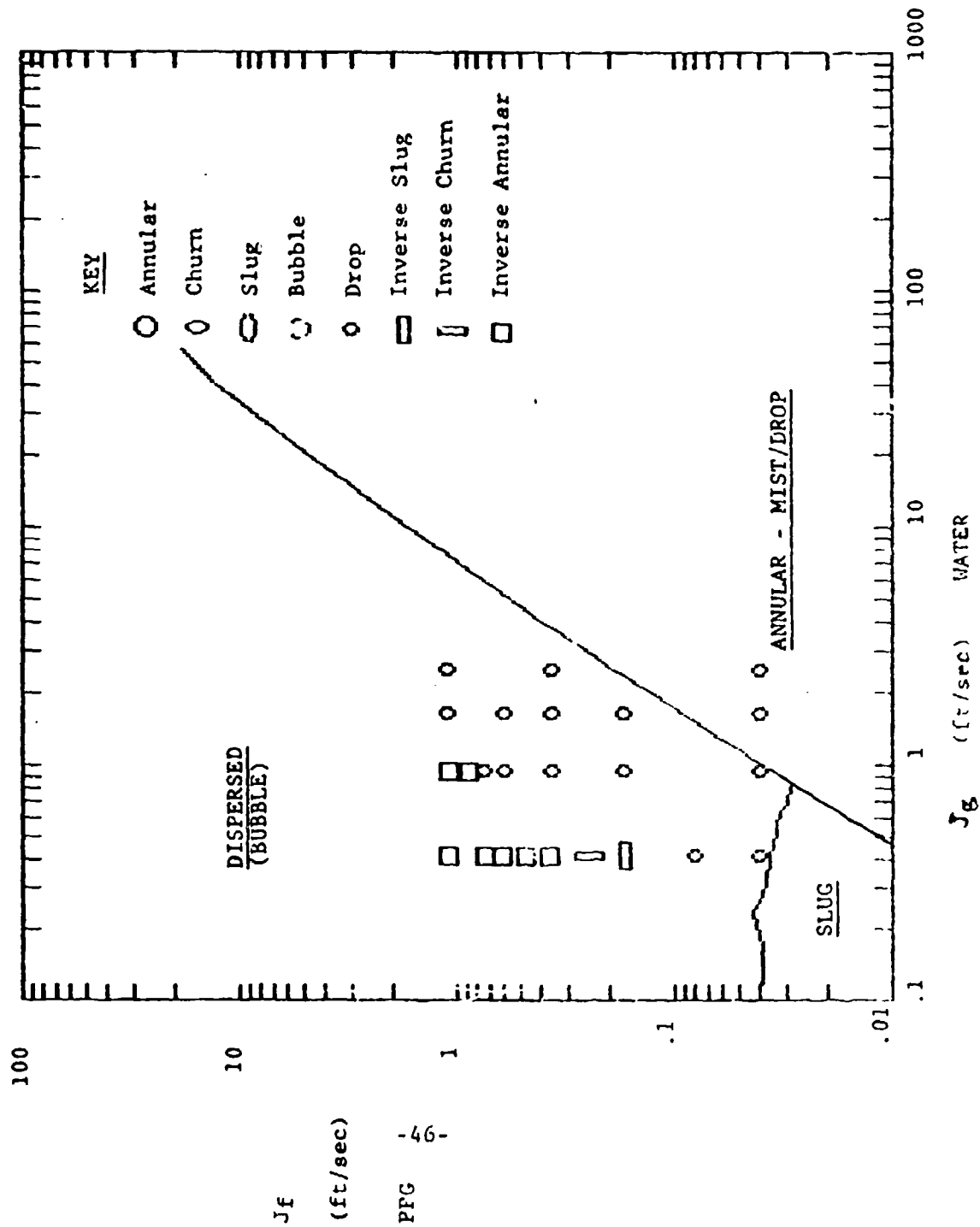


FIGURE 33

LABDATA 4  
 PPG-2000 and WATER at 77° F  
 Compared to Dukler-Taitel Horizontal Flow Regime Map Predictions  
 (Predicted Flow Regimes are UNDERLINED)

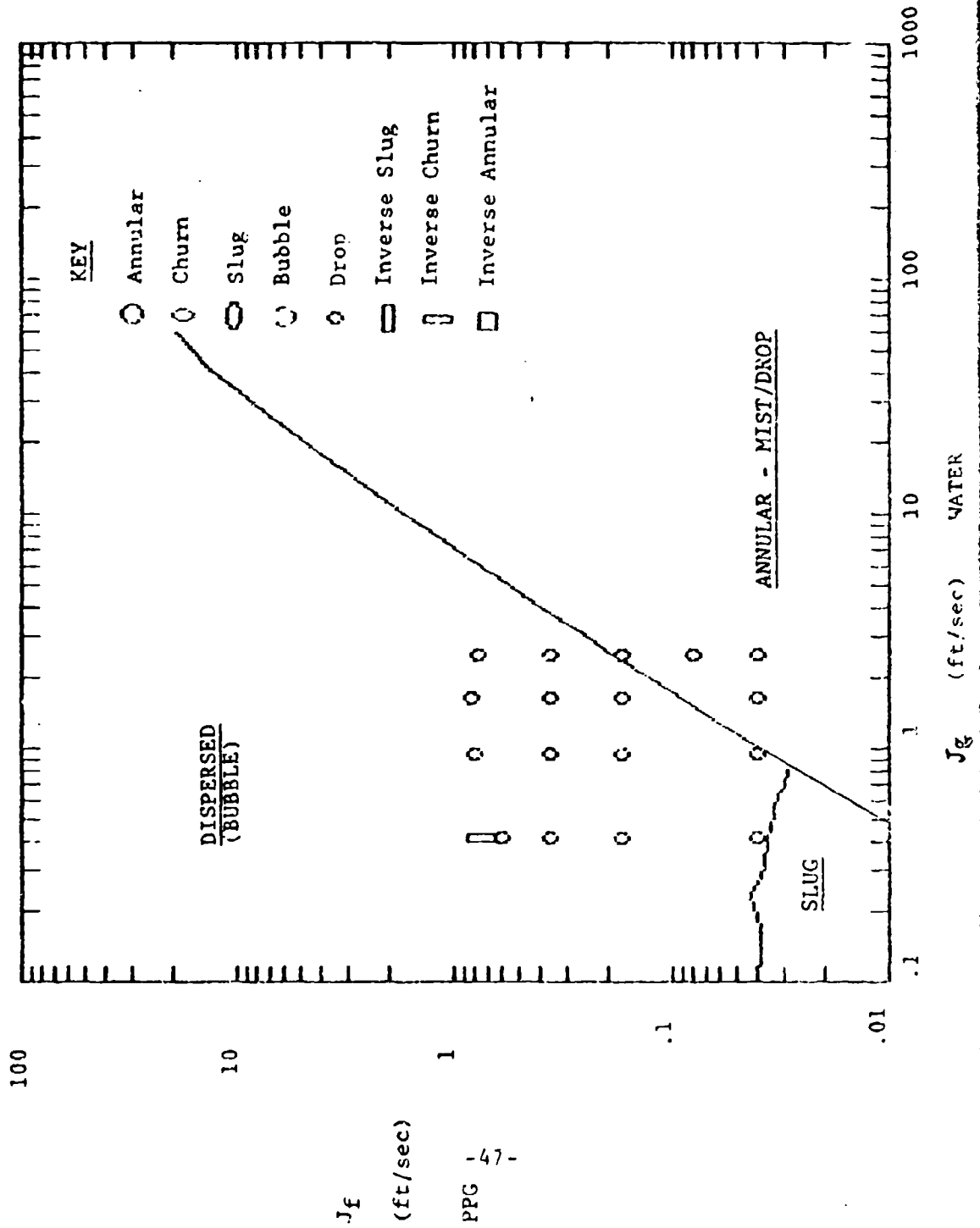


FIGURE 34

LABDATA 5  
 PPG - 2000 and WATER at 77°F  
 Compared to Dukler-Taitel Horizontal Flow Regime Map Predictions  
 (Predicted Flow Regimes are UNDERLINED)

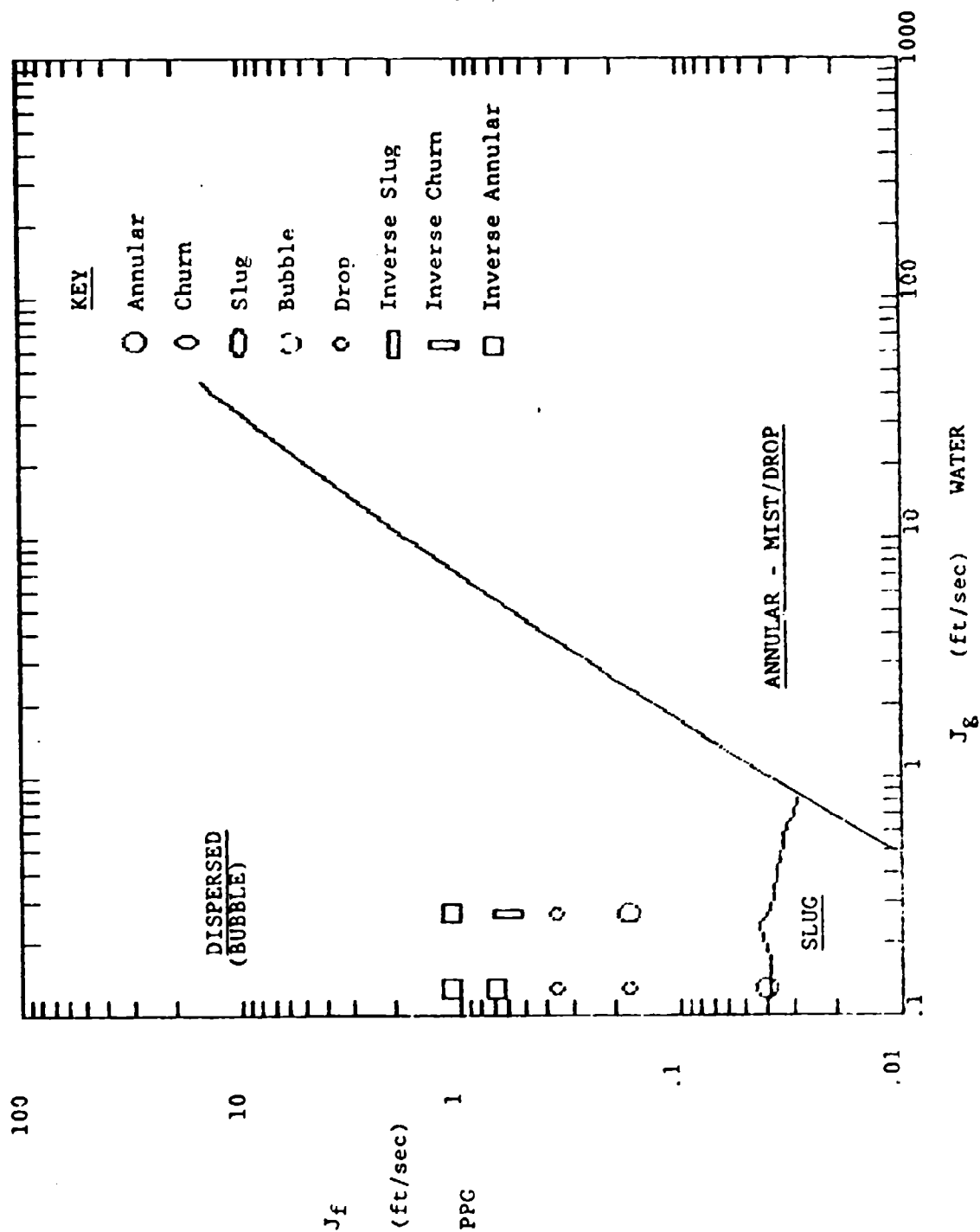
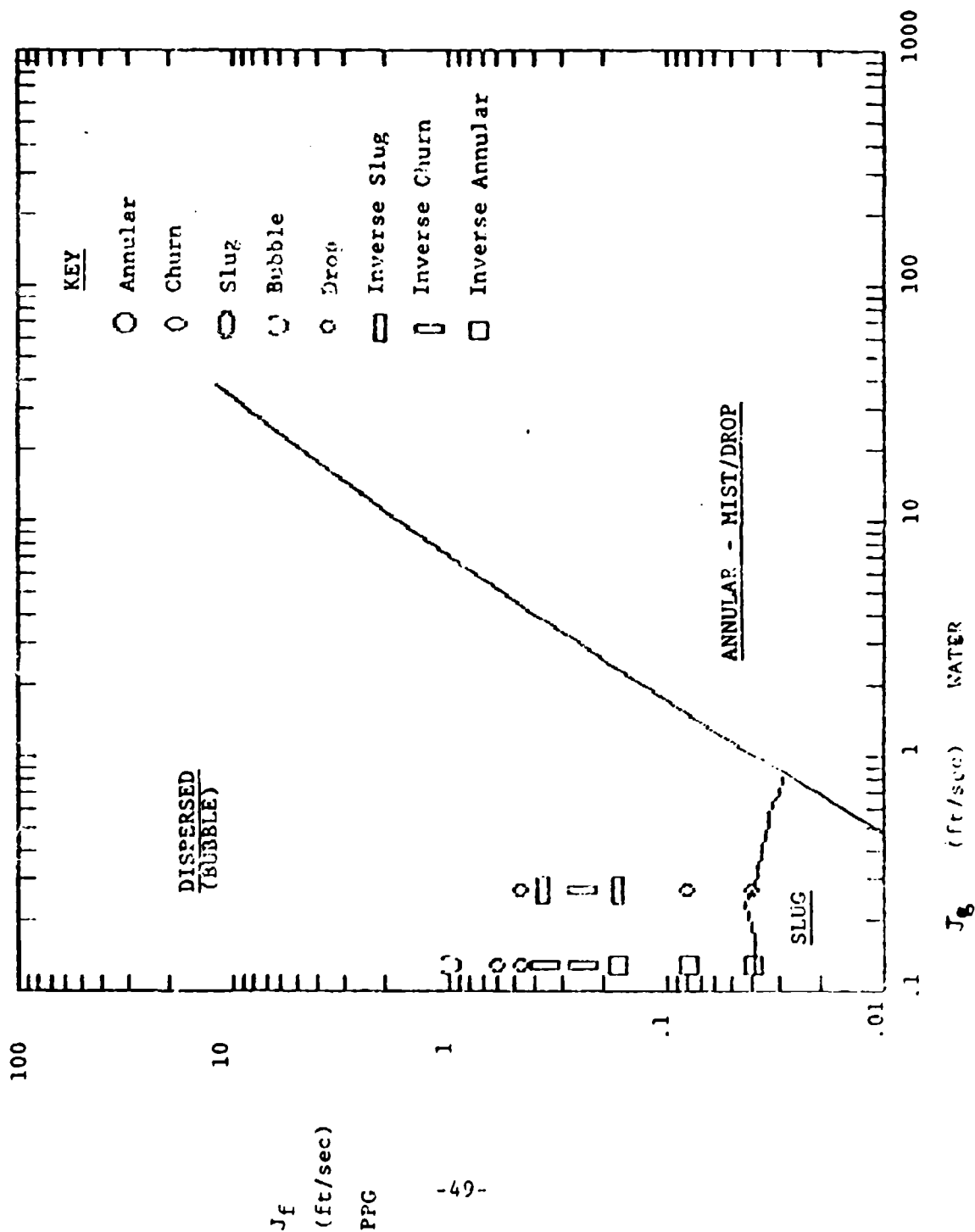


FIGURE 35

LABDATA 6  
PPG-200C and WATER at 77° F  
Compared to Dukler-Taitel Horizontal Flow Regime Map Predictions  
(Predicted Flow Regimes are UNDERLINED)



mathematics of the model is concerned, reduced gravity is similar in effect to equalized fluid densities, as one would expect.

It is immediately apparent that the Dukler-Taitel horizontal map is not a good predictor of observed flow regimes for the fluids and conditions we tested. This is true for every entrance conditions and virtually every flow rate we used. The only observed flow regime that was correctly predicted is some of the drop flow (if an annular-mist prediction is interpreted as drop flow). However, drop flow occurred in many regions where it was not predicted. Inverse annular, inverse churn, and inverse slug flow (not predicted at all), occurred where dispersed (i.e., bubbly) flow was predicted. The Dukler predicted slug (i.e., intermittent) flow is a tiny area outside the range of most of our data. However, data points closest to this region were mostly drop flow. Some data points near this region were bubble, annular or inverse annular flow. There was never any form of intermittent (i.e., inverse slug or churn) flow as predicted in the slug flow region. We conclude that the Dukler horizontal flow regime map is inadequate to predict or even describe the flow regimes which occur in situations of minimal buoyancy.

#### **Weisman Horizontal Flow Regime Map**

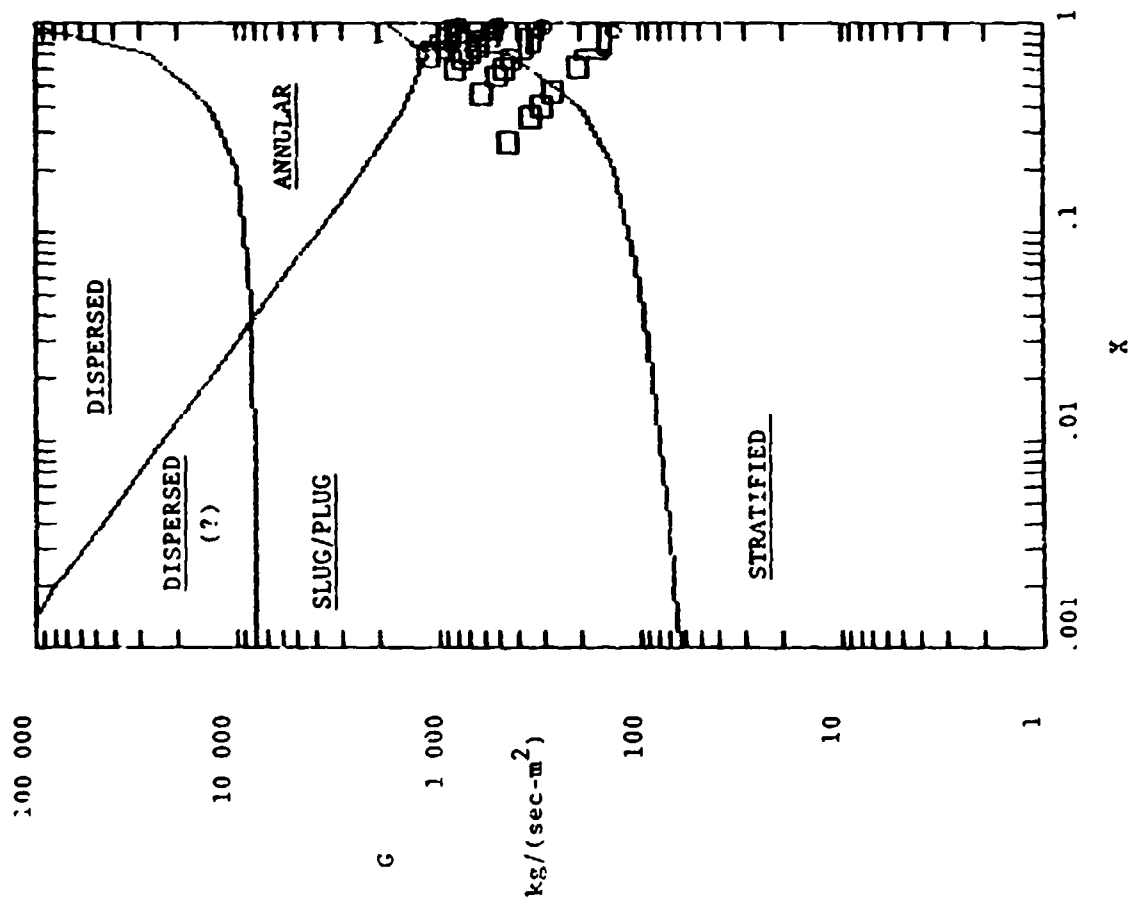
Figure 36 shows one set of Lab data ("LABDATA 1") plotted on a log G - log X Weisman horizontal flow regime map. Because of the similarity in liquid densities, the data are compressed. This is not a useful plotting method for observing our particular laboratory data. Therefore, figures 37-42 plot the Weisman prediction curves and the lab data on log  $J_f$  - log  $J_g$  plots. Again, it is immediately apparent that the predicted flow regimes do not match observed data. A major part of the Weisman prediction is for stratified flow which occurs in none of the experiments whatsoever. The other major part of the Weisman horizontal prediction is for slug/plug flow. Occasionally inverse slug or inverse churn flow do occur in this region predicted as slug/plug flow. But most occurrences of any type of intermittent flow are in the region predicted as stratified. drop flow does occur, but in the "stratified" prediction, not in the annular (i.e., "annular-mist/drop") where it would be expected.

Furthermore, inverse annular flow occurs and is unpredicted. We conclude that the Weisman flow regime map is inadequate to predict or even describe the flow regimes which occur in situations of minimal density.

#### **Dukler-Taitel Vertical Flow Regime Map:**

Figures 43-48 show the same lab data described previously, but with the Dukler-Taitel Vertical flow regime map predictions over-laid on the same scale. These predictions are based on the

FIGURE 36



WEISMAN Horizontal  
Flow Regime Map Predictions  
for PPG - 2000 and WATER at  
77° F (PPG taken as the liquid)

Mass Velocity plotted against  
Quality (MKS units)  
LABDATA 1 plotted to show that  
with nearly equal liquid (PPG)  
and "Gas" (WATER) Densities, Data  
is compressed and unreadable on  
this particular co-ordinate system  
and scale.

FIGURE 37

LABDATA 1 (HORIZONTAL DATA)  
 PPG-2000 and WATER at 77 F  
 Compared to Weisman Horizontal Flow Regime Map Predictions  
 (Predicted Flow Regimes are UNDERLINED)

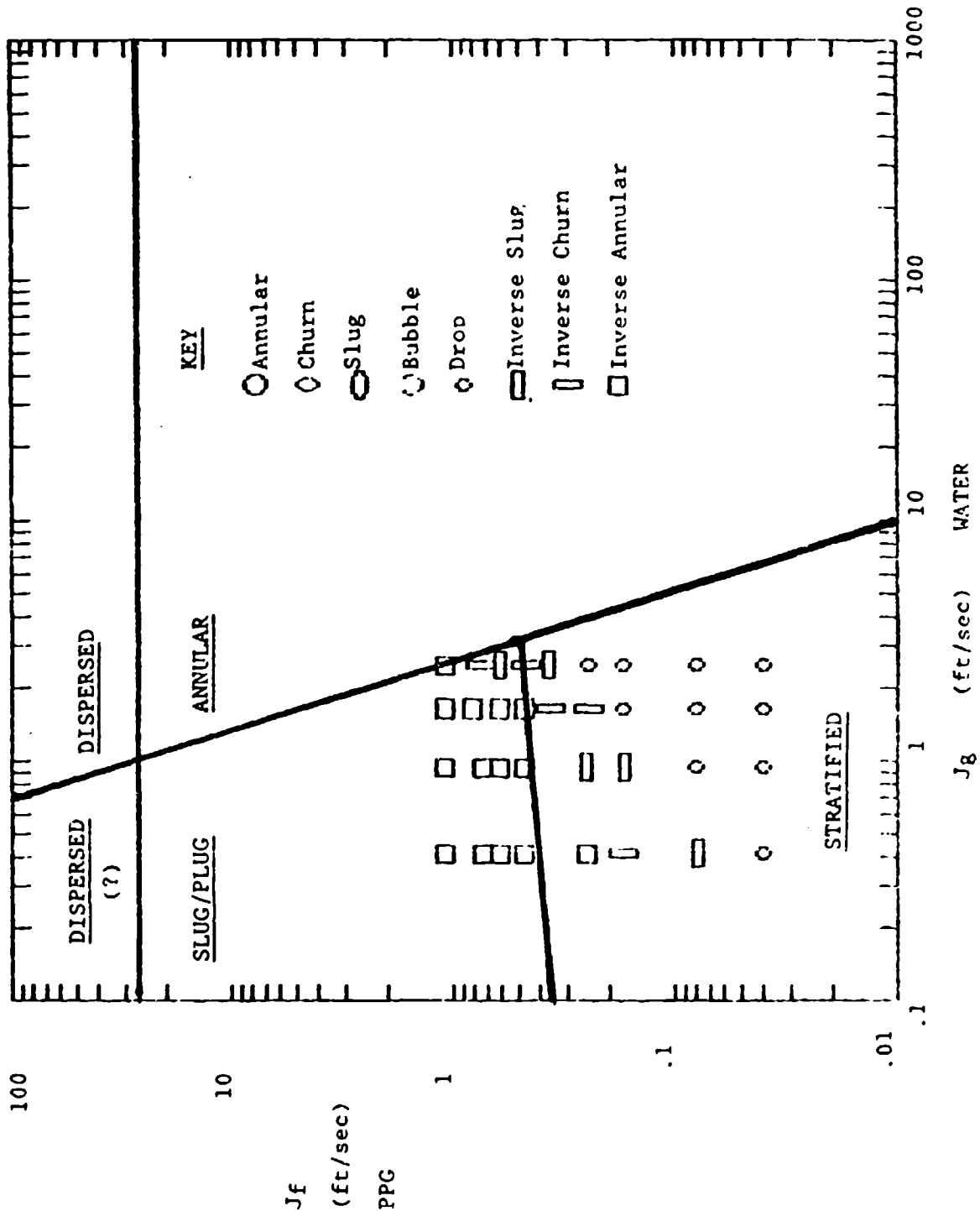


FIGURE 30

LABDATA 2 (HORIZONTAL DATA)  
PPG-2060 and WATER at 77 F  
Compared to Weisman Horizontal Flow Regime Map Predictions  
(Predicted Flow Regimes are UNDERLINED)

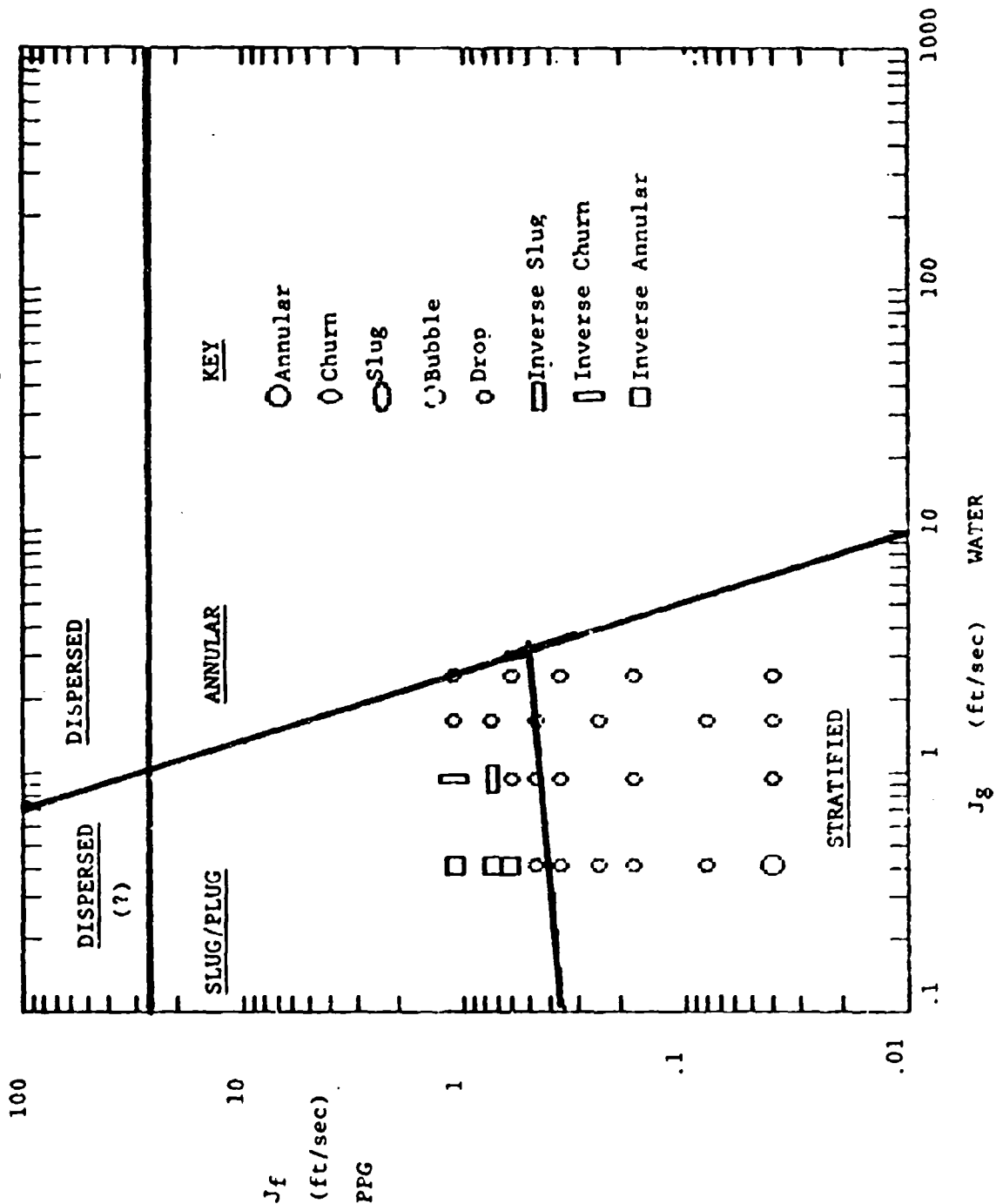


FIGURE 39

LABDATA 3 (HORIZONTAL DATA)  
PPG-2000 and WATER at 77 F  
Compared to Weisman Horizontal Flow Regime Map Predictions  
(Predicted Flow Regimes are UNDERLINED)

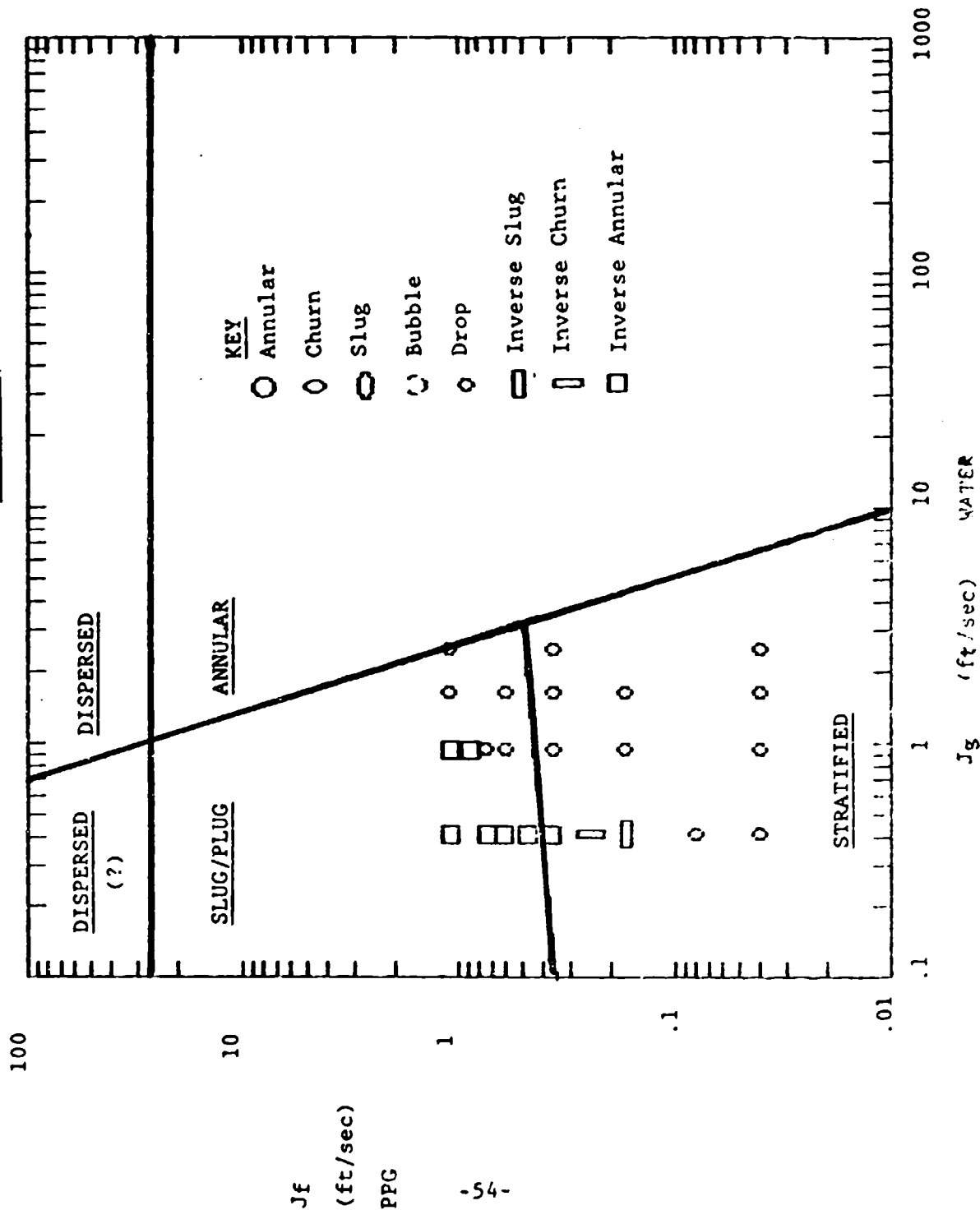
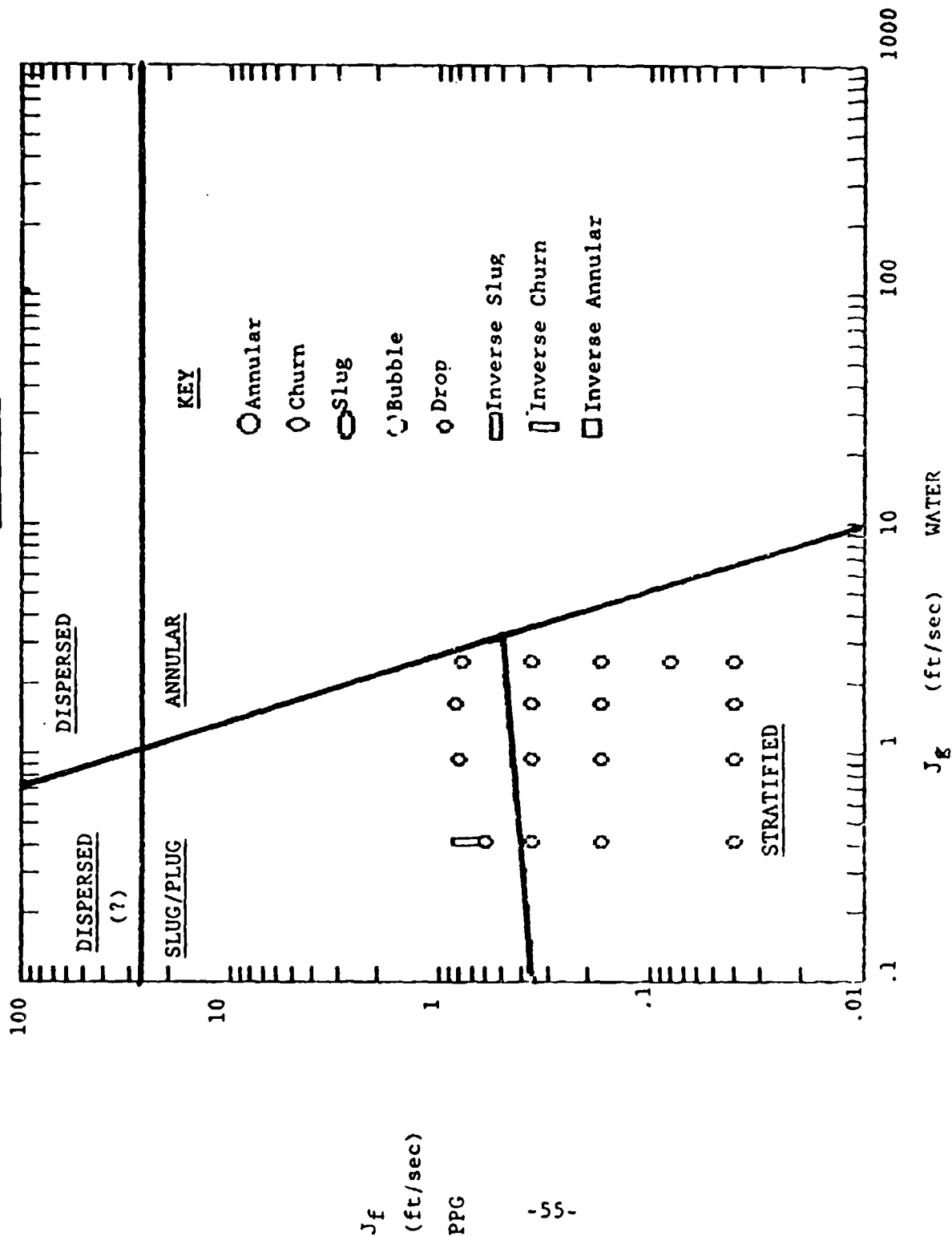


FIGURE 40

LABDATA <sup>2</sup> (HORIZONTAL DATA)  
 PPG-2000 and WATER at 77 F  
 Compared to Weisman Horizontal Flow Regime Map Predictions  
 (Predicted Flow Regimes are UNDERLINED)



$J_f$   
 (ft/sec)  
 PPG

$J_g$  (ft/sec) WATER

FIGURE 41

**LABDATA 5 (HORIZONTAL DATA)**  
 PPG-2000 and WATER at 77 F  
 Compared to Weisman Horizontal Flow Regime Map Predictions  
 (Predicted Flow Regimes are UNDERLINED)

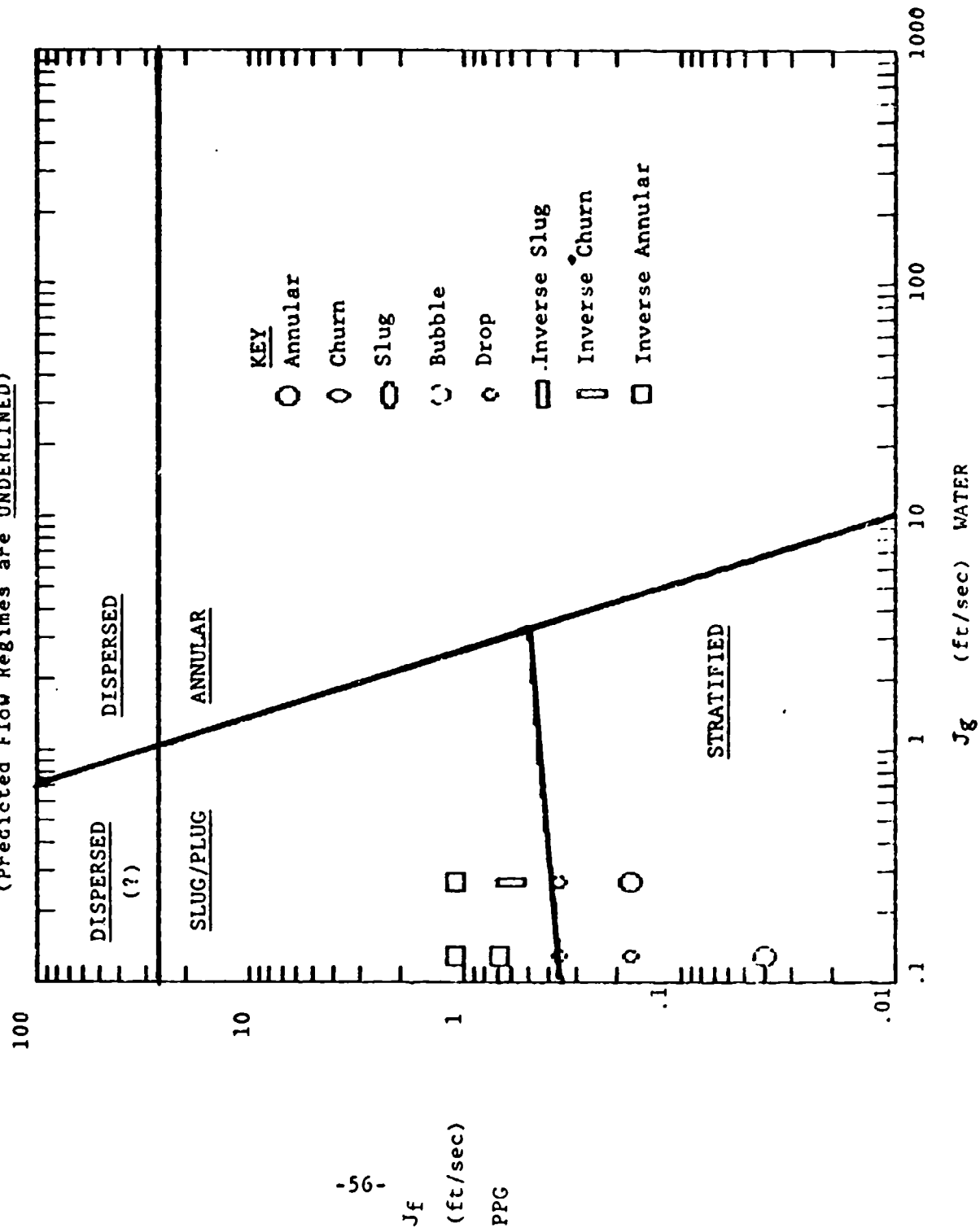


FIGURE 42

LABDATA 6 (HORIZONTAL DATA)  
 PPG-2000 and WATER at 77 F  
 Compared to Weisman Horizontal Flow Regime Map Predictions  
 (Predicted Flow Regimes are UNDERLINED)

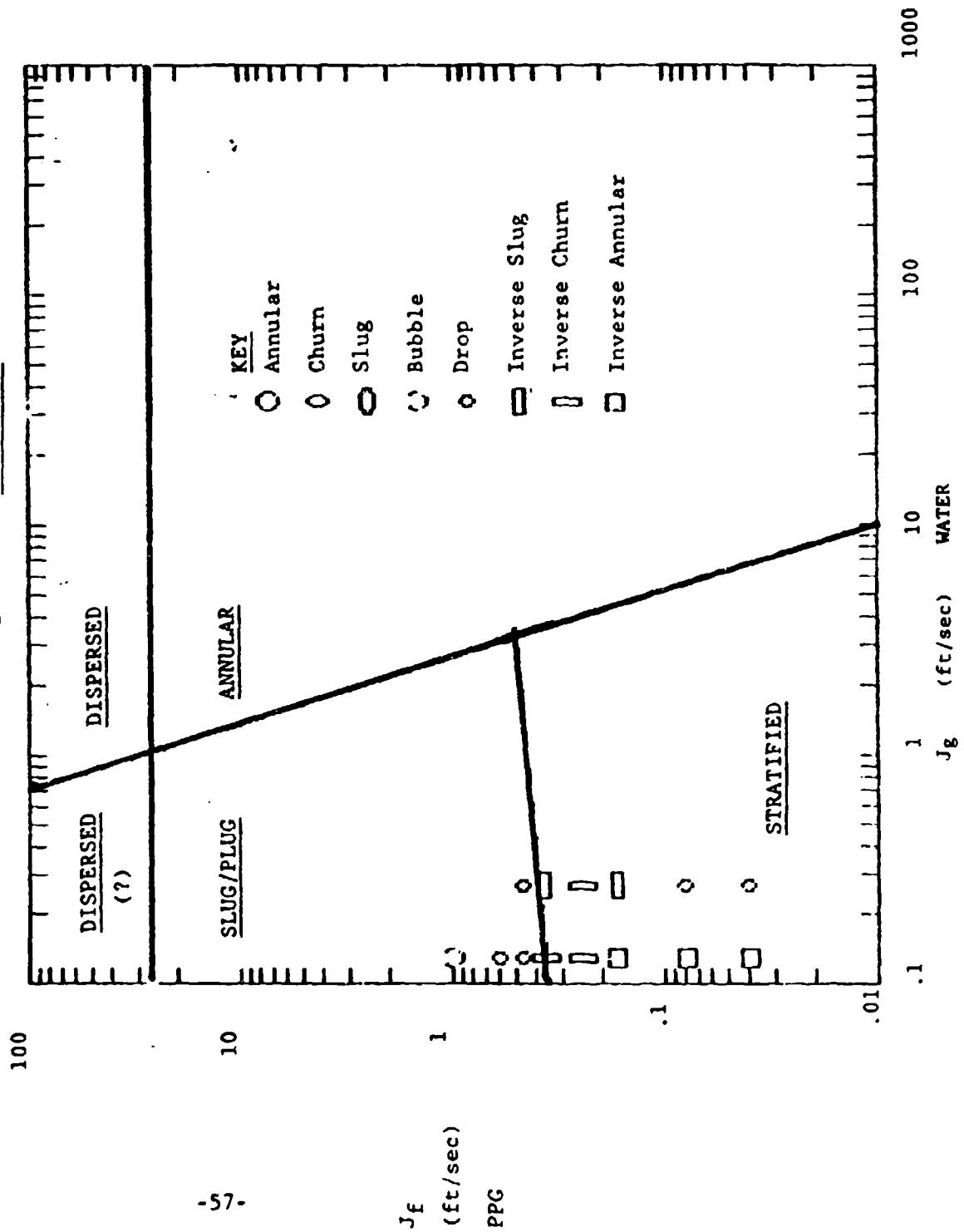


FIGURE 43

LABDATA 1 (HORIZONTAL DATA)  
 PPG - 2000 and WATER at 77° F  
 Compared to Dukler-Taitel Vertical Flow Regime Map Predictions  
 (Predicted Flow Regimes are UNDERLINED)

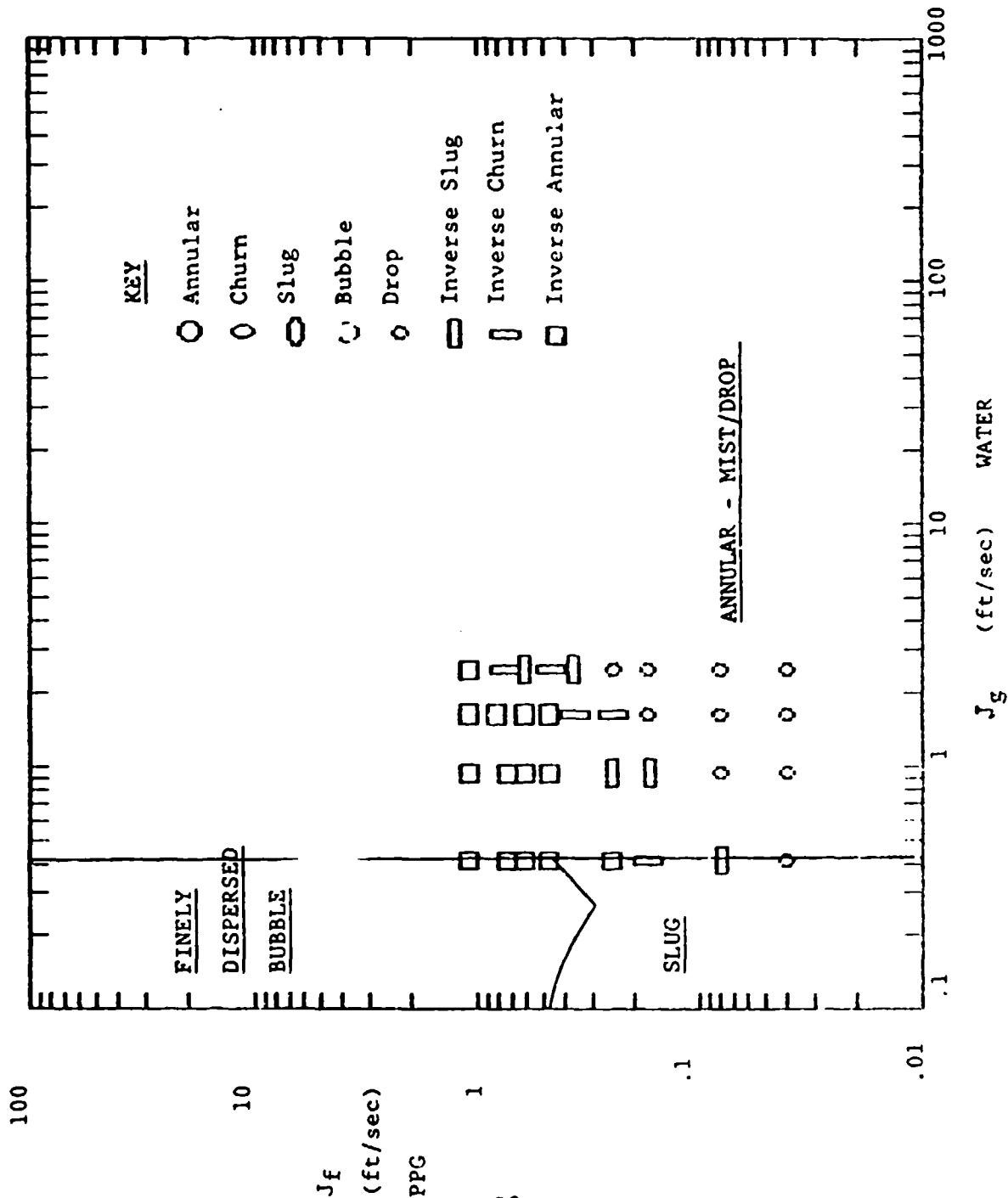


FIGURE 44

LABDATA 2 (HORIZONTAL DATA)  
 PPG - 2000 and WATER at 77°F  
 Compared to Dukler-Taitel Vertical Flow Regime Map Predictions  
 (Predicted Flow Regimes are UNDERLINED)

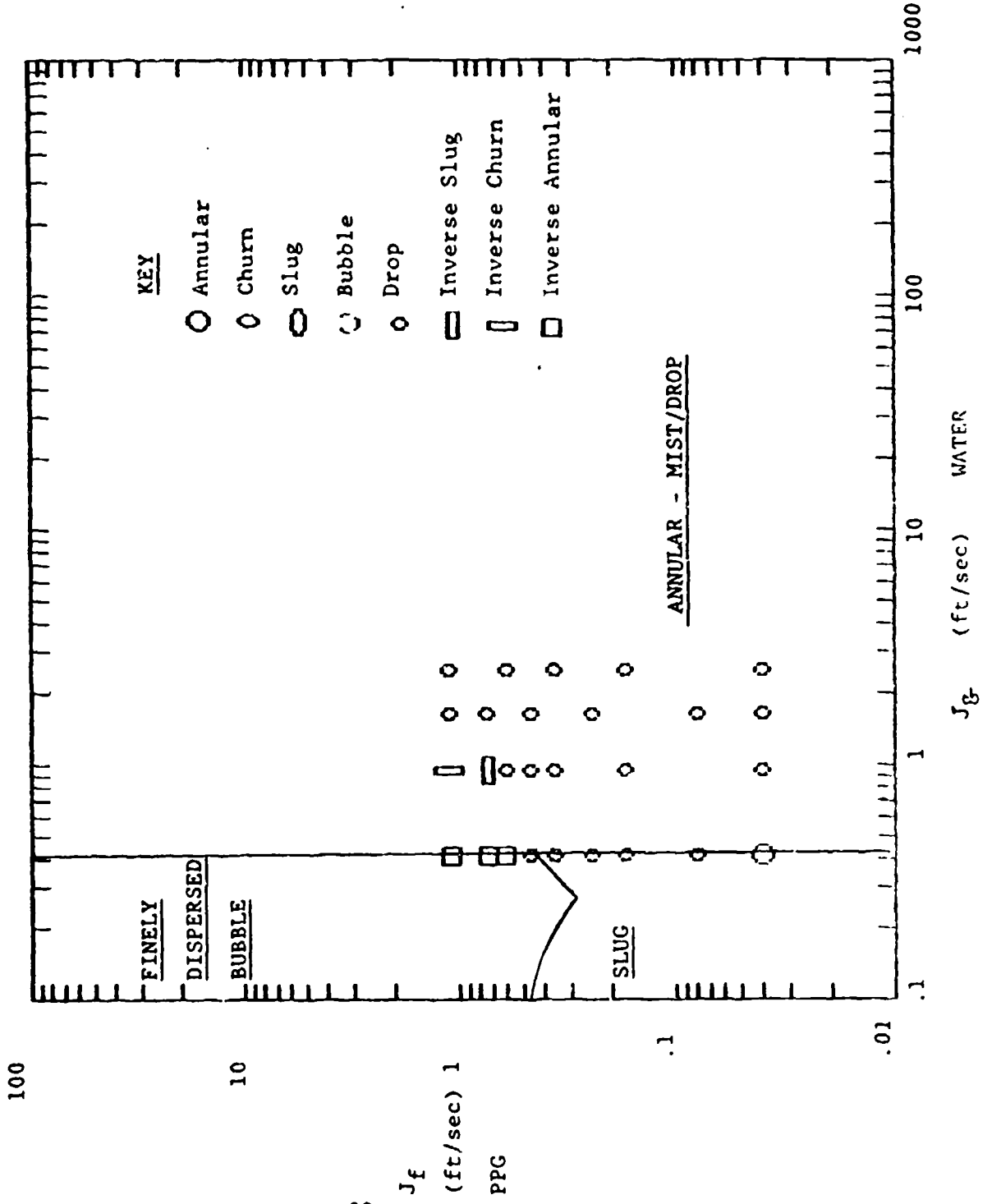


FIGURE 45

LABDATA 3 (HORIZONTAL DATA)  
 PPG - 2000 and WATER at 77°F  
 Compared to Dukler-Taitel Vertical Flow Regime Map Predictions  
 (Predicted Flow Regimes are UNDERLINED)

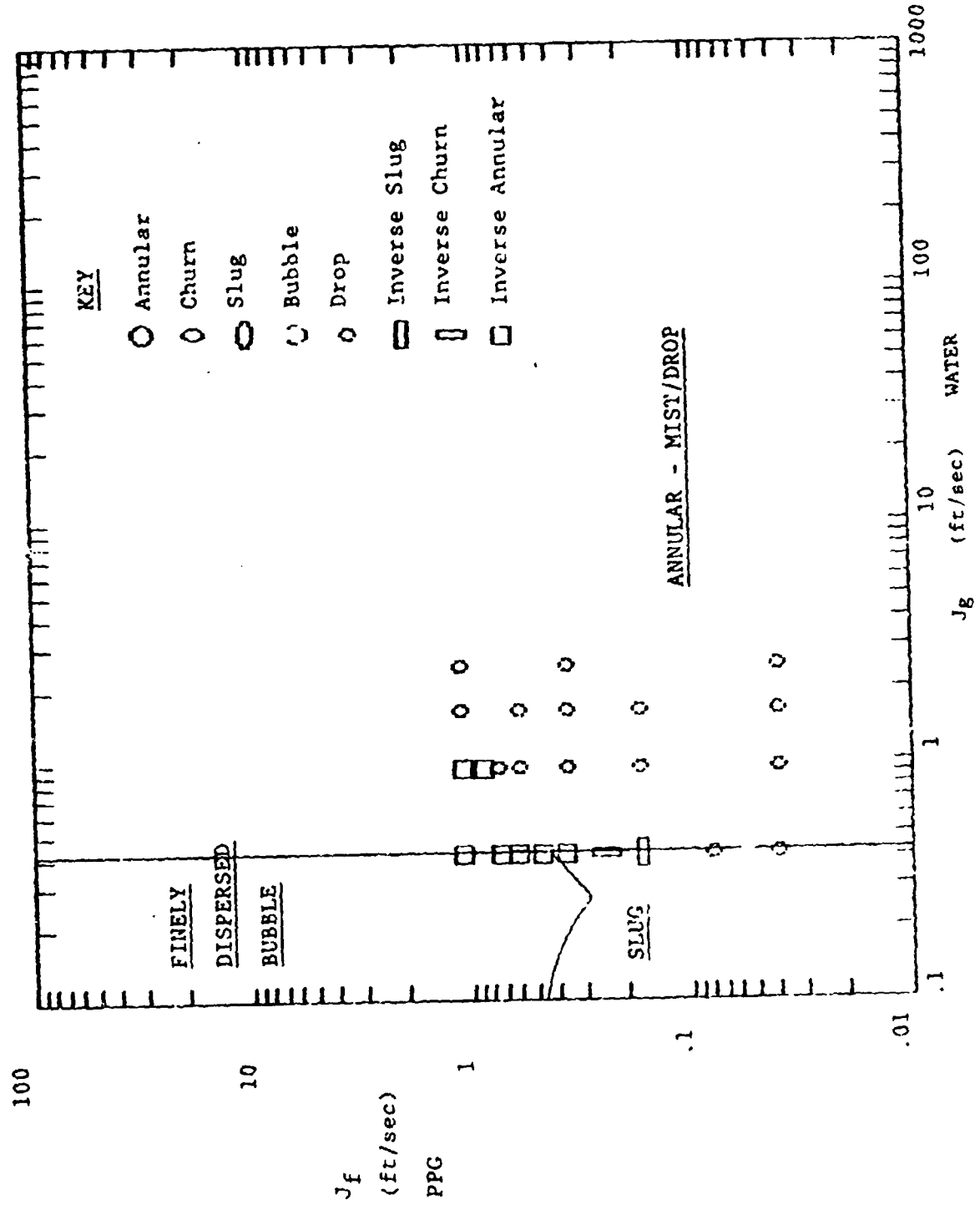


FIGURE 46

LABDATA 4 (HORIZONTAL DATA)  
 PPC - 2000 and WATER at 77°F  
 Compared to Dukler - Taitel Vertical Flow Regime Map Predictions  
 (Predicted Flow Regimes are UNDERLINED)

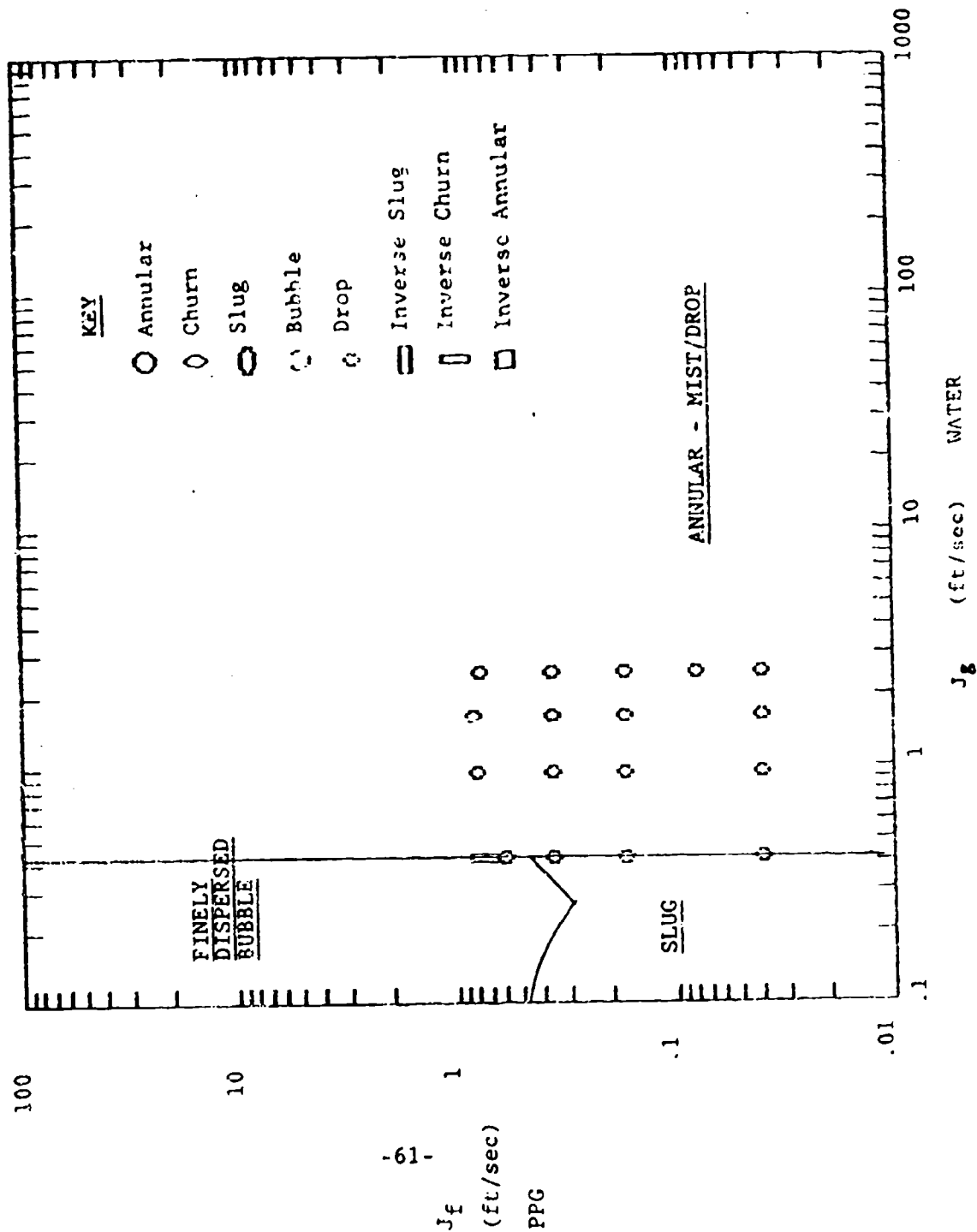


FIGURE 47

LABDATA 5 (HORIZONTAL DATA)  
 PPG - 2000 and WATER at 77°F  
 Compared to Dukler-Taitel Vertical Flow Regime Map Predictions  
 (Predicted Flow Regimes are UNDERLINED)

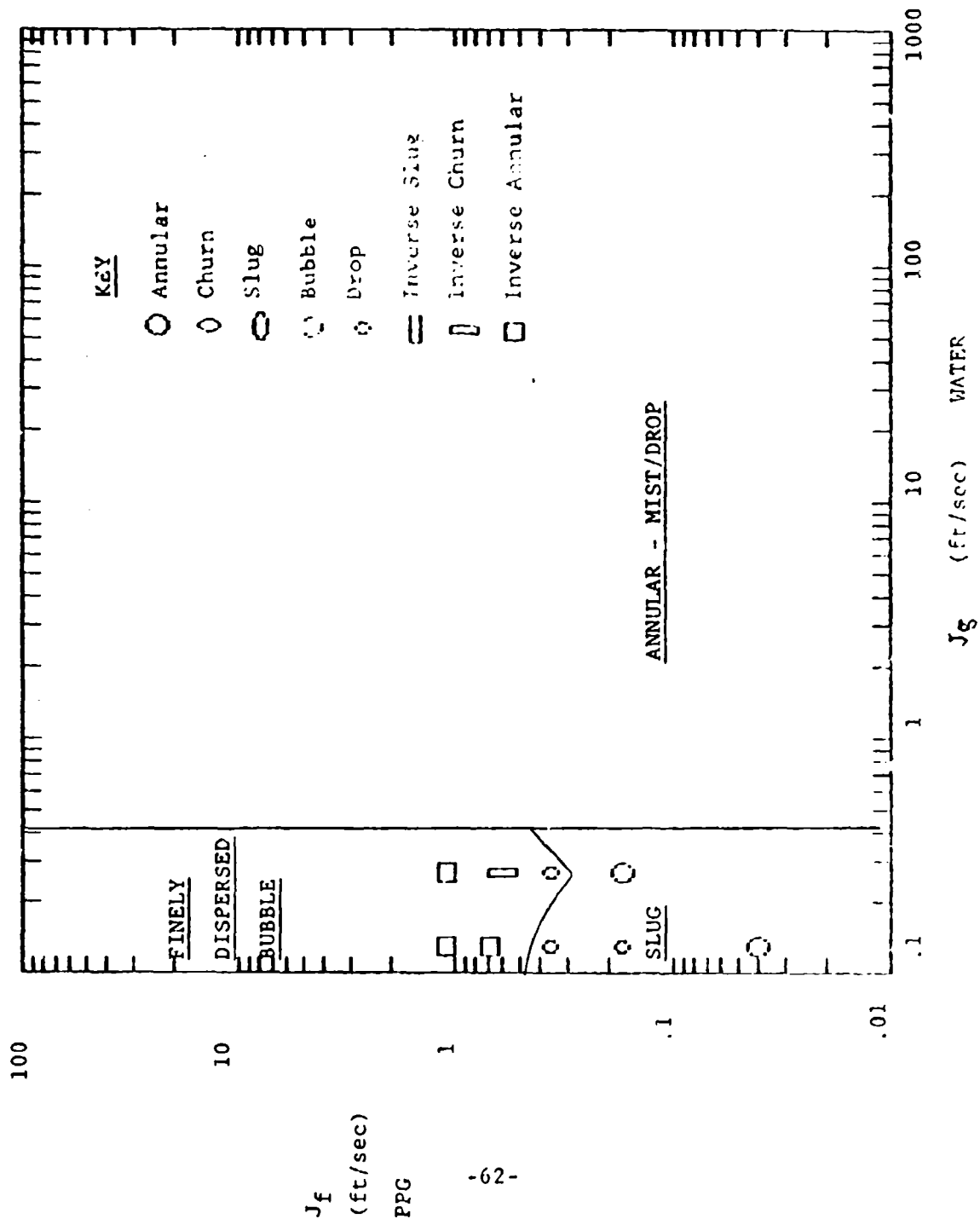
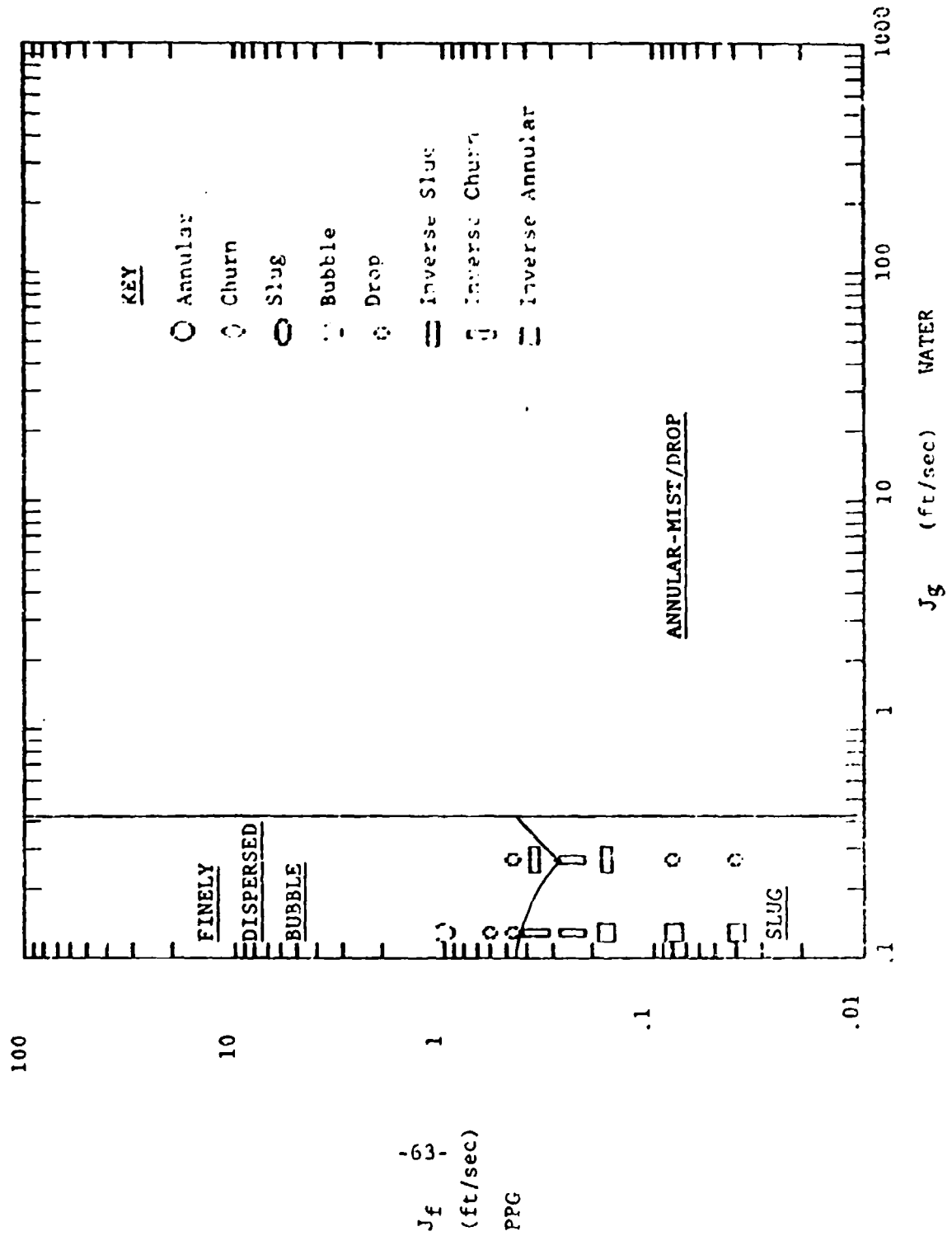


FIGURE 48

LABDATA 6 (HORIZONTAL DATA)  
 PPG - 2000 and WATER at 77°F  
 Compared to Dukler - Taitel Vertical Flow Regime Map Predictions  
 (Predicted Flow Regimes are UNDERLINED)



actual laboratory conditions. Again, it is immediately apparent that the Dukler-Taitel Vertical Flow Regime Map does not fit the laboratory data. Comparing our lab data (from horizontal tubes) to the vertical Dukler-Taitel predictions is admittedly a misapplication of the Vertical Dukler-Taitel Flow Regime Map. Much of its math depends on the vertical buoyancy effect. However, since this effect is so small in our experiments, we have compared it with our lab data. The comparison is offered with the reasoning that it might be of benefit, since logically, a fully general vertical flow regime map would predict correct horizontal behavior as long as the gravity or buoyancy term was zero or very close to zero. In any event, the results of this comparison with our lab data do not encourage the use of the Dukler-Taitel vertical flow regime map for fluids of near or equal densities.

The majority of data falls in the region predicted as annular flow. Without going into further details, it is clear that this flow regime map, like the other, fails to differentiate the flow regimes observed.

#### **Weisman Vertical Flow Regime Map**

Figure 49 shows the Weisman Vertical flow regime map on its familiar  $\log G$  vs.  $\log X$  co-ordinates. Note that the dispersed and annular boundaries intersect in a way that is difficult to understand what regime is predicted. We assumed the dispersed regime is predicted in the region in question.

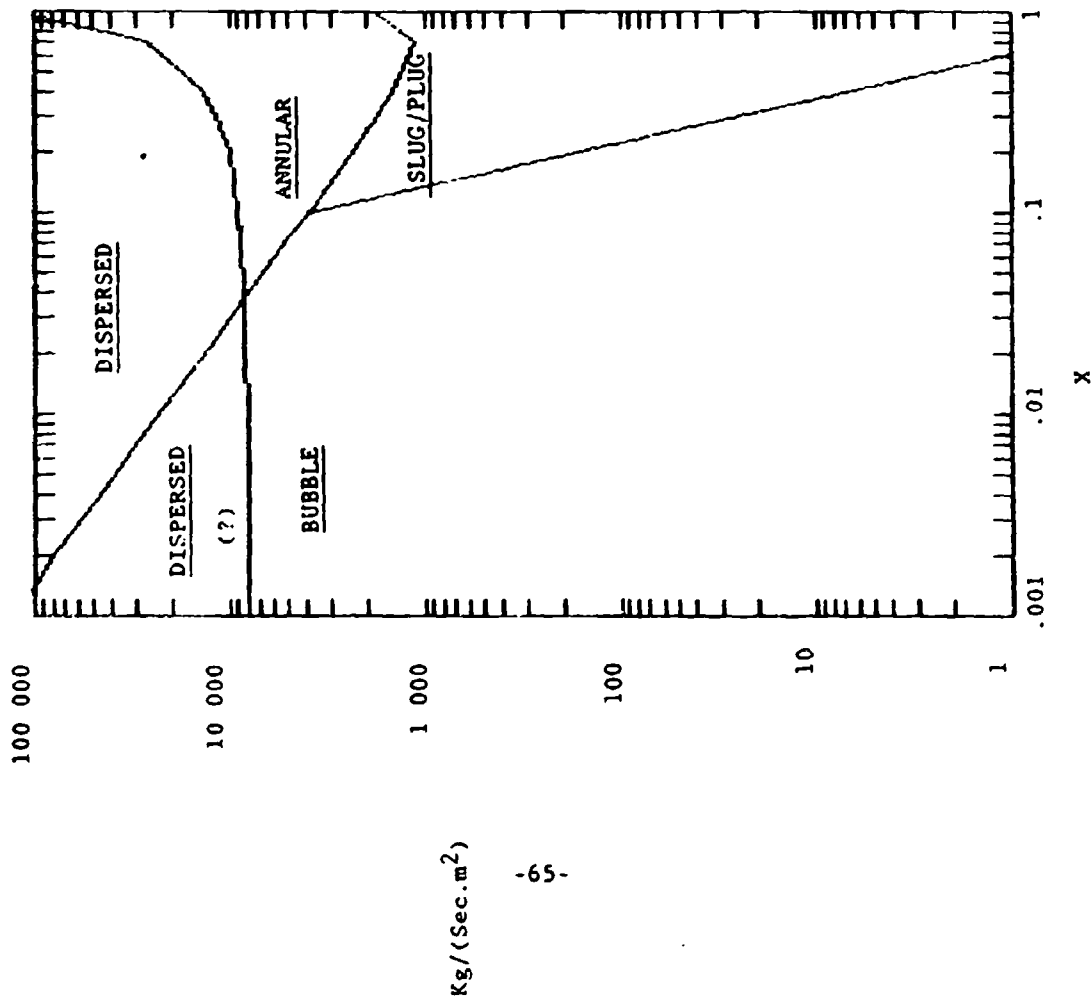
Figures 50-55 show the Weisman Vertical flow regime map predictions plotted with our lab data on a  $\log J_f - \log J_g$  plot. Since the buoyancy effect is so small, and the horizontal model predicted the results so poorly, we present this comparison as a point of interest. Virtually all the various flow regimes observed in our experiments fall into the region predicted as "slug/plug". Clearly, this particular flow regime map fails to differentiate or predict the observed flow regimes when the buoyancy force is minimized.

### **VI. COMMENTARY ON FLOW REGIME MAPS**

#### **The Weisman Maps (Vertical and Horizontal)**

Beyond the observations already offered, we have no commentary on the Weisman flow regime predictions. The Weisman flow regime models are apparently based on correlation schemes which include relevant physical properties, but which do not seem to reflect any particular physical model. Therefore, analytical critique or modification is difficult.

FIGURE 49



WEISMAN VERTICAL  
Flow Regime Map Predictions  
for PPG - 2000 and WATER  
at 77° F (PPG taken as the  
liquid)  
Mass Velocity plotted against  
Quality (MKS units)

$\text{Kg}/(\text{Sec} \cdot \text{m}^2)$

FIGURE 50

LABDATA 1 (HORIZONTAL DATA)  
 PPG-2000 and WATER at 77 F  
 Compared to Weisman Vertical Flow Regime Map Predictions  
 (Predicted Flow Regimes are UNDERLINED)

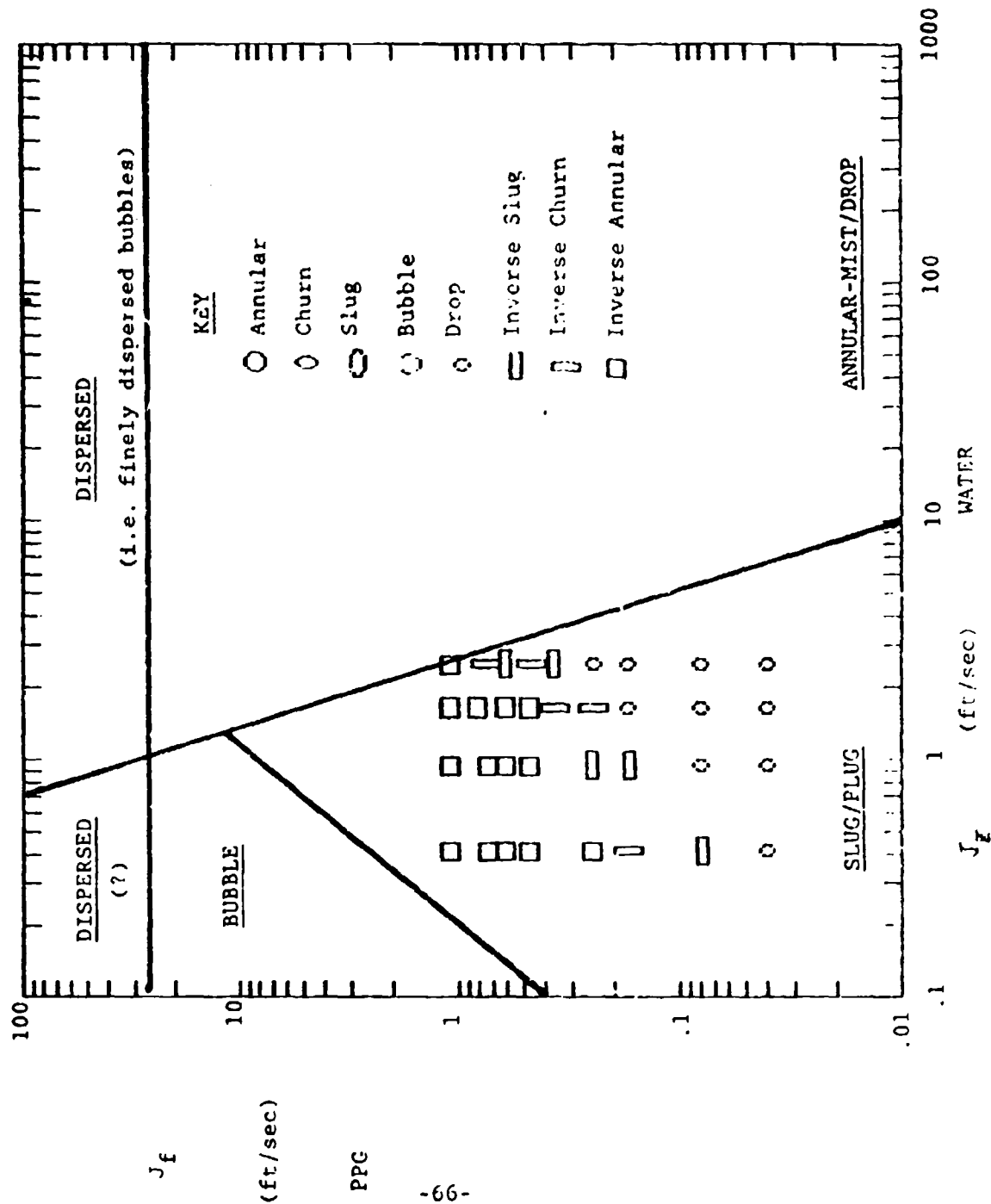


FIGURE 51

LABDATA 2 (HORIZONTAL DATA)  
 PPG-2000 and WATER at 77 F  
 Compared to Weisman Vertical Flow Regime Map Predictions  
 (Predicted Flow Regimes are UNDERLINED)

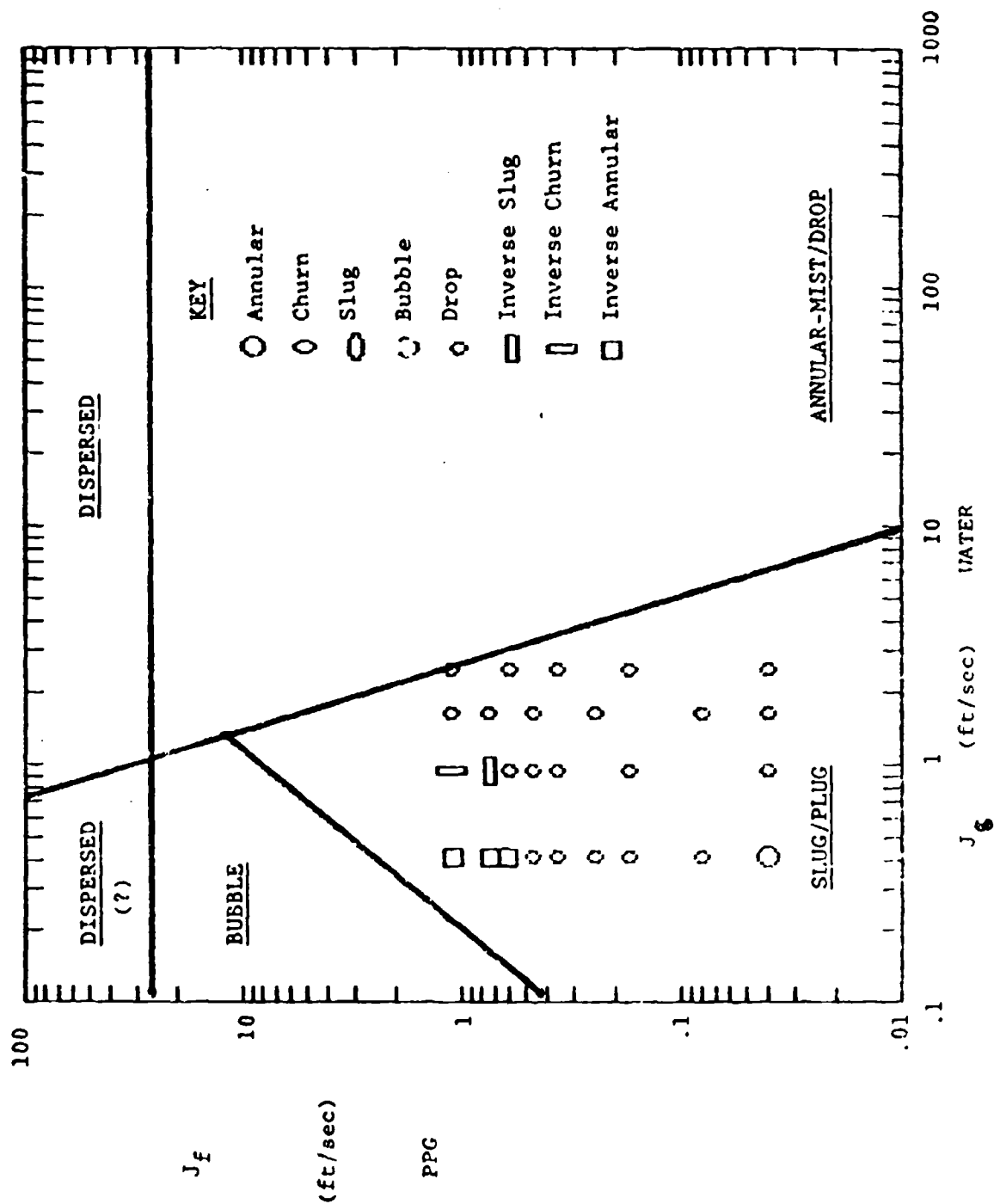


FIGURE 52

LABDATA 3 (HORIZONTAL DATA)  
 PPG-2000 and WATER at 77 F  
 Compared to Weisman Vertical Flow Regime Map Predictions  
 (Predicted Flow Regimes are UNDERLINED)

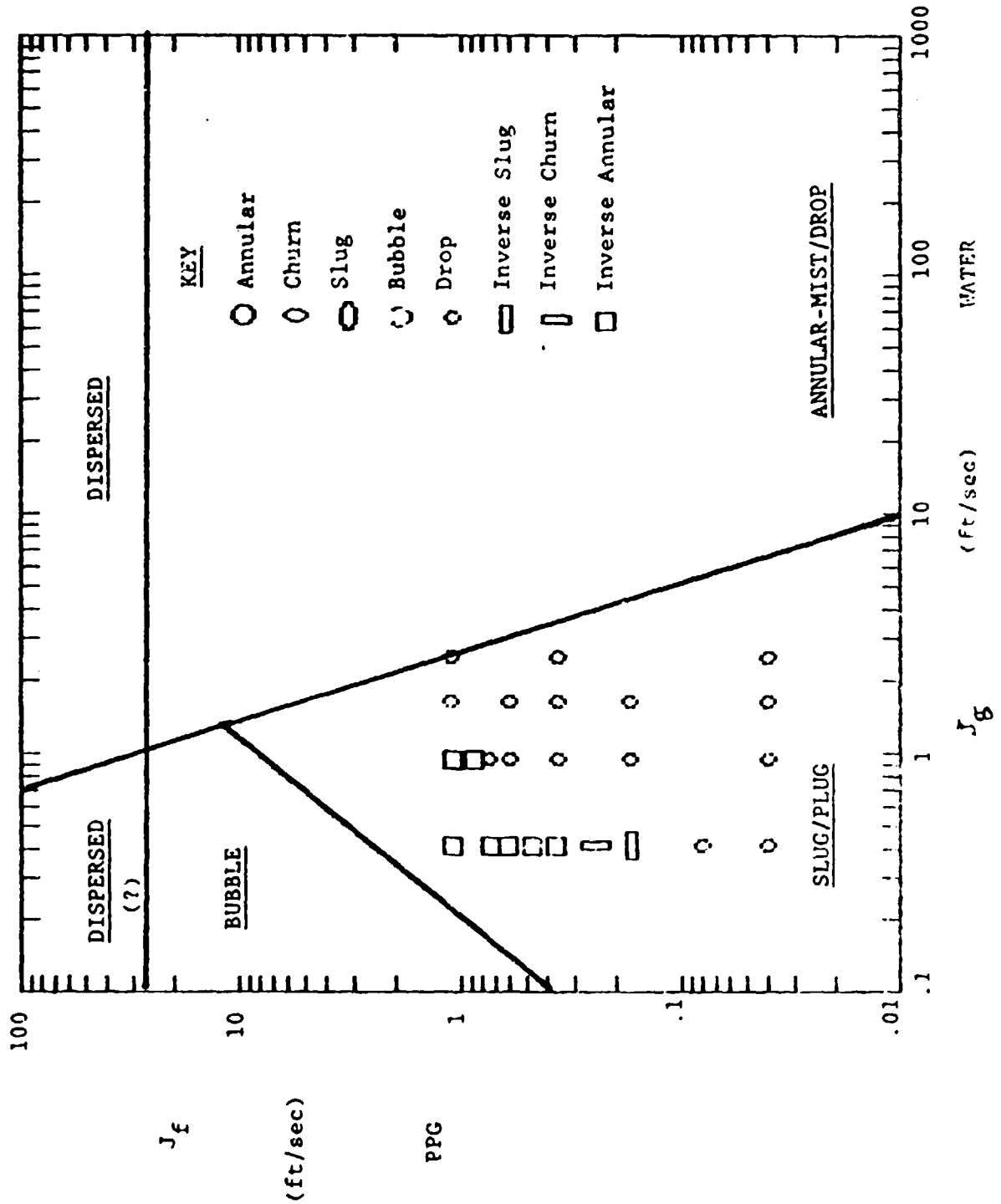


FIGURE 53

LABDATA 4 (HORIZONTAL DATA)  
 PPG-2000 and WATER at 77 F  
 Compared to Weisman Vertical Flow Regime Map Predictions  
 (Predicted Flow Regimes are UNDERLINED)

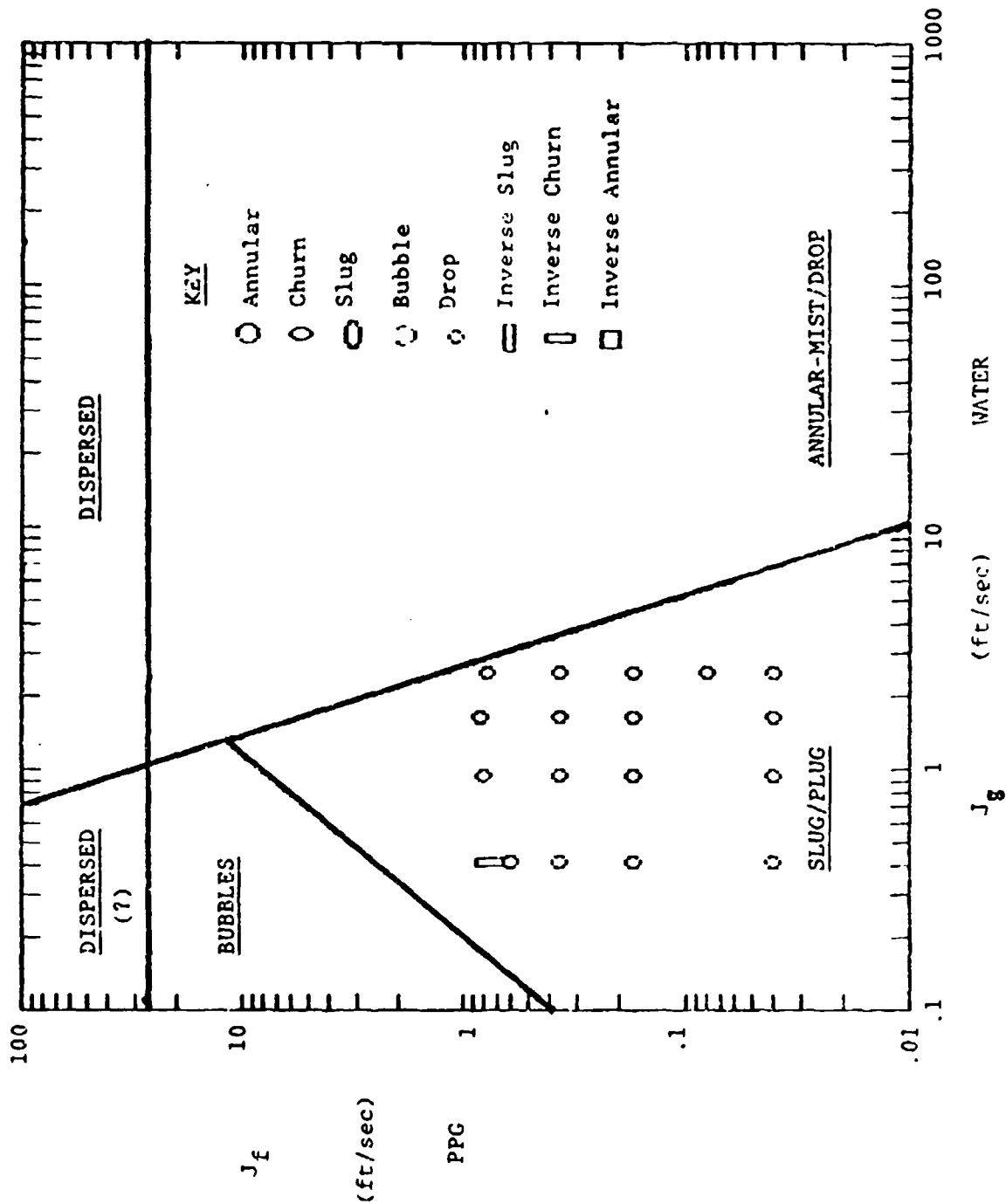


FIGURE 54

LABDATA 5 (HORIZONTAL DATA)  
 PPG-2000 and WATER at 77 F  
 Compared to Weisman Vertical Flow Regime Map Predictions  
 (Predicted Flow Regimes are UNDERLINED)

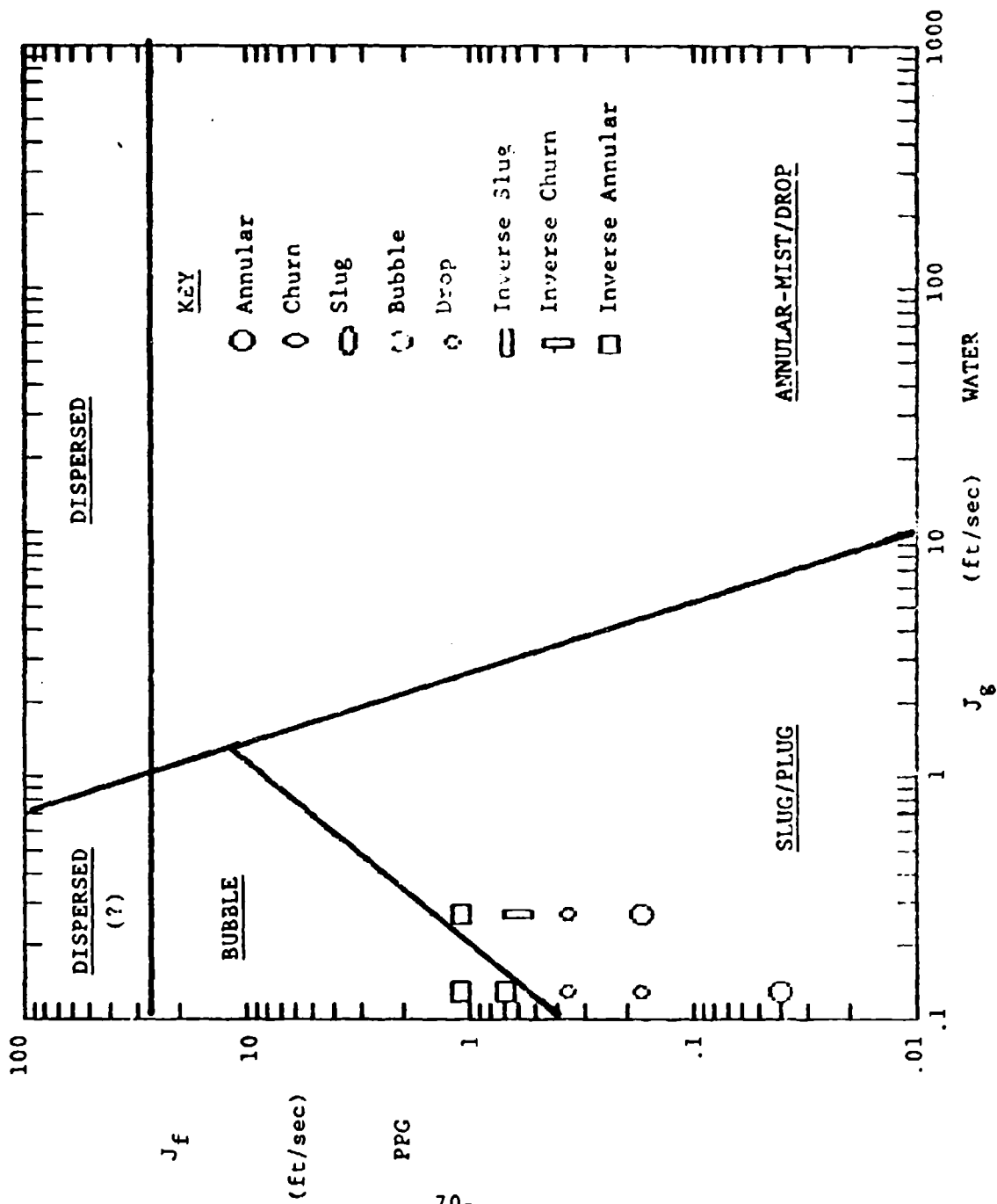
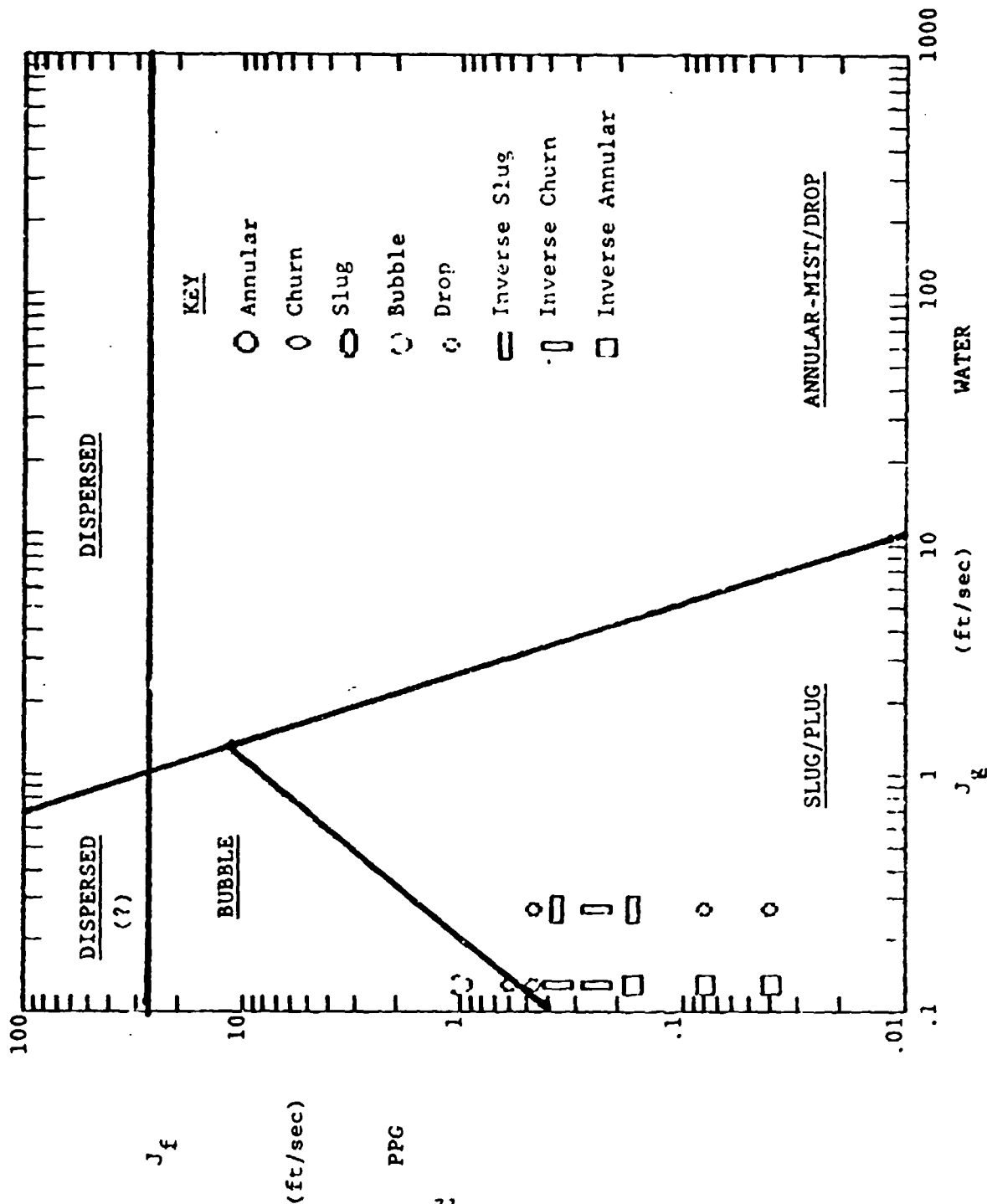


FIGURE 55

LABDATA 6 (HORIZONTAL DATA)  
 PPG-2000 and WATER at 77 F  
 Compared to Weisman Vertical Flow Regime Map Predictions  
 (Predicted Flow Regimes are UNDERLINED)



## The Dukler-Taitel Horizontal Flow Regime Map

The Dukler-Taitel Horizontal flow regime map is based on the assumption that the vapor-liquid flow always tends toward stratified flow, and that instability conditions create other, (non-stratified) flow regimes. That is, the (non-linear differential) equations of flow are always solved assuming that the flow starts in the stratified flow regime. A force balance is solved between the vapor and liquid flow and the wall shear, assuming a stratified condition. Then stability conditions are applied to see if:

- a. Waves form (which gives WAVY flow);
- b. Waves grow beyond the tube diameter (i.e., "exponentially" and unstably);
  1. which give INTERMITTENT (i.e., "SLUG") flow if the originally assumed stratified flow equations at this vapor-liquid flow rate had a void fraction of 50% or greater;
  2. which give ANNULAR-MIST/DROP flow if the originally assumed stratified force balance at this vapor-liquid flow rate had a void fraction of less than 50%;
- c. The liquid flow rate is sufficient to break up and disperse the vapor slugs into bubbles, and DISPERSED (or BUBBLY) flow is predicted, given intermittent flow.

The most important point for the Dukler-Taitel horizontal flow regime map is that the whole map is predicated on the calculated physical relationships arising from an assumed initial stratified flow. Thus, on theoretical grounds alone, zero gravity conditions are obviously beyond the range of validity of the Dukler-Taitel horizontal flow regime map.

Experimentally we have shown the same result, even where the gravity term is non-zero, but minimal. That is, with minimal buoyancy forces, our experiments showed that the Dukler-Taitel horizontal flow regime map did not predict flow regime behavior well at all.

## The Dukler-Taitel Vertical Flow Regime Map

The Dukler-Taitel Vertical flow regime map bases a number (but not all) of its curves on either a bubble rise velocity or a slip velocity based on a gravity field. The annular curve, for example, is based on the Kutateladze Number, a dimensionless group which balances the vapor inertial force against gravity and surface tension. This same analysis has been used to predict the

upper limit (i.e., no liquid downflow) to counter-current vapor-liquid vertical flow.

Without discussing every curve of Dukler-Taitel in detail, it is clear that this flow regime map assumes a gravity term. The assumed physics and therefore the mathematical modeling, is inappropriate when a zero, or possibly minimal gravity term is assumed. Thus, analytical considerations indicate that the Dukler-Taitel vertical map cannot be extrapolated to zero gravity.

Again, our experiments indicate the same conclusion. The Vertical Dukler-Taitel map is not valid in ranges of zero or minimal gravity (i.e., buoyancy) effects.

## VII. ANALYTICAL WORK

Initial work for zero gravity two-phase flow regime analysis is presented here. Appendix A contains a tentative analysis of entrainment. In that discussion and the abbreviated summary below we show that:

1. A shear velocity exists in zero gravity or in our experiments as one fluid phase experiences wall drag and the other fluid phase flows more freely in the core of the pipe;
2. Entrainment mechanisms, which are driven by the above shear velocity, cause the formation of a drop flow;
3. Sufficient drops in the core will form inverse slug flow, then inverse churn flow, then inverse annular flow;
4. In general, de-entrainment balances against entrainment to determine the steady-state concentration of drops in the core. In our own experiments, since  $\rho_f = \rho_g$ , a de-entrainment mechanism is lacking. Therefore, inverse annular flow occurs sooner than where  $\rho_f > \rho_g$ , since there is no way for droplets of equal density, once entrained, to leave the core. The core becomes overloaded with droplets, which coalesce to form inverse annular flow. A de-entrainment mechanism would exist if  $\rho_f > \rho_g$ , since droplets, unable to closely follow every movement of the core gas flow, would impinge on the liquid film on the pipe perimeter.

For zero-gravity two phase flow, the important parameters and properties are:

$$J_f, J_g \propto \rho_f, \rho_g, D, \mu_f, \mu_g, \sigma^{(1)}$$

In our experiments to simulate zero-gravity on earth we used two immiscible liquids of approximately the same density. This prevents stratification effects in horizontal tube flow and countercurrent flow in vertical flow which would both normally occur on earth if the fluids were of unequal density. However, the use of equal density fluids also prevents large relative velocities between the two phases. Large relative velocities occur when inertia is the dominant factor in the overall pressure drop. It is well known that when inertia is a dominant factor:

$$\Delta P \propto \rho_f V_f^2 \quad (2a)$$

and also that:

$$\Delta P \propto \rho_g V_g^2 \quad (2b)$$

These two relations imply:  $V_g / V_f = \sqrt{\rho_f / \rho_g}$  (3)

However, equation 3 results in unrealistically large velocity ratios (slip ratios) of the two phases. In reality, inter-phase shear forces will keep the slip velocity much less than Eqn 3 indicates. Nevertheless, slip velocities will be present. In cases of large slip velocity the gravity term becomes secondary. That is, stratification does not occur. Therefore already existing data on the earth's surface are probably quite valid for zero gravity flow as well.

Because our simulation of zero-gravity two-phase flow was accomplished with two liquids of equal densities the flow in our experiments is close to homogeneous flow. However, even with the same density for the two phases, relative velocities do exist. Namely, at certain flow rates, one of the two phases flows preferentially along the walls of the duct. Thus, the average velocity of this "wall" phase is smaller than the average velocity of the phase in the core. The relative velocity between the two phases gives rise to a shear force at the interface which in turn results in entrainment, if the shear force is sufficiently large. A discussion and tentative analysis of this relative velocity and the resulting entrainment is given in Appendix A.

From the above considerations of zero gravity two-phase flow, we can deduce several nondimensional parameters:

$$Re_f = \frac{\rho_f J_f D}{\mu_f} \quad (4)$$

$$Re_g = \frac{\rho_g J_g D}{\mu_g} \quad (5)$$

Further we need one parameter which contains surface tension. A surface tension parameter can be deduced from the ratio of the dimensionless inverse viscosity (eqn. 10.16 of Ref. 10) to the Eotvos - number, (eqn. 10.14 of Ref. 10). (The EOTVOS number is the ratio of density effects to surface tension).

$$N = \frac{N_f^2}{N_{eo}} = \frac{D^3 g (\rho_f - \rho_g) \rho_f \sigma}{\mu_f g D^2 (\rho_f - \rho_g)} = \frac{\rho_f \sigma D}{\mu_f} \quad (6)$$

We should be aware that N is a constant in any apparatus (or in our experiments) as long as the geometry and the fluids used remain the same.

Equations 4, 5, and 6 contain all the parameters necessary to describe zero gravity two phase flow. These parameters were listed in equation 1. However, before an analysis can proceed, void fraction (or equivalently, slip velocity) must be determined.

Appendix A shows one way to deduce void fraction from a slug flow relationship. The result from Appendix A is

$$\alpha = \frac{1/C_1}{1 + J_f/J_g} \quad (7)$$

This relationship was used because slug flow was observed in our experiments. This result needs to be verified quantitatively.

In Appendix A the reasoning to produce an analysis of entrainment was performed. However, this analysis is still tentative at this point. More experiments with other fluids in zero gravity will have to be done before general conclusions can be drawn.

If entrainment of liquid occurs in actual zero-gravity vapor-liquid flow there will also be a certain amount of de-entrainment. That is, some entrained liquid droplets, swept along by the vapor flow, will be deposited on the continuous liquid phase, usually at the wall. This de-entrainment is due to the density difference between vapor and liquid. Droplets of liquid have a high inertia, and are moving laterally to the vapor flow, probably due to the vapor's turbulence. An analysis of de-entrainment is necessary to fully predict zero gravity two phase flow. The balance of entrainment and de-entrainment mechanisms will yield a net quantity of entrained liquid, which will be a major factor in determining the flow regime. For example, as more drops remain entrained in the core vapor flow, they will tend to coalesce. The flow regime would then change successively from drop to inverse slug to inverse annular flow.

## VIII. CONCLUSIONS

In Phase I it was proven that a useful simulation of zero-gravity vapor-liquid behavior can be accomplished with two immiscible liquids of equal density. With this experimental approach it has been shown that such phenomena as inverse annular flow do readily occur. The existing flow regime models are not able to predict the experimentally observed flow regimes in our experiments. The predicted flow regimes either did not occur at all or occurred where they were not predicted to occur. Furthermore, flow regimes such as inverse annular or inverse slug which were observed, weren't included in any of the flow regime models.

The present experiments also provided insights into a useful analysis of zero-gravity two-phase flow. Three dimensionless groups have been proposed which together should contain the necessary parameters to describe zero gravity two phase flow.

The agreement among the different flow regime models is rather poor when the gravity constant or the density difference between the phases is reduced. This suggests limited applicability of such models outside their range of experimental verification. It can thus be concluded that a universal theory for flow regime prediction does not exist at this point and data is needed to develop flow regime maps, particularly for zero gravity flow. It is hoped that these new flow regime maps can be combined with the considerations and comparisons of existing flow regime maps to produce a more universally applicable analytical model.

The data produced in this work, the important findings and parameters outlined above, and the initiation of an analysis are an encouraging start for the task of producing a true flow regime simulation scheme. As soon as a flow regime map for zero-gravity exists, correct pressure drop and heat transfer coefficients can be obtained much more easily. [11,12] Subsequently, the design of efficient heat exchanger equipment for spacecraft utilizing evaporation and/or condensation can be pursued more effectively.

## REFERENCES

1. Keshock, E.G.; Spencer, G.; French, B.L.; Williams, J.L., "A Photographic Study of Flow Condensation in I-G and Zero-Gravity Environments" (Appendix B to NASA-CR-144395) 1973
2. Heppner, D.B.; King, C.D.; Littles, J.W., "Zero-G Experiments in Two-Phase Fluids Flow Regimes", ME paper 75-ENAs-24 for Mtng July 1975.
3. Taitel, Y.; Dukler, A.E., "A Model For Predicting Flow Regime Transitions in Horizontal and Near Horizontal Gas-Liquid Flow", ASME paper 75-WA/HT -29 for mtng December 1975.
4. Cooper, M.G.; Judo, A.M.; Pike, R.A., "Shape and Departure of Single Bubbles Growing at a Wall", Cambridge University Engineering Department, 1978.
5. Oker, e.; Merte, Jr., H., "Transient Boiling Heat Transfer in Saturated Liquid Nitrogen and F113 at Standard and Zero Gravity", NASA - CR - 120202, 1973.
6. Vaughan, Jr., O.H.; Huny, R.J.; "Skylab Fluid Mechanics Simulations: Oscillations, Rotation, Collision and Coalescence of Water Droplets Under Low-Gravity Environment", Space Simulation, NASA SP-379 pp 563-574, 1975.
7. Williams, J.L.; Keshock, E.G.; Wiggins, C.L., "Development of a Direct Condensing Radiator for Use in a Spacecraft Vapor Compression Refrigeration System", Journal of Engineering for Industry (Transactions of the ASME), November 1973.
8. Taitel, Y.; Bornea, D.; Dukler, A.E., "Modeling Flow Pattern Transitions for Steady Upward Gas-Liquid Flow in Vertical Tubes", AIChE Journal (Vol. 26, No. 3) May, 1980.
9. Ishii, M.; De Jarlais, G.; "Flow Regime Transitions and Interfacial Characteristics of Inverted Annular Flow", Argonne National Laboratory, 1985.
10. Wallis, G.B., "One-Dimensional Two Phase Flow, McGraw-Hill, N.Y., 1969.
11. Collier, J.G., "Boiling and Condensation", McGraw Hill, N.Y. 1977.
12. Wolf, K.D., H.J. Richter, "Computer Program for Prediction of Pressure Drop and Heat Transfer in Evaporating Two Phase Flow", Dartmouth College, Hanover, NH 1983.
13. Eastman, R.E. Feldmanis C.J., Haskin, W.L., Weaver, K.L., "Two Phase Fluid Thermal Transport For Spacecraft" AFWAL-TR-84-3028, Wright Patterson Air Force Base, October 1984.

## APPENDIX A

### ENTRAINMENT ANALYSIS

A preliminary analysis of entrainment is presented here. The analysis shows promise of matching the data, although it is still too sensitive to several parameters to be completely satisfactory. As yet, no analysis of droplets coalescing to form inverse slugs, inverse churn flow, or inverse annular flow is being presented.

In the main analysis section of this report it was pointed out that at certain flow rates, one of the two phases flows preferentially along the walls of the flow duct. Thus, the average velocity of the "wall" phase is smaller than the average velocity of the phase in the core. The relative velocity between the two phases gives rise to a shear force at the interface. This shear force results in entrainment, if the shearing force is sufficiently large.

The relative velocity between the two phases can probably be described similarly to horizontal slug flow. (See p. 301, eqn (10.59) of Ref. 10):

$$V_g = C_1 J \approx 1.2 J = 1.2 (J_f + J_g) \quad (1)$$

In the referenced equation, the constant is more precisely described as

$$C_1 = \frac{V_g}{J} = 1 + 1.27 \left( 1 - e^{-3.8 \left( \frac{\mu_f}{J\sigma} \right)^{0.8}} \right) \quad (2)$$

Assuming that  $C_1$  = constant, then the void fraction is expressed as:

$$\alpha = \frac{J_g}{V_g} = \frac{J_g}{C_1 (J_g + J_f)} = \frac{1/C_1}{1 + J_f/J_g} \quad (3)$$

The above equation can be re-written as:

$$\frac{J_f}{J_g} = \frac{1}{C_1 \alpha} - 1 \quad (4)$$

A very common value for  $C_1$  is 1.2, (see Zuber REF 10). In this case equation (4) indicates that the void fraction must be less than 84% if there are to be reasonable values for  $J_f/J_g$ . Otherwise  $J_f/J_g$  is less than zero, which is impossible in zero gravity flow. However, this limitation should not be of concern

because the slug flow relationship (from which Eqn 3 is derived) is probably not valid at these high void fractions.

But Eqn. (4) gives lines of constant void fraction in the  $\log J_f$  vs.  $\log J_g$  plot used for plotting the data from the experiments (see enclosed figure). Also plotted was the function:

$$\frac{J_f}{J_g} = \frac{1}{\alpha} - 1 \quad (5)$$

which is valid for homogeneous flow (i.e.,  $C_1 = 1$  in eqn. (4)).

It is interesting to note that the transition line from "annular-mist" to "dispersed" flow is nothing but a line of constant void fraction.

The entrainment process can be examined in greater detail. Because of the relative velocity identified in Eqn.(4), entrainment would be expected if this relative velocity is sufficient to cause waves and subsequently entrainment from these waves.

Steen and Wallis claim that onset of entrainment occurs at

$$\frac{V_s \mu_g}{\sigma} \left( \frac{\rho_g}{\rho_f} \right)^{1/2} > 2.46 \times 10^{-4} \quad (6)$$

(see eqn. (12.43) from Reference 10)

It is safe to assume that  $V_s$  is the shear velocity causing the entrainment, thus

$$V_s = V_g - V_f \quad (7)$$

In this equation,  $V_g$  is the bulk velocity of the phase flowing in the center and  $V_f$  is the bulk velocity of the phase flowing at the wall. Thus it makes sense to use  $V_s$ , rather than the superficial velocity  $J_g$  as claimed by Steen.

With:  $V_f = J_f / (1 - \alpha) \quad (8)$

and Eqns. (10), (12) and (13) we get for the onset of entrainment

$$V_g - V_f = V_s > (2.46 \times 10^{-4}) \frac{\sigma}{\mu_g} \quad (9)$$

Remember that in the present case:  $\rho_f \approx \rho_g$

$$C_1(J_f + J_g) - \frac{J_f}{(1-\alpha)} > 2.46 \cdot 10^{-4} \frac{\sigma}{\mu_g} \quad (10)$$

These equations yield:

$$C_1(J_f + J_g) \left( 1 - \frac{J_f}{C_1(J_f + J_g) - J_g} \right) > 2.46 \cdot 10^{-4} \frac{\sigma}{\mu_g} \quad (11)$$

The surface tension between PPG and water is:

$$\sigma = \sigma_w + \sigma_{PPG} - 2(\sigma_w^d \sigma_{PPG}^d)^{1/2} \quad (12)$$

where it is estimated:  $\sigma_{PPG}^d \approx 20 \text{ dyne/cm}$ .

Where  $\sigma_w^d$  is the dispersion force contribution to surface tension of water in air.

From this it is concluded that:

$$\sigma = 62 \text{ dyne/cm}$$

With these values Eqn. (11) can be solved for onset of entrainment for different constants  $C_1$ . For  $C_1 = 1$  the left hand side of Eqn. (11) is zero, and entrainment will never occur. This is an expected result.

It is very disturbing that according to Eqn.(11) the result becomes very sensitive to the value of  $C_1$ . From Eqn. (11) it is seen for the present properties:

$$\frac{C_1(C_1 - 1)(J_f + J_g)^2}{C_1 J_f + (C_1 - 1)J_g} = 1.53 \times 10^{-2} \text{ m/s} \quad (13)$$

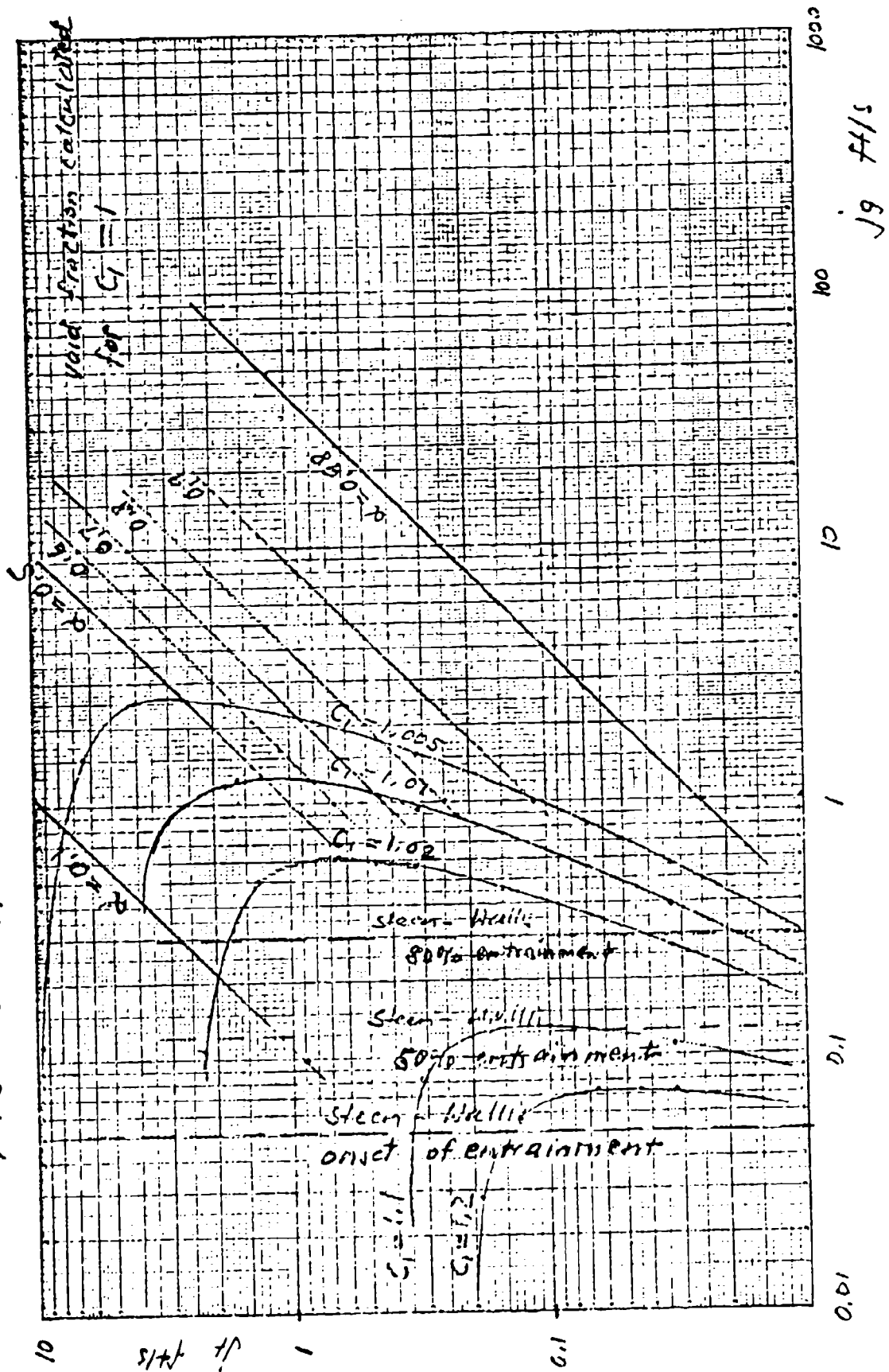
Here the equal sign is for onset of entrainment. Notice also that the right hand side is much smaller than unity. Thus, the denominator has to be much larger than the numerator.

It seems that a value of  $C_1 = 1.1$  to  $1.2$  is reasonable as suggested by Zuber. [10] Thus entrainment occurs already at  $J_f$  and  $J_g$  values smaller than  $0.01$  and  $0.1$  fps, as was observed.

Figure A1 shows Equation (11) plotted on a  $\log J_f$  v  $\log J_g$  plot. There are two solutions of  $J_f$  for each value of  $J_g$ . Only the larger value of  $J_f$  is physically reasonable for initiation of entrainment because only in this part of the curve does the onset of entrainment occur at decreasing liquid flows as the gas flow is increased. Qualitatively, this branch of the curve describes the transition from slug to dispersed flow quite well.

$s_4/s_3 \approx 1, \mu_4/\mu_3 = 1.5$

FIGURE A1



APPENDIX B  
LABORATORY DATA

# LABDATA 1

DATA POINT	COMMENTS
1	Large spherical drops of PPG almost fill tube; 6-10" apart; sometimes 2-3 drops pair up.
2	PPG forms bullet shaped "slugs" 2-4" long, 10-16" apart.
3	Irregular long PPG "slugs", almost inverse annular flow.
4	Inverse annular.
5	Inverse annular.
6	Inverse annular; some PPG drops in perimeter flow of water.
7	Same as above. More PPG drops in perimeter flow.
8	Same as above; many more PPG drops in perimeter flow.
9	PPG drops approximately 5 mm diameter.
10	Large PPG drops 2-3 at a time almost fill pipe; some small satellite drops.
11	Bullet shaped slugs of PPG; some small satellite drops.
12	Almost inverse annular; slugs are 24" long and touch each other.
13	Inverse annular.
14	Same as above; core has larger diameter. Some PPG drops in perimeter.
15	Same; more PPG drops in perimeter.
16	Same; but perimeter very cloudy due to many PPG drops. Almost looks emulsified.
17	PPG drops 1-2 mm diameter.
18	Same; 2 mm diameter PPG drops.
19	Same; 2-3 mm diameter PPG drops.
20	Same; 3-4-5 mm diameter PPG drops.

# LABDATA 1 (CONT.)

DATA POINT	COMMENTS
21	PPG drops: 5mm - 1 cm and not spherical; irregular shapes.
22	Irregular PPG drops lined up in core. Small spherical PPG drops in perimeter flow of water.
23	Almost inverse annular; PPG slugs touching each other.
24	Almost inverse annular. Breaks up occasionally to inverse churn or inverse slug flow.
25	Inverse annular.
26	PPG drops, 2-3 mm diameter.
27	PPG drops, 3-4 mm diameter.
28	PPG drops all sizes 1-10 mm in diameter, most 5 mm diameter.
29	Messy flow, irregular drops (inverse slug ? inverse churn?) PPG drops forming up in center.
30	Almost inverse annular 3-4" long PPG slugs; chaotic.
31	Inverse annular; less chaotic; PPG drops on perimeter (few), but large 5 mm diameter.
32	Very smooth continuous core of PPG. Very few PPG drops in perimeter flow of water.
33	Inverse annular flow, no perimeter flow of PPG drops; very "clean" rippling core, quite smooth.
34	Inverse annular, larger core. Less smooth. Some perimeter PPG drops.

## LABDATA 2

DATA POINT	COMMENTS
1	Thin PPG perimeter film; PPG drops in core diameter of 0-5 mm; last 12-18" PPG film is washing off perimeter.
2	Same as above; PPG drop diameters are 0-3 mm; last 2 - 2 1/2 ft are washed clean of PPG film.
3	Same; more PPG drops, 0 - 4,5 mm diameter.
4	Same; up to 6 mm diameter PPG drops.
5	Same, but "chimney effect" starts (PPG drops tend towards center of pipe). Diameter of PPG drops are all about same, 10mm.
6	Same, some large irregular shaped PPG drops prefer core (center of pipe).
7	Inverse annular flow.
8	Inverse annular; many PPG drops almost emulsified outside of PPG core.
9	Same, fatter core of PPG.
10	Almost a mist of PPG some PPG drops to 2-3 mm diameter; very thin PPG film on wall.
11	Same; more drops of PPG some to 4,5 mm diameter.
12	Same; many small "emulsified" PPG drops; a few large PPG drops, irregular shape; possibly to 8,10 mm diameter.
13	Same; up to 5 mm diameter drops of PPG.
14	Same; more PPG drops; more irregular ones 5-8 mm diameter is the common size.
15	1-2" slugs of PPG in core forming a "train" of slugs.
16	More irregular; lots of drops of PPG; irregular shapes; almost a continuous core.
17	Tiny PPG drops almost emulsified; wall is washed of all PPG.

# LABDATA 2 (CONT.)

DATA POINT	COMMENTS
18	Same (many small drops); up to 1-2 mm diameter PPG drops.
19	Same ("emulsion" of small PPG drops); some drops up to 2-3 mm. Some thin PPG film exists up to 10 feet from entrance.
20	Thin PPG film for 17-20 feet; most PPG drops emulsified, a few as large as 4 mm diameter.
21	Same; mostly emulsified; some irregular drops up to 10 mm.
22	Same, a few more large, irregular drops PPG. Beginning to show signs of PPG large drops preferring core.
23	Fine PPG emulsion. <u>Thin</u> annular PPG film, some washing off of film at entrance.
24	Same.
25	Same.
26	Same. Some PPG drops are larger. PPG film remains on wall.
27	Same. Some PPG drops larger (up to 1-2 mm diameter).

### LABDATA 3

DATA POINT	COMMENTS
1	Drops of PPG; PPG film on wall. Some film is washing off. PPG drops up to 5,8 mm diameter a few of irregular shape.
2	PPG drops; large, many of irregular shape some 1-2 cm. Some tendency of PPG drops to flow in core.
3	"Train" of PPG slugs, 2-4" long, orderly; some small satellite PPG drops.
4	Train of PPG slugs 6-12" long each; orderly. Almost inverse annular flow.
5	Inverse annular; also large PPG drops (3-4 mm) in perimeter flow of water.
6	Same.
7	Same; fatter core, some 5-8 mm diameter PPG drops in perimeter.
8	Same; fatter PPG core "squishes" against PPG drops in perimeter flow.
9	Same. Some water bubbles in PPG core.
10	No PPG film; some large PPG drops up to 10 mm.
11	Same; some PPG film.
12	Same; a few irregular PPG large drops; PPG beginning to show preference for core.
13	Same; more irregular drops; small tendency of PPG to flow in core.
14	PPG shows strong preference to flow in core.
15	Inverse annular flow first forms.
16	Inverse annular; also some large PPG drops elsewhere (in perimeter flow of water).
17	Emulsified PPG (tiny drops); some PPG film, very thin.
18	Same; minimal PPG film.

LABDATA 3 (CONT.)

DATA POINT	COMMENTS
19	Same; some PPG drops to 1-2 mm diameter.
20	Same; minimal PPG film.
21	Emulsified PPG drops (tiny); some very thin PPG film on wall.
22	Thin PPG film. Tiny PPG emulsified drops.
23	Same.
24	Same.

# LABDATA 4

DATA POINT	COMMENTS
1	Small (0-1 mm) PPG drops; PPG film is totally washed off wall.
2	Same; more PPG drops (0-2 mm); some PPG thin annular film remains.
3	Same; no PPG film.
4	Same; fine emulsion of PPG drops.
5	Small, few PPG drops (0-1, 2 mm diameter); semi-cloudy due to large number of small drops.
6	Same; more cloudy, PPG drops 0-2, 3 mm in diameter.
7	Very cloudy; cannot see drop size (or PPG drops are all too small to see).
8	Same.
9	Same.
10	Small PPG drops 0-2 mm diameter no PPG film.
11	PPG drops 0-4 mm diameter; semi-cloudy.
12	Cloudy; PPG drops 0-3 mm diameter.
13	Cloudy emulsion of PPG drops; no annular PPG film ; more drops of PPG than above.
14	Some PPG film on wall; PPG drops 0-4 mm diameter.
15	Same; PPG film; PPG drops are "packed".
16	Same; PPG diameter of 4-5 mm; drops "packed" no preference for core.
17	Same.
18	Irregular PPG shapes; PPG film on wall; definite preference of PPG to flow in core.

# LABDATA 5

DATA POINT	COMMENTS
1	Simultaneous annular and inverse annular flow significant PPG film (i.e., thick film of PPG on perimeter, center core of PPG flow, with water inbetween).
2	Simultaneous annular and inverse annular; significant PPG film; also, PPG irregular shaped drops in water.
3	Annular; but core of H <sub>2</sub> O is full of PPG drops large and small sizes, jammed together.
4	Annular; large PPG drops; in places PPG film is quite thick; washed off in other places.
5	Annular; thick perimeter PPG film re-establishing itself; a few small and large PPG drops in core.
6	Simultaneous annular/ inverse annular.
7	Almost same; PPG core is segmented.
8	No PPG core preference; packed PPG drops of irregular shape.
9	Annular (water core) large PPG drops, not very packed. Mostly regular spherical shape.

# LABDATA 6

DATA POINT	COMMENTS
1	Continuous slow "core" of PPG moves in bottom of pipe.
2	Same; some large drops PPG in water.
3	Same; some small PPG drops; an occasional break in PPG core.
4	Messy flow; PPG core broken; slugs/"plugs" 2" - 8" long of PPG (churn flow?).
5	Same; very irregular PPG drops; still tendency for PPG to be in core.
6	Large PPG drops (1 cm), some irregular shape; water at entrance tends to flow in core (annular flow).
7	Same; water at entrance tends to flow in core.
8	Water bubbles in core; water bubbles are full of PPG drops; annular (water core) for first 5 feet.
9	PPG drops 5-10 mm diameter.
10	Same; some 20 mm diameter irregular PPG drops; packed.
11	PPG slugs 2-3" long.
12	Same, 4-6" long irregular shapes.
13	PPG slugs packed together.
14	Large PPG drops 1-2" diameter irregular shape in core.

B:LABDATA1

UNITS ARE ft/sec & lbf/sq ft

Jf =	.04	Flow Reg:	D
Jg =	.41		
Re f =	1.169591	'alpha' =	.9111111
Re g =	3673.835	Dyn. Press =	.196425
J =	.45	(f) =	.001552
		(g) =	.163057
Jf =	.08	Flow Reg:	IS
Jg =	.41		
Re f =	2.339181	'alpha' =	.8367346
Re g =	3673.835	Dyn. Press =	.232897
J =	.49	(f) =	.006208
		(g) =	.163057
Jf =	.17	Flow Reg:	IC
Jg =	.41		
Re f =	4.97076	'alpha' =	.7068966
Re g =	3673.835	Dyn. Press =	.326308
J =	.58	(f) =	.028033
		(g) =	.163057
Jf =	.25	Flow Reg:	IA
Jg =	.41		
Re f =	7.309942	'alpha' =	.6212121
Re g =	3673.835	Dyn. Press =	.422532
J =	.66	(f) =	.060625
		(g) =	.163057
Jf =	.47	Flow Reg:	IA
Jg =	.41		
Re f =	13.74269	'alpha' =	.4659091
Re g =	3673.835	Dyn. Press =	.751168
J =	.88	(f) =	.214273
		(g) =	.163057

Jf =	.61		Flow Reg:	IA
Jg =	.41			
Re f =		17.83626	'alpha' =	.4019608
Re g =		3673.835	Dyn. Press =	1.009188
J =		1.02	(f) =	.360937
			(g) =	.163057
Jf =	.74		Flow Reg:	IA
Jg =	.41			
Re f =		21.63743	'alpha' =	.3565218
Re g =		3673.835	L . Press =	1.282825
J =		1.15	(f) =	.5311721
			(g) =	.163057
Jf =	1.1		Flow Reg:	IA
Jg =	.41			
Re f =		32.16374	'alpha' =	.2715232
Re g =		3673.835	Dyn. Press =	2.211697
J =		1.51	(f) =	1.1737
			(g) =	.163057
Jf =	.04		Flow Reg:	D
Jg =	.94			
Re f =		1.169591	'alpha' =	.9591836
Re g =		8422.939	Dyn. Press =	.9315881
J =		.98	(f) =	.001552
			(g) =	.857092
Jf =	.08		Flow Reg:	D
Jg =	.94			
Re f =		2.339181	'alpha' =	.9215686
Re g =		8422.939	Dyn. Press =	1.009188
J =		1.02	(f) =	.006208
			(g) =	.857092
Jf =	.17		Flow Reg:	IS
Jg =	.94			
Re f =		4.97076	'alpha' =	.8468468
Re g =		8422.939	Dyn. Press =	1.195137
J =		1.11	(f) =	.028033
			(g) =	.857092

Jf =	.25	Flow Reg:	IS
Jg =	.94		
Re f =	7.309942	'alpha' =	.789916
Re g =	8422.939	Dyn. Press =	1.373617
J =	1.19	(f) =	.060625
		(g) =	.857092
Jf =	.47	Flow Reg:	IA
Jg =	.94		
Re f =	13.74269	'alpha' =	.6666667
Re g =	8422.939	Dyn. Press =	1.928457
J =	1.41	(f) =	.214273
		(g) =	.857092
Jf =	.61	Flow Reg:	IA
Jg =	.94		
Re f =	17.83626	'alpha' =	.6064516
Re g =	8422.939	Dyn. Press =	2.330425
J =	1.55	(f) =	.360937
		(g) =	.857092
Jf =	.74	Flow Reg:	IA
Jg =	.94		
Re f =	21.63743	'alpha' =	.5595238
Re g =	8422.939	Dyn. Press =	2.737728
J =	1.68	(f) =	.5311721
		(g) =	.857092
Jf =	1.1	Flow Reg:	IA
Jg =	.94		
Re f =	32.16374	'alpha' =	.4607843
Re g =	8422.939	Dyn. Press =	4.036752
J =	2.04	(f) =	1.1737
		(g) =	.857092
Jf =	.04	Flow Reg:	D
Jg =	2.49		
Re f =	1.169591	'alpha' =	.9841898
Re g =	22311.83	Dyn. Press =	6.208873
J =	2.53	(f) =	.001552
		(g) =	6.014097

Jf = .08  
Jg = 2.49

Re f = 2.339181  
Re g = 22311.83  
J = 2.57

Flow Reg: D

'alpha' = .9688716  
Dyn. Press = 6.406753  
(f) = .006208  
(g) = 6.014097

Jf = .17  
Jg = 2.49

Re f = 4.97076  
Re g = 22311.83  
J = 2.66

Flow Reg: D

'alpha' = .9360902  
Dyn. Press = 6.863333  
(f) = .028033  
(g) = 6.014097

Jf = .25  
Jg = 2.49

Re f = 7.309942  
Re g = 22311.83  
J = 2.74

Flow Reg: D

'alpha' = .9087591  
Dyn. Press = 7.282372  
(f) = .060625  
(g) = 6.014097

Jf = .37  
Jg = 2.49

Re f = 10.81871  
Re g = 22311.83  
J = 2.86

Flow Reg: IS

'alpha' = .8706293  
Dyn. Press = 7.934213  
(f) = .132793  
(g) = 6.014097

Jf = .47  
Jg = 2.49

Re f = 13.74269  
Re g = 22311.83  
J = 2.96

Flow Reg: IC

'alpha' = .8412162  
Dyn. Press = 8.498752  
(f) = .214273  
(g) = 6.014097

Jf = .61  
Jg = 2.49

Re f = 17.83626  
Re g = 22311.83  
J = 3.1

Flow Reg: IS

'alpha' = .8032258  
Dyn. Press = 9.3217  
(f) = .360937  
(g) = 6.014097

Jf =	.74		Flow Reg:	IC
Jg =	2.49			
Re f =		21.63743	'alpha' =	.7708978
Re g =		22311.83	Dyn. Press =	10.11991
J =		3.23	(f) =	.5311721
			(g) =	6.014097
Jf =	1.1		Flow Reg:	IA
Jg =	2.49			
Re f =		32.16374	'alpha' =	.6935933
Re g =		22311.83	Dyn. Press =	12.50146
J =		3.59	(f) =	1.1737
			(g) =	6.014097
Jf =	.04		Flow Reg:	D
Jg =	1.64			
Re f =		1.169591	'alpha' =	.9761905
Re g =		14695.34	Dyn. Press =	2.737728
J =		1.68	(f) =	.001552
			(g) =	2.608912
Jf =	.08		Flow Reg:	D
Jg =	1.64			
Re f =		2.339181	'alpha' =	.9534884
Re g =		14695.34	Dyn. Press =	2.869648
J =		1.72	(f) =	.006208
			(g) =	2.608912
Jf =	.17		Flow Reg:	D
Jg =	1.64			
Re f =		4.97076	'alpha' =	.9060774
Re g =		14695.34	Dyn. Press =	3.177817
J =		1.81	(f) =	.028033
			(g) =	2.608912
Jf =	.25		Flow Reg:	IC
Jg =	1.64			
Re f =		7.309942	'alpha' =	.8677249
Re g =		14695.34	Dyn. Press =	3.464937
J =		1.89	(f) =	.060625
			(g) =	2.608912

Jf =	.37		Flow Reg:	IC
Jg =	1.64			
	Re f =	10.81871	'alpha' =	.8159205
	Re g =	14695.34	Dyn. Press =	3.918897
	J =	2.01	(f) =	.132793
			(g) =	2.608912
Jf =	.47		Flow Reg:	IA
Jg =	1.64			
	Re f =	13.74269	'alpha' =	.7772513
	Re g =	14695.34	Dyn. Press =	4.318537
	J =	2.11	(f) =	.214273
			(g) =	2.608912
Jf =	.61		Flow Reg:	IA
Jg =	1.64			
	Re f =	17.83626	'alpha' =	.7288889
	Re g =	14695.34	Dyn. Press =	4.910625
	J =	2.25	(f) =	.360937
			(g) =	2.608912
Jf =	.81		Flow Reg:	IA
Jg =	1.64			
	Re f =	23.68421	'alpha' =	.6693878
	Re g =	14695.34	Dyn. Press =	5.822426
	J =	2.45	(f) =	.636417
			(g) =	2.608912
Jf =	1.1		Flow Reg:	IA
Jg =	1.64			
	Re f =	32.16374	'alpha' =	.5985401
	Re g =	14695.34	Dyn. Press =	7.282372
	J =	2.74	(f) =	1.1737
			(g) =	2.608912
Jf =	30		Flow Reg:	A
Jg =	30			
	Re f =	877.1929	'alpha' =	.5
	Re g =	268817.2	Dyn. Press =	3492
	J =	60	(f) =	873
			(g) =	873

Jf =	17.54	Flow Reg:	C
Jg =	30		
Re f =	512.8655	'alpha' =	.6310476
Re g =	268817.2	Dyn. Press =	2192.25
J =	47.54	(f) =	298.4221
		(g) =	873
Jf =	10.25	Flow Reg:	S
Jg =	30		
Re f =	299.7076	'alpha' =	.7453416
Re g =	268817.2	Dyn. Press =	1571.461
J =	40.25	(f) =	101.9106
		(g) =	873
Jf =	5.99	Flow Reg:	B
Jg =	30		
Re f =	175.1462	'alpha' =	.833565
Re g =	268817.2	Dyn. Press =	1256.422
J =	35.99	(f) =	34.8037
		(g) =	873
Jf =	3.5	Flow Reg:	D
Jg =	30		
Re f =	102.3392	'alpha' =	.8955224
Re g =	268817.2	Dyn. Press =	1088.583
J =	33.5	(f) =	11.8825
		(g) =	873
Jf =	2.05	Flow Reg:	IS
Jg =	30		
Re f =	59.94152	'alpha' =	.9360375
Re g =	268817.2	Dyn. Press =	996.3864
J =	32.05	(f) =	4.076425
		(g) =	873
Jf =	1.2	Flow Reg:	IC
Jg =	30		
Re f =	35.08772	'alpha' =	.9615384
Re g =	268817.2	Dyn. Press =	944.2369
J =	31.2	(f) =	1.3968
		(g) =	873

Jf =  
Jg =

.7  
30

Flow Reg: IA

Re f = 20.46784  
Re g = 268817.2  
J = 30.7

'alpha' = .9771987  
Dyn. Press = 914.2154  
(f) = .4753  
(g) = 873

B:LABDATA2

UNITS ARE ft/sec & lbf/sq ft

Jf =	.04		Flow Reg:	A
Jg =	.41			
	Re f =	1.169591	'alpha' =	.9111111
	Re g =	3673.835		
	J =	.45	Dyn. Press =	.196425
			(f) =	.001552
			(g) =	.163057
Jf =	.08		Flow Reg:	D
Jg =	.41			
	Re f =	2.339181	'alpha' =	.8367346
	Re g =	3673.835		
	J =	.49	Dyn. Press =	.232897
			(f) =	.006208
			(g) =	.163057
Jf =	.17		Flow Reg:	D
Jg =	.41			
	Re f =	4.97076	'alpha' =	.7068966
	Re g =	3673.835		
	J =	.58	Dyn. Press =	.326308
			(f) =	.028033
			(g) =	.163057
Jf =	.25		Flow Reg:	D
Jg =	.41			
	Re f =	7.309942	'alpha' =	.6212121
	Re g =	3673.835		
	J =	.66	Dyn. Press =	.422532
			(f) =	.060625
			(g) =	.163057
Jf =	.37		Flow Reg:	D
Jg =	.41			
	Re f =	10.81871	'alpha' =	.525641
	Re g =	3673.835		
	J =	.78	Dyn. Press =	.590148
			(f) =	.132793
			(g) =	.163057

17 Flow Reg: D

Jf =	.77		Flow Reg:	D
Jg =	.41			
	Re f =	13.74269	'alpha' =	.4659091
	Re g =	3673.835	Dyn. Press =	.751168
	J =	.88	(f) =	.214273
			(g) =	.163057
Jf =	.61		Flow Reg:	IA
Jg =	.41			
	Re f =	17.83626	'alpha' =	.4019608
	Re g =	3673.835	Dyn. Press =	1.009188
	J =	1.02	(f) =	.360937
			(g) =	.163057
Jf =	.74		Flow Reg:	IA
Jg =	.41			
	Re f =	21.63743	'alpha' =	.3565218
	Re g =	3673.835	Dyn. Press =	1.282825
	J =	1.15	(f) =	.5311721
			(g) =	.163057
Jf =	1.1		Flow Reg:	IA
Jg =	.41			
	Re f =	32.16374	'alpha' =	.2715232
	Re g =	3673.835	Dyn. Press =	2.211697
	J =	1.51	(f) =	1.1737
			(g) =	.163057
Jf =	.04		Flow Reg:	D
Jg =	.94			
	Re f =	1.169591	'alpha' =	.9591836
	Re g =	8422.939	Dyn. Press =	.9315881
	J =	.98	(f) =	.001552
			(g) =	.857092
Jf =	.17		Flow Reg:	D
Jg =	.94			
	Re f =	4.97076	'alpha' =	.8468468
	Re g =	8422.939	Dyn. Press =	1.195137
	J =	1.11	(f) =	.028033
			(g) =	.857092
Jf =	.77		Flow Reg:	D
Jg =				

Jf =	.94	Re f =	10.81871	'alpha' =	.7175573
Jg =		Re g =	8422.939	Dyn. Press =	1.664617
		J =	1.31	(f) =	.132793
				(g) =	.857092
Jf =	.47	Re f =	13.74269	'alpha' =	.6666667
Jg =	.94	Re g =	8422.939	Dyn. Press =	1.928457
		J =	1.41	(f) =	.214273
				(g) =	.857092
Jf =	.61	Re f =	17.83626	'alpha' =	.6064516
Jg =	.94	Re g =	8422.939	Dyn. Press =	2.330425
		J =	1.55	(f) =	.360937
				(g) =	.857092
Jf =	.74	Re f =	21.63743	'alpha' =	.5595238
Jg =	.94	Re g =	8422.939	Dyn. Press =	2.737728
		J =	1.68	(f) =	.5311721
				(g) =	.857092
Jf =	1.1	Re f =	32.16374	'alpha' =	.4607843
Jg =	.94	Re g =	8422.939	Dyn. Press =	4.036752
		J =	2.04	(f) =	1.1737
				(g) =	.857092
Jf =	.04	Re f =	1.169591	'alpha' =	.9761903
Jg =	1.64	Re g =	14695.34	Dyn. Press =	2.737728
		J =	1.68	(f) =	.001552
				(g) =	2.608912
Jf =	.00	Re f =		'alpha' =	
Jg =		Re g =		Dyn. Press =	
		J =		(f) =	
				(g) =	

U =	1.00	Flow Reg:	D
Jg =	1.64		
Re f =	2.339181	'alpha' =	.9534884
Re g =	14695.34	Dyn. Press =	2.869648
J =	1.72	(f) =	.006208
		(g) =	2.608912
Jf =	.25	Flow Reg:	D
Jg =	1.64		
Re f =	7.309942	'alpha' =	.8677249
Re g =	14695.34	Dyn. Press =	3.464937
J =	1.89	(f) =	.060625
		(g) =	2.608912
Jf =	.47	Flow Reg:	D
Jg =	1.64		
Re f =	13.74269	'alpha' =	.7772513
Re g =	14695.34	Dyn. Press =	4.318537
J =	2.11	(f) =	.214273
		(g) =	2.608912
Jf =	.74	Flow Reg:	D
Jg =	1.64		
Re f =	21.63743	'alpha' =	.6890756
Re g =	14695.34	Dyn. Press =	5.494469
J =	2.38	(f) =	.5311721
		(g) =	2.608912
Jf =	1.1	Flow Reg:	D
Jg =	1.64		
Re f =	32.16374	'alpha' =	.5985401
Re g =	14695.34	Dyn. Press =	7.282372
J =	2.74	(f) =	1.1737
		(g) =	2.608912
Jf =	.04	Flow Reg:	D
Jg =	2.49		
Re f =	1.169591	'alpha' =	.9841898
Re g =	22311.83	Dyn. Press =	6.208873
J =	2.53	(f) =	.001552
		(g) =	6.014097
Jf =	.17	Flow Reg:	D
Jg =	1.64		

Jg =	2.49		Flow Reg:	
	Re f =	4.97076	'alpha' =	.9360902
	Re g =	22311.83	Dyn. Press =	6.863333
	J =	2.66	(f) =	.028033
			(g) =	6.014097

Jf =	.37		Flow Reg:	D
Jg =	2.49			
	Re f =	10.81871	'alpha' =	.8706293
	Re g =	22311.83	Dyn. Press =	7.934213
	J =	2.86	(f) =	.132793
			(g) =	6.014097

Jf =	.61		Flow Reg:	D
Jg =	2.49			
	Re f =	17.83626	'alpha' =	.8032258
	Re g =	22311.83	Dyn. Press =	9.3217
	J =	3.1	(f) =	.360937
			(g) =	6.014097

Jf =	1.1		Flow Reg:	D
Jg =	2.49			
	Re f =	32.16374	'alpha' =	.6935933
	Re g =	22311.83	Dyn. Press =	12.50146
	J =	3.59	(f) =	1.1737
			(g) =	6.014097

B:LABDATA3

UNITS ARE ft/sec & lbf/sq ft

Jf =	.04		Flow Reg:	D
Jg =	.41			
Re f =		1.169591	'alpha' =	.9111111
Re g =		3673.835	Dyn. Press =	.196425
J =		.45	(f) =	.001552
			(g) =	.163057
Jf =	.08		Flow Reg:	D
Jg =	.41			
Re f =		2.339181	'alpha' =	.8367346
Re g =		3673.835	Dyn. Press =	.232897
J =		.49	(f) =	.006208
			(g) =	.163057
Jf =	.17		Flow Reg:	IS
Jg =	.41			
Re f =		4.97076	'alpha' =	.7068966
Re g =		3673.835	Dyn. Press =	.326308
J =		.58	(f) =	.028033
			(g) =	.163057
Jf =	.25		Flow Reg:	IC
Jg =	.41			
Re f =		7.309942	'alpha' =	.6212121
Re g =		3673.835	Dyn. Press =	.422532
J =		.66	(f) =	.060625
			(g) =	.163057
Jf =	.37		Flow Reg:	IA
Jg =	.41			
Re f =		10.81871	'alpha' =	.525641
Re g =		3673.835	Dyn. Press =	.590148
J =		.78	(f) =	.132793
			(g) =	.163057

Jf =	.47		Flow Reg:	IA
Jg =	.41			
Re f =		13.74269	'alpha' =	.4659091
Re g =		3673.835	Dyn. Press =	.751168
J =		.88	(f) =	.214273
			(g) =	.163057
Jf =	.61		Flow Reg:	IA
Jg =	.41			
Re f =		17.83626	'alpha' =	.4019608
Re g =		3673.835	Dyn. Press =	1.009188
J =		1.02	(f) =	.360937
			(g) =	.163057
Jf =	.74		Flow Reg:	IA
Jg =	.41			
Re f =		21.63743	'alpha' =	.3565218
Re g =		3673.835	Dyn. Press =	1.282825
J =		1.15	(f) =	.5311721
			(g) =	.163057
Jf =	1.1		Flow Reg:	IA
Jg =	.41			
Re f =		32.16374	'alpha' =	.2715232
Re g =		3673.835	Dyn. Press =	2.211697
J =		1.51	(f) =	1.1737
			(g) =	.163057
Jf =	.04		Flow Reg:	D
Jg =	.94			
Re f =		1.169591	'alpha' =	.9591836
Re g =		8422.939	Dyn. Press =	.9315881
J =		.98	(f) =	.001552
			(g) =	.857092
Jf =	.17		Flow Reg:	D
Jg =	.94			
Re f =		4.97076	'alpha' =	.8468468
Re g =		8422.939	Dyn. Press =	1.195137
J =		1.11	(f) =	.026033
			(g) =	.857092

Jf = .37  
Jg = .94

Re f = 10.81871  
Re g = 8422.939  
J = 1.31

Flow Reg: D

'alpha' = .7175573  
Dyn. Press = 1.464617  
(f) = .132793  
(g) = .857092

Jf = .61  
Jg = .94

Re f = 17.83626  
Re g = 8422.939  
J = 1.55

Flow Reg: D

'alpha' = .6064516  
Dyn. Press = 2.330425  
(f) = .360937  
(g) = .857092

Jf = .74  
Jg = .94

Re f = 21.63743  
Re g = 8422.939  
J = 1.68

Flow Reg: D

'alpha' = .5595238  
Dyn. Press = 2.737728  
(f) = .5311721  
(g) = .857092

Jf = .87  
Jg = .94

Re f = 25.4386  
Re g = 8422.939  
J = 1.81

Flow Reg: IA

'alpha' = .5193371  
Dyn. Press = 3.177817  
(f) = .734193  
(g) = .857092

Jf = 1.1  
Jg = .94

Re f = 32.16374  
Re g = 8422.939  
J = 2.04

Flow Reg: IA

'alpha' = .4607843  
Dyn. Press = 4.036752  
(f) = 1.1737  
(g) = .857092

Jf = .04  
Jg = 1.64

Re f = 1.169591  
Re g = 14693.34  
J = 1.68

Flow Reg: D

'alpha' = .9761905  
Dyn. Press = 2.737728  
(f) = .001552  
(g) = .857092

Jf = .17  
Jg = 1.64

Re f = 4.97076  
Re g = 14695.34  
J = 1.81

Flow Reg: D

'alpha' = .9060774  
Dyn. Press = 3.177817  
(f) = .028033  
(g) = 2.608912

Jf = .37  
Jg = 1.64

Re f = 10.81871  
Re g = 14695.34  
J = 2.01

Flow Reg: D

'alpha' = .8159205  
Dyn. Press = 3.918897  
(f) = .132793  
(g) = 2.608912

Jf = .61  
Jg = 1.64

Re f = 17.83626  
Re g = 14695.34  
J = 2.25

Flow Reg: D

'alpha' = .7288889  
Dyn. Press = 4.910625  
(f) = .360937  
(g) = 2.608912

Jf = 1.1  
Jg = 1.64

Re f = 32.16374  
Re g = 14695.34  
J = 2.74

Flow Reg: D

'alpha' = .5985401  
Dyn. Press = 7.282372  
(f) = 1.1737  
(g) = 2.608912

Jf = .04  
Jg = 2.49

Re f = 1.169591  
Re g = 22311.83  
J = 2.53

Flow Reg: D

'alpha' = .9841898  
Dyn. Press = 6.208873  
(f) = .001552  
(g) = 6.014097

Jf = .37  
Jg = 2.49

Re f = 10.81871  
Re g = 22311.83  
J = 2.86

Flow Reg: D

'alpha' = .8706293  
Dyn. Press = 7.934213  
(f) = .132793  
(g) = 6.014097

Jf = 1.1  
Jg = 2.49

Re f = 32.16374  
Re g = 223'1.83  
J = 3.59

Flow Reg: D

'alpha' = .6935933

Dyn. Press = 12.50146

(f) = 1.1737

(g) = 6.014097

B:LAPDATA4

UNITS ARE ft/sec & lbf/sq ft

Jf =	.04		Flow Reg:	D
Jg =	1.64			
Re f =	1.169591	'alpha' =	.9761905	
Re g =	14695.34	Dyn. Press =	2.737728	
J =	1.66	(f) =	.001552	
		(g) =	2.608912	
Jf =	.17		Flow Reg:	D
Jg =	1.64			
Re f =	4.97076	'alpha' =	.9060774	
Re g =	14695.34	Dyn. Press =	3.177817	
J =	1.81	(f) =	.028073	
		(g) =	2.608912	
Jf =	.37		Flow Reg:	D
Jg =	1.64			
Re f =	10.81871	'alpha' =	.8159205	
Re g =	14695.34	Dyn. Press =	3.918897	
J =	2.01	(f) =	.132793	
		(g) =	2.608912	
Jf =	.84		Flow Reg:	D
Jg =	1.64			
Re f =	24.5614	'alpha' =	.6612903	
Re g =	14695.34	Dyn. Press =	5.965889	
J =	2.48	(f) =	.684432	
		(g) =	2.608912	
Jf =	.04		Flow Reg:	D
Jg =	2.49			
Re f =	1.169591	'alpha' =	.9841896	
Re g =	22311.83	Dyn. Press =	6.208873	
J =	2.53	(f) =	.001552	
		(g) =	6.014097	

Jf =	.08		Flow Reg:	D
Jg =	2.49			
Re f =		2.339181	'alpha' =	.9688716
Re g =		22311.83	Dyn. Press =	6.406757
J =		2.57	(f) =	.006208
			(g) =	6.014097
Jf =	.17		Flow Reg:	D
Jg =	2.49			
Re f =		4.97076	'alpha' =	.9360902
Re g =		22311.83	Dyn. Press =	6.863333
J =		2.66	(f) =	.028033
			(g) =	6.014097
Jf =	.37		Flow Reg:	D
Jg =	2.49			
Re f =		10.81871	'alpha' =	.8706293
Re g =		22311.83	Dyn. Press =	7.934213
J =		2.86	(f) =	.132793
			(g) =	6.014097
Jf =	.79		Flow Reg:	D
Jg =	2.49			
Re f =		23.09942	'alpha' =	.7591463
Re g =		22311.83	Dyn. Press =	10.47565
J =		3.28	(f) =	.605377
			(g) =	6.014097
Jf =	.04		Flow Reg:	D
Jg =	.94			
Re f =		1.169591	'alpha' =	.9591836
Re g =		8422.939	Dyn. Press =	.9315881
J =		.98	(f) =	.001552
			(g) =	.857092
Jf =	.17		Flow Reg:	D
Jg =	.94			
Re f =		4.97076	'alpha' =	.8468468
Re g =		8422.939	Dyn. Press =	1.195137
J =		1.11	(f) =	.028033
			(g) =	.857092

Jf =	.37		Flow Reg:	D
Jg =	.94			
Re f =		10.81871	'alpha' =	.7175577
Re g =		8422.939	Dyn. Press =	1.664617
J =		1.31	(f) =	.132787
			(g) =	.857092
Jf =	.81		Flow Reg:	D
Jg =	.94			
Re f =		23.68421	'alpha' =	.5371429
Re g =		8422.939	Dyn. Press =	2.970625
J =		1.75	(f) =	.636417
			(g) =	.857092
Jf =	.04		Flow Reg:	D
Jg =	.41			
Re f =		1.169591	'alpha' =	.9111111
Re g =		3673.835	Dyn. Press =	.196425
J =		.45	(f) =	.001552
			(g) =	.163057
Jf =	.17		Flow Reg:	D
Jg =	.41			
Re f =		4.97076	'alpha' =	.7068966
Re g =		3673.835	Dyn. Press =	.326308
J =		.58	(f) =	.028033
			(g) =	.163057
Jf =	.37		Flow Reg:	D
Jg =	.41			
Re f =		10.81871	'alpha' =	.525641
Re g =		3673.835	Dyn. Press =	.590148
J =		.78	(f) =	.132793
			(g) =	.163057
Jf =	.61		Flow Reg:	D
Jg =	.41			
Re f =		17.83626	'alpha' =	.4019600
Re g =		3673.835	Dyn. Press =	1.009168
J =		1.02	(f) =	.360937
			(g) =	.163057

Re f =  
Jg =

.74  
.41

Re f =  
Re g =  
J =

21.63743  
3673.835  
1.15

Flow Reg: 10

'alpha' = .3565218  
Dyn. Press = 1.282925  
(f) = .5311721  
(g) = .163057

EXLARDATAS

UNITS ARE ft/sec & lbf/sq ft

Jf =	1.1		Flow Reg:	IA
Jg =	.13			
	Re f =	32.16374	'alpha' =	.1056911
	Re g =	1164.875	Dyn. Press =	1.487517
	J =	1.23	(f) =	1.1737
			(g) =	.016393
Jf =	.68		Flow Reg:	IA
Jg =	.13			
	Re f =	19.88304	'alpha' =	.1604938
	Re g =	1164.875	Dyn. Press =	.636417
	J =	.81	(f) =	.448528
			(g) =	.016393
Jf =	.37		Flow Reg:	D
Jg =	.13			
	Re f =	10.81871	'alpha' =	.26
	Re g =	1164.875	Dyn. Press =	.2425
	J =	.5	(f) =	.132783
			(g) =	.016393
Jf =	.17		Flow Reg:	D
Jg =	.13			
	Re f =	4.97076	'alpha' =	.4333333
	Re g =	1164.875	Dyn. Press =	.0873
	J =	.3	(f) =	.028001
			(g) =	.016393
Jf =	.04		Flow Reg:	A
Jg =	.13			
	Re f =	1.169591	'alpha' =	.7647059
	Re g =	1164.875	Dyn. Press =	.028001
	J =	.17	(f) =	.001552
			(g) =	.016393

Jf =	1.1		Flow Reg:	IC
Jg =	.27			
Re f =		32.16374	'alpha' =	.1970803
Re g =		2419.355	Dyn. Press =	1.820597
J =		1.27	(f) =	1.1737
			(g) =	7.071301E-02
Jf =	.61		Flow Reg:	IC
Jg =	.27			
Re f =		17.87626	'alpha' =	.3068182
Re g =		2419.355	Dyn. Press =	.751168
J =		.88	(f) =	.360937
			(g) =	7.071301E-02
Jf =	.37		Flow Reg:	D
Jg =	.27			
Re f =		10.81871	'alpha' =	.4218751
Re g =		2419.355	Dyn. Press =	.397312
J =		.64	(f) =	.152797
			(g) =	7.071301E-02
Jf =	.17		Flow Reg:	A
Jg =	.27			
Re f =		4.97076	'alpha' =	.6136364
Re g =		2419.355	Dyn. Press =	.187792
J =		.44	(f) =	.028933
			(g) =	7.071301E-02

B:LABDATA6

UNITS ARE ft/sec & lbf/sq ft

Jf =	.04		Flow Reg:	IA
Jg =	.13			
Re f =		1.169591	'alpha' =	.7647059
Re g =		1164.875	Dyn. Press =	.028033
J =		.17	(f) =	.001552
			(g) =	.016393
Jf =	.08		Flow Reg:	IA
Jg =	.13			
Re f =		2.339181	'alpha' =	.6190476
Re g =		1164.875	Dyn. Press =	.042777
J =		.21	(f) =	.006208
			(g) =	.016393
Jf =	.17		Flow Reg:	IA
Jg =	.13			
Re f =		4.97076	'alpha' =	.4333333
Re g =		1164.875	Dyn. Press =	.0873
J =		.3	(f) =	.028033
			(g) =	.016393
Jf =	.25		Flow Reg:	IC
Jg =	.13			
Re f =		7.309942	'alpha' =	.3421052
Re g =		1164.875	Dyn. Press =	.140068
J =		.38	(f) =	.060623
			(g) =	.016393
Jf =	.37		Flow Reg:	IC
Jg =	.13			
Re f =		10.61871	'alpha' =	.26
Re g =		1164.875	Dyn. Press =	.2825
J =		.5	(f) =	.155793
			(g) =	.016393

Jf =	.47	Flow Reg:	D
Jg =	.13		
Re f =	13.74269	'alpha' =	.2166667
Re g =	1164.875	Dyn. Press =	.3492
J =	.6	(f) =	.214273
		(g) =	.016393
Jf =	.61	Flow Reg:	D
Jg =	.13		
Re f =	17.83626	'alpha' =	.1756757
Re g =	1164.875	Dyn. Press =	.5311721
J =	.74	(f) =	.360937
		(g) =	.016393
Jf =	.99	Flow Reg:	B
Jg =	.13		
Re f =	28.94737	'alpha' =	.1160714
Re g =	1164.875	Dyn. Press =	1.216768
J =	1.12	(f) =	.9506971
		(g) =	.016393
Jf =	.04	Flow Reg:	D
Jg =	.27		
Re f =	1.169591	'alpha' =	.8709678
Re g =	2419.355	Dyn. Press =	9.321701E-02
J =	.31	(f) =	.001552
		(g) =	7.071301E-02
Jf =	.08	Flow Reg:	D
Jg =	.27		
Re f =	2.339181	'alpha' =	.7714285
Re g =	2419.355	Dyn. Press =	.118825
J =	.35	(f) =	.006208
		(g) =	7.071301E-02
Jf =	.17	Flow Reg:	IS
Jg =	.27		
Re f =	4.97076	'alpha' =	.6136764
Re g =	2419.355	Dyn. Press =	.187792
J =	.44	(f) =	.028077
		(g) =	7.071301E-02

Jf = .25  
Jg = .27

Re f = 7.309942  
Re g = 2419.355  
J = .52

Flow Reg: IC

'alpha' = .5192308  
Dyn. Press = .262288  
(f) = .060625  
(g) = 7.071301E-02

Jf = .37  
Jg = .27

Re f = 10.81871  
Re g = 2419.355  
J = .64

Flow Reg: IS

'alpha' = .4218751  
Dyn. Press = .397312  
(f) = .132792  
(g) = 7.071301E-02

Jf = .47  
Jg = .27

Re f = 13.74269  
Re g = 2419.355  
J = .74

Flow Reg: D

'alpha' = .3648649  
Dyn. Press = .5311721  
(f) = .214273  
(g) = 7.071301E-02